MECHANISMS DURING CATHEPSIN INHIBITION AND THE EFFECTS ON SUBSTRATE DEGRADATION AND BREAST CANCER CELL INVASION

A Dissertation
Presented to
The Academic Faculty

by

Catera Wilder

In Partial Fulfillment
of the Requirements for the Degree
Doctor of Philosophy in the
School of Wallace H. Coulter Department of Biomedical Engineering

Georgia Institute of Technology
May 2016

MECHANISMS DURING CATHEPSIN INHIBITION AND THE EFFECTS ON SUBSTRATE DEGRADATION AND BREAST CANCER CELL INVASION

Approved by:

Dr. Manu Platt, Advisor
School of Biomedical Engineering
Georgia Institute of Technology

Dr. Shelly Peyton
School of Chemical Engineering
University of Massachusetts Amherst

Dr. Melissa Kemp
School of Biomedical Engineering
Georgia Institute of Technology

Dr. Johnna Temenoff
School of Biomedical Engineering
Georgia Institute of Technology

Dr. Valerie Odero-Marah
School of Biological Sciences
Clark Atlanta University

Date Approved: February 22, 2016

To My Family

TABLE OF CONTENTS

LIST OF FIGURES

LIST OF SYMBOLS AND ABBREVIATIONS

Adipo	adipogenic
Cat	cathepsin
CysC	cystatin C
Cyclo	cycloheximide
DC	direct contact
DTT	dithiothreitol
EC	endothelial cell
ECM	extracellular matrix
ER	estrogen receptor
Exp	expansion
GM	GM6001
HER	human epidermal growth factor receptor
HIV	human immunodeficiency virus
L	cathepsin L
K	cathepsin K
Mac	macrophages
MDA	MDA-MB-231 cells
MMPs	matrix metalloproteinases
MSC	mesenchymal stem cell
OCL	osteoclasts
OS	osteogenic
pCR	pathological complete response
PBMCs	peripheral blood mononuclear cells

PMA	phorbol myristate acetate
PR	progesterone receptor
RAW	RAW 264.7 macrophages
SDS-PAGE	sodium dodecyl sulfate-polyacrylamide gel electrophoresis
S	cathepsin S
TAMs	tumor associated macrophages
TNFα	tumor necrosis factor α
TW	transwell
V	cathepsin V

SUMMARY

Currently, one out of every eight women in the U.S. will be diagnosed with breast cancer in their lifetime. Cysteine cathepsin proteases are powerful collagenases and elastases that play an important role in matrix remodeling and are upregulated in various diseases such as atherosclerosis, osteoporosis, and cancer. During cancer progression, tumor cells upregulate cysteine cathepsins to assist with the invasion and metastasis of the tumor. This has motivated pharmaceutical companies to develop protease inhibitors, but many have failed clinical trials due to adverse side effects. Currently there is limited research investigating cellular feedback mechanisms caused by cathepsin inhibitors. This highlights a need to understand how cathepsin inhibition affects cathepsin production. The objective of this work is to elucidate cellular feedback regulations of cysteine cathepsins during broad spectrum inhibition and possible mechanisms in order to develop more effective cathepsin inhibitors for breast cancer therapies.

This was accomplished by developing tools to selectively distinguish active cathepsins K, L, S, and V to appropriately quantify their levels in cells and tissue. Next, the inhibitor-induced effects on cathepsin activity with chemical or protein inhibitors in breast cancer cells was determined. Mechanisms by which inhibition of cathepsin activity induced active cathepsins were elucidated, and finally, the role in substrate degradation and cell invasion was investigated. The results of this work provide tools to selectively distinguish cathepsins by taking advantage of pH and substrate regulation and identifies a feedback response that elevates active cathepsins in response to cathepsin inhibition. These findings also demonstrate an interaction that occurs between two cathepsins within the

cathepsin proteolytic network. Currently, there are limited studies investigating the effects of cathepsin inhibition on the cellular regulation of cathepsin amounts. Not only are these findings important for providing more effective treatment options for breast cancer, but this work has broad implications since cathepsins have been implicated in diseases such as HIV, atherosclerosis, and osteoporosis.

CHAPTER 1

INTRODUCTION

1.1 Motivation

Currently, one out of every eight women in the U.S. will be diagnosed with breast cancer in their lifetime. The American Cancer Society reported that survival rates decrease dramatically to 26% for metastatic or distant tumors compared to 85% for regionally migrated tumors and 99% for localized tumors [1]. With a dismal survival rate, there is a dire need for more research focused on metastatic cancer detection and treatment. Cysteine cathepsin proteases are powerful collagenases and elastases that play an important role in matrix remodeling and are upregulated in various diseases such as atherosclerosis, osteoporosis, and cancer [2-7]. During cancer progression, tumor cells upregulate cysteine cathepsins to assist with the invasion and metastasis of the tumor [5, 8-11]. Under physiological conditions, cathepsins are inhibited intracellularly and extracellularly by the family of protein inhibitors cystatins including cystatin B, also known as stefin B, and cystatin C, respectively [12]. Reduced protein levels of cystatin M, were reported to occur in invasive ductal carcinoma tissue [10]. This has motivated pharmaceutical companies to develop protease inhibitors, but many have failed clinical trials due to adverse side effects [13]. However, more focus has been directed toward targeting these proteases for cancer treatments due to the research demonstrating the important role of cysteine cathepsins in cancer progression and metastasis [13, 14]. Moreover, clinical studies have primarily used cysteine cathepsin inhibitors to treat bone related diseases such as osteoporosis and bone metastasis [15-17] even though *in vivo*

studies have suggested the need for cysteine cathepsin inhibitors to inhibit cancer invasion and metastasis [7, 10, 13, 18-20].

This is in contrast to therapies developed to target matrix metalloproteinases (MMPs), another family of proteases also identified as players in cancer invasion, which were not effective in reducing cancer progression during clinical trials using MMP broad-spectrum family inhibitors [13, 18, 19, 21-23]. Compared to the MMP clinical trials, the clinical trials using cathepsin inhibitors have shown that the inhibitors are efficacious, although they do cause adverse side effects [13, 24]. Currently there is limited research investigating cellular feedback mechanisms caused by cathepsin inhibitors. This highlights a need to understand how cathepsin inhibition affects cathepsin production, and for the development of tools capable of reliably measuring active cathepsins.

The cathepsin proteolytic network is a dynamic system involving 11 proteases, 11 endogenous inhibitors, pro-peptide cleavage, auto-activation, substrate promiscuity, competitive inhibition, and enzyme inactivation, along with interactions among different protease families. Thus, it is important to understand how perturbations within the cathepsin network due to inhibition affects the system and induces any compensatory mechanisms. However, little research has examined such compensatory mechanisms. This thesis investigates the cellular regulation of cysteine cathepsins during broad spectrum inhibition and possible mechanisms in order to develop more effective cathepsin inhibitors for cancer therapies.

1.2 Research Objectives

The **objective of this research** is to elucidate cellular feedback mechanisms due to broad spectrum cysteine cathepsin inhibitors in breast cancer. This objective will assist with achieving the overall goal to understand cathepsin inhibitor-induced cellular mechanisms that could be contributing to adverse side effects that occur during therapeutic cathepsin inhibitor administration.

The **central hypothesis** is that perturbing the cathepsin proteolytic network with a small molecule or protein cathepsin inhibitor induces a feedback between cathepsin inhibition and production which upregulates cathepsin protein expression and activity. This hypothesis will be evaluated using the following aims:

Specific Aim 1: Develop tools to distinguish pro-, mature, and inactive cathepsins K, L, S, and V to appropriately quantify their levels in cells and tissue

Hypothesis: If cathepsins K, L, S, and V have different regulatory properties for activity, then selectivity for cathepsins K, L, S, or V can be obtained by varying the assay buffer pH and the substrate within the electrophoresis gel. The electrophoretic migration of recombinant cathepsins K, L, S, and V was identified using the modified sodium dodecyl sulfate-polyacrylamide gel electrophoresis (SDS-PAGE) method, zymography. Recombinant cathepsins K, L, S, and V were incubated at various pHs and with different substrates and the activity measured to determine conditions for selectivity. Cell lysates and tissue samples were assayed using gelatin cathepsin zymography to confirm selectivity in systems containing more cathepsins, cell types, and matrices. It was found that by taking advantage of different pH and substrate preferences of cathepsins, proteolytic activity of

cathepsins K, L, S and V in human cells and tissue samples was selectively detected. The selectivity was accomplished even when distinguishing between homologous cathepsins.

Specific Aim 2: Determine inhibitor-induced effects on cathepsin activity with chemical or protein inhibition in breast cancer cells

Hypothesis: During cathepsin inhibition, the amount of active and total cathepsins will be decreased in breast cancer cells. MDA-MB-231 breast cancer cells were assayed using multiplex zymography and Western blots to quantify the amount and time dependent activation of cathepsins when either stimulated with broad spectrum cathepsin inhibitors E-64, cystatin C, or transfected with cystatin C overexpression plasmids. The cathepsin cellular localization was identified using immunostaining and confocal imaging. The effect of cathepsin inhibitors on secreted cathepsins was detected using multiplex zymography and Western blots. Active cathepsins S and L were detected in the MDA-MB-231 cells. E-64 incubation with MDA-MB-231 cells upregulated the amount of active cathepsin S while reducing cathepsin L. Cystatin C incubation and overexpression also caused elevation in cathepsin S. The differential response of cathepsin S and L was due in part to differences in cellular location.

Specific Aim 3: Elucidate mechanisms by which inhibition of cathepsin activity induces active cathepsins and investigate its role in substrate degradation and cell invasion

Hypothesis: Inhibitor-induced upregulation of active cathepsin S is due to active cathepsin L and the cathepsin S upregulation will increase substrate degradation and

cancer cell invasion. The amount of active and total cathepsin protein amounts in non-transformed and cancerous human epithelial cells, macrophages, and tissue treated with E-64 was determined. In addition, effects of cathepsin L protein on the inhibitor-induced elevation of cathepsin S were assessed in murine models which do not express cathepsin L. Cystatin overexpression models were used to investigate the role of cathepsin inhibitors on breast cancer cell substrate degradation and invasion. Cathepsin inhibition increased the amount of active cathepsin S in the non-cancerous human breast tissue and macrophages. The upregulation of cathepsin S was regulated by cathepsin L as validated in the murine models lacking cathepsin L expression.

The results of this work provide tools to selectively distinguish cathepsins by taking advantage of pH and substrate regulation and identifies a feedback mechanism that elevates active cathepsins in response to cathepsin inhibition. These findings also demonstrate an interaction that occurs between two cathepsins within the cathepsin proteolytic network. Currently, there are limited studies investigating the effects of cathepsin inhibition on the cellular regulation of cathepsin amounts. Not only are these findings important for providing more effective treatment options for breast cancer, but this work has broad implications since cathepsins have been implicated in diseases such as HIV, atherosclerosis, and osteoporosis.

CHAPTER 2

Background

2.1 Breast Cancer

In 2012, there was an estimated 14.1 million new cancer cases worldwide and this number is expected to increase to 21.7 million by 2030 [25, 26]. While this disease effects millions of people world-wide, the U.S alone has 1.6 million new cases expected in 2016. While progress in treatments and diagnosis has risen the five-year relative survival rate up at least 20% since 1977, in 2016, an estimated 595,690 deaths will occur due to the disease. In the U.S., cancer is the 2nd leading cause of death, and in 2011 the medical costs had reached up to $88.7 billion [1, 27].

In women, breast cancer is one of the most common cancers diagnosed in women with one in eight women being diagnosed in their lifetime. An estimated 29% of new cancer cases diagnosed in women will be breast cancer [28, 29]. Breast cancer can be grouped into two main categories: carcinomas and sarcomas. Sarcomas arise due to transformations that occur in the cells that make up the connective tissue including adipocytes, myofibroblasts, fibroblasts or other cell types located in soft tissue. This is in contrast to carcinomas, of which make up a majority of breast cancers, which occur due to transformation of epithelial cells that serve as lining of the lobules within the breast tissue.

Currently, the TNM system is used to classify a patient's tumor stage. With this system, the extent of primary tumor growth, spread to any lymph node, and the establishment of distant metastasis to other organs is used as markers for classification. There are four stages of cancer along with stage 0, which is known as *in situ* and is often

considered to be non-invasive or pre-cancerous. In Stage I and stage II the tumor cells have only invaded the local surrounding tissue and the survival rate is 99%. By stage III, which has regional invasion, the survival rate is lowered to 85%. Once the classification reaches stage IV, the cancer cell invasion is distant and usually metastatic. The survival rate at stage IV drops dramatically to only 26%. This dismal survival rate has led 36% of women with stage I or II to undergo double mastectomy surgery, an invasive surgery in which both breasts are removed and is often used as a preventative measure [28, 30].

Breast cancers can be further classified based on the presence of different hormone or growth factor receptors. Estrogen and progesterone are major sex hormones that bind to nuclear receptors in target tissues and act as transcription factors [31-33]. Estrogen receptor (ER)- or progesterone receptor (PR)-positive tumors accounted for 84% of diagnosed breast cancer in 2012 [28]. Human epidermal growth factor receptor (HER) is a family of receptor tyrosine kinases which bind to members of the epidermal growth factor family such as epidermal growth factor (EGF). Overexpression of HER2 increases cell proliferation due to the sensitivity toward growth factors such as EGF that promote proliferation [34-36], and approximately 14% of breast cancers cases in 2012 were HER2-positive [28]. Tumors classified as triple negative are characterized as being negative for ER, PR, and HER2. Triple-negative breast cancers tend to be more aggressive [37], occur in younger women along with non-Hispanic black or Hispanic women, and have a lower 5 year survival rate compared to other types of breast cancers [38].

Mutations in the BRCA1 and BRCA2 genes have also been associated with increased risk of breast cancer [39-41]. The relative risk of breast cancer incidence for BRCA1

mutation carriers peaks at 33% for the age range 30-39 years. The peak for BRCA2 mutation carriers occurs in the 20-29 year old age group with a 19% relative risk [42]. Thus, genetic testing for BRCA1 and BRCA2 gene mutations has been used to guide decisions on interventions such as preventative surgery [43, 44].

2.2 Cathepsins in Breast Cancer

Human epithelial breast cancer cells have been reported to acidify the extracellular milieu [45], which provides an optimal environment for cathepsin activity in the pericellular environment since the optimal pH for most cathepsin activity ranges from five to six [46-48]. During cancer progression, transformed cancer cells reduce cell-cell and cell-matrix attachments and elevate protease expression and activity [49-55]. The loss of adhesion and increased proteolysis is thought to promote cancer cell invasion and metastasis [56] especially for breast carcinoma cells which tend to migrate in chains and clusters [57, 58]. Zhang et al indirectly demonstrated cathepsins' involvement in tumor growth by orthotopically injecting breast cancer cells overexpressing cystatin M, one of the cathepsin protein inhibitors from the cystatin family, into mice. Cystatin M overexpression reduced primary tumor volume and the number of metastasized cells. The involvement of cathepsins in tumor growth and metastasis is important to understand especially since minimal cystatin M protein expression was reported in the invasive ductal carcinoma human breast tissue compared to normal human breast tissue [10]. Other studies also showed cystatin C overexpression reduced human fibrosarcoma lung metastasis and cystatin A overexpressing esophageal squamous carcinoma cells reduced tumor weight, growth, and lung metastasis [7, 11]. Tumor-associated cells that are recruited to the tumor site also have increased protease expression and activity

contributing to the overabundant amount of cathepsins compared to cystatins in cancer [5, 59, 60]. While pharmaceutical companies have focused on developing cathepsins K inhibitors for bone related diseases in which it is involved such as osteoporosis, these inhibitors are now being used in trials for the treatment of bone metastasis [13, 15-17].

Recently, more evidence suggests that some proteases can have tumor-promoting or tumor-suppressing roles depending on the cell type the protease is expressed in, and thus, broad spectrum inhibitors might reduce cathepsin activity from tumor-suppressing proteases [61]. It has also been reported that the expression profiles of active cathepsins varies in breast cancer tissue. While the amount of cathepsin K and L was upregulated in breast cancer tissue and peaked at stage II, active cathepsin S amounts remained comparable to that detected in the normal tissue regardless of cancer stage [9]. In addition, Kopitz et al showed that cathepsin B expression correlated with lung metastasis, while cathepsin L expression did not [7]. All of this highlights the differential regulation of each cathepsin, and the need to understand how the amount of each cathepsin might change during the various cancer stages.

2.3 Current Cancer Therapies and Cathepsin Inhibitors

The type of breast cancer treatment option selected after diagnosis depends on the tumor extent and cancer stage. Lumpectomy or mastectomy surgical procedures are used for local treatment and include excision of the tumor or breast tissue, respectively [62]. Lumpectomy treatment, also known as breast-conserving surgery, has similar rates of recurrences and deaths compared to radical mastectomy [63]. Depending on the extent of invasion, axillary lymph node dissection may also be conducted. Prophylactic and bilateral mastectomy are other intervention methods, and the rates of these treatment

options have increased since 1998 [64, 65]. Although, more studies have to be conducted to determine the long-term benefits of prophylactic and bilateral mastectomy treatments [65-67]. These surgical procedures can be followed with whole-breast or accelerated partial breast irradiation radiation therapy to reduce the risk of recurrence [68-70]. Neoadjuvant or adjuvant chemotherapy regimens can also be used with lumpectomy or mastectomy. Neoadjuvant chemotherapy which is administered before surgery, has been shown to be associated with a 16.6% decrease in mastectomy rate, when compared to adjuvant chemotherapy, which is administered post-surgery [71]. To provide the most effective treatments, combination therapies are usually used. A clinical trial in patients with HER2-overexpressing tumors demonstrated that chemotherapy plus trastuzumab, an antibody based competitive antagonist of the HER2 receptor, and lapatinib, a small molecule inhibitor of the HER2 receptor, had a 51.3% rate of pathological complete response (pCR), which is associated with good prognosis. Chemotherapy plus either lapatinib or trastuzumab had lower pCR rates: 29.5% with trastuzumab; and 24.7% with lapatinib [71]. Although effective, these systemic treatments often have severe adverse side effects associated with them that can lower the quality of life.

There are no current cancer therapies utilizing cathepsin inhibitors, but clinical trials of cathepsin inhibitors have been conducted. Odanacatib is a selective cathepsin K inhibitor and is currently in phase III. This drug has been seen to increase bone mineral density and reduce the amount of bone fractures in subjects and could be used for metastatic bone treatment. Though the phase III clinical trial was terminated early due to an external data monitoring committee recommendation after 158 out of 16,071 participants had an osteoporotic hip fracture incident, it was indicated that the subjects

who were administered Odanacatib had better benefit/risk profiles compared to the placebo group [15-17].

2.4 Properties of Cysteine Cathepsins

Cathepsins K, L, S, and V are members of the lysosomal cysteine cathepsin family belonging to the papain family of peptidases and share 60% sequence homology [4, 72]. Their overexpression in disease states has resulted in implications in a number of pathological roles.

Human macrophages use cathepsin S for major histocompatibility complex (MHC) and antigen processing, but in disease, it is involved in atherosclerosis [2, 73-75], emphysema [75], abdominal aortic aneurysms [75-77], arthritis [78], and other diseases associated with elastinolytic remodeling [79]. Even though cathepsins normally have optimal activity at acidic pH, cathepsin S is capable of maintaining its potent elastase activity even at neutral pH [75, 80].

Similar to cathepsin S, cathepsin K also has strong elastase activity, which diminishes at neutral pH [75].

Additionally, cathepsin K is the most potent mammalian collagenase and is critical in bone resorption [81]. It was shown to cleave collagen from cortical bone more effectively than that of MMP-9, -1, and -13 due to the additional intrahelical and telopeptide cleavage while other mammalian collagenases can only cleave at one site or the other [81]. Cathepsin K is also upregulated in breast and prostate cancer [82, 83]and is involved in cardiovascular disease, osteoporosis, and arthritis [3, 73, 84, 85].

Cathepsin V is overexpressed in colon and breast carcinomas [82, 86], although it was first identified in the human thymus, testis, and macrophages[87]. With elastolytic

activity higher than cathepsins K and S, and pancreatic and leukocyte elastases by two to eight fold, cathepsin V is the most potent mammalian elastase. Human cathepsin V has an 80% homologous sequence with human cathepsin L [4, 88], and human cathepsin V, and not human cathepsin L was shown to be orthologous to mouse cathepsin L [89, 90].

Detection and distinction of individual active cathepsin by current and traditional methods has been difficult due to sequence homology of the cathepsins, instability of the mature form at neutral pH, and substrate promiscuity. Fluorogenic substrates and active site labeling probes have been developed and have improved sensitivity [91-94], but structural similarities between family members still impede desired specificity when used with cells.

2.5 Cellular Activation and Trafficking of Cathepsins

Initially, cathepsins were identified in lysosomes in which lysosomal cargo is degraded. It was originally thought that this was the only subcellular location in which cathepsins were located [75, 95]. Now it is known that cathepsins are also secreted by cells such as osteoclasts, macrophages, and tumor cells [96-99].

Cathepsins have also been implicated in apoptotic pathways due to their release into the cytoplasmic space [100-102]. Due to the numerous locations of cathepsins, cathepsins are tightly regulated using pro-peptides, endogenous inhibitors, pH, and glycosylation to prevent off-target cleavage of proteins [3, 12, 80, 103]. Cathepsins are synthesized as zymogens that are inactive due to a pro-peptide piece that has to be proteolytically cleaved in order to become active [80, 103, 104]. This activation can occur due to autoactivation or activation within a family. Cystatins, the endogenous cathepsin inhibitors, bind to the active site of the cathepsins blocking the active site and acting as a

competitor for other substrates. The type 1 cystatins, also known as stefins, inhibit cytosolic cathepsins, while the type 2 cystatins are secreted and inhibit secreted cathepsins [12, 105, 106].

Inactive cathepsins were thought to be trafficked in secretory vesicles while active cathepsins are trafficked in endo-lysosomal vesicles, both of which can be targeted for secretion [107]. Albeit, an active form of cathepsin L was recently reported to be secreted via secretory vesicles not associated with lysosomal exocytosis pathways [98]. Cathepsins are also trafficked to other subcellular locations including the cytosol and the nucleus, which contains truncated forms of cathepsin L [108, 109]. When in the nucleus, cathepsin L is suggested to cleave the CCAAT-displacement protein/cut homeobox transcription factor [108]. The targeting of these cysteine proteases to specific locations is dependent on glycosylation in the Golgi apparatus regulates [110]. Overexpression of cathepsins overloads the Golgi and lysosomal targeting pathway, leading to improper glycosylation and subsequent mis-targeting of the enzymes, such that they are secreted instead of being sorted to lysosomes to other cellular compartments [107, 111, 112], which occurs during pathological overexpression of cathepsins.

2.6 Proteolytic Networks and Compensatory Mechanisms

Others have shown compensatory mechanisms within the cathepsin proteolytic network. A recent report showed that deletion of multiple cathepsins, in this case cathepsins S and B, causes an upregulation of cathepsin Z in a tumor mice model [113]. Murine cathepsin L mRNA was upregulated in a cathepsin K knockout mouse model; active cathepsin X elevation was detected in a cathepsin B knockout mouse model; increases in cathepsin D, Z, and B proteins occurred in a murine cathepsin L knockout mouse; and elevated

cathepsin Z protein was observed in a cathepsin B knockout mouse model [60, 114, 115]. Even though human cathepsin V, not human cathepsin L, is orthologous to mouse cathepsin L, human cathepsin V has an 80% homologous sequence with human cathepsin L. All of these reports of compensatory feedback responses in knockout mouse models highlights the harm in studying one protease without consideration of the entire proteolytic complex and points to a need to understand the effects of cathepsin downregulation or inhibition.

CHAPTER 3

Manipulating substrate and pH in zymography protocols selectively distinguishes cathepsins K, L, S, and V activity in cells and tissues[1]

3.1 Introduction

Proper measurement of changes in levels of cathepsin activity in disease states would be beneficial to understand the roles of cathepsins and to develop therapies. The sequence homology of cathepsins K, L, S, and V, instability of the mature form at neutral pH, and substrate promiscuity all confuse detection and distinction of individual cathepsin activities by current and traditional methods. Fluorogenic substrates and active site labeling probes have been used to advantage and improved sensitivity [91-94], but structural similarities between family members still impede desired specificity when used with cells or mixtures of different cathepsin family members.

Most of these cathepsins have been defined with cell- or tissue-specific expression under normal physiology [72, 75, 90, 116-118], but in disease states are turned on by a number of other cell types. In doing so, post-translational processing is altered. Glycosylation that normally occurs to target cathepsins for sorting to lysosomes [111], propeptide cleavage to activate the enzymes [119, 120], and other changes affect enzyme structure and ultimately their electrophoretic migration distance in a non-reduced preparation which relies solely on SDS to add negative charge and partially denature the

---

1Used with permission from: Wilder CL, Park KY, Keegan PM, Platt MO. (2011). Manipulating substrate and pH in zymography protocols selectively distinguishes cathepsins K, L, S, and V activity in cells and tissues. Arch Biochem Biophys. Dec 1;516(1):52-7. doi: 10.1016/j.abb.2011.09.009.

protein. Additionally, cathepsins have disulfide bonds that may differ between family members [3, 121].

Among the four, they share 60% sequence homology [75, 89, 90] but each has unique properties and different homeostatic functions. Cathepsin S is a potent elastase notable for its activity at neutral pH [75]. Cathepsin K serves a critical role in bone resorption and is the most potent mammalian collagenase described [81]. Cathepsin V was first identified in the human thymus, testis, and macrophages[87] and has been identified recently as the most potent mammalian elastase with elastolytic activity higher than cathepsins K and S.

Here a method of zymography, or substrate gel electrophoresis, to detect the activity of cathepsins K, L, S, and V from one cell extract/preparation is detailed. Zymography is a method whereby a substrate is polymerized into a polyacrylamide gel such that, upon activation, the enzymes hydrolyze the embedded substrate in situ, and proteolytic activity can be visualized as cleared bands on a Coomassie stained background. This technique has many benefits: 1) it does not require antibodies making it relatively inexpensive and species-independent, 2) separation of proteins by molecular mass and non-reducing electrophoretic migration visually confirm enzyme identity, 3) densitometry can be used for quantitative analysis, and 4) pH change can confirm specific cathepsin activity. Cathepsin L zymography protocols have been described [99, 122, 123], and in a recent study, we reported that cathepsin K activity is detectable at femtomole quantities through gelatin zymography [124]. This study is the first report of a zymography protocol for cathepsin S and cathepsin V, and slight modifications that allow for specific determination and quantification of cathepsins K, S, L, and V in cell and tissue extracts is

further described. Then this method is applied to monocyte derived macrophages and osteoclasts, endothelial cells exposed to the inflammatory cytokine TNFα, and normal and cancerous human lung tissue to demonstrate its utility in detecting cathepsins in health and disease states.

3.2 Materials and Methods

3.2.1 Materials

Recombinant human cathepsin K isolated from insect cells (Enzo); recombinant human cathepsin K from *E. coli* (EMD Bioscience); human cathepsin L isolated from human liver (Enzo); recombinant human cathepsin S from *E. coli* (EMD Biosciences); recombinant human cathepsin S from insect cells (Enzo); recombinant human cathepsin V from NSO cells (Enzo); Cathepsin V with mutated glycosylation site was expressed in *P. pastoris* and was a kind gift from Dieter Brömme; E-64 protease inhibitor (EMD Biosciences); Murine macrophage RAW 264.7 cell line (ATCC); Human breast and lung tissue lysates (Protein Biotechnologies). Tumor necrosis factor alpha (TNFα; Invitrogen), Macrophage colony stimulating factor (M-CSF; Peprotech), and receptor activator of nuclear factor kappa B ligand (RANKL).

3.2.2 Cell Culture

Murine macrophage RAW 264.7 cells were cultured in Dulbecco's Modified Eagle Medium (Lonza) containing 10% fetal bovine serum (FBS), 1% L-glutamine, and 1% penicillin/streptomycin. Human aortic endothelial cells (ECs) (Lonza) were cultured in MCDB medium 131 (Mediatech) containing 10% fetal bovine serum (FBS), 1% L-

glutamine, 1% penicillin/streptomycin, and 1% endothelial cell growth serum (ECGS). ECs were stimulated with or without 10 ng/mL TNFα (Invitrogen) for twenty hours. Cells were maintained with 5% CO2 at 37˚C.

3.2.3 Primary Monocyte isolation

This study was approved by an institutional review board committee and the subjects gave informed consent. Whole blood samples obtained from consenting donors were centrifuged against a Ficoll-Paque density gradient (density: 1.077g/mL; GE Healthcare) for 30 minutes at 900g to separate the buffy coat layer. After centrifugation, peripheral blood mononuclear cells (PBMCs) were aspirated, washed in PBS, and pelleted by centrifugation for 10 minutes. The isolated cells were then washed with a red blood cell (RBC) lysis buffer (0.83% ammonium chloride, 0.1% potassium bicarbonate, and 0.0037% EDTA) for seven minutes to remove any contaminating RBCs. The PBMCs were then washed in sterile PBS, and cell number and viability were determined using a Vi-Cell (Beckman Coulter). Monocytes were isolated by adhesion, and then differentiated into either macrophages with 30ng/µl M-CSF in RPMI or osteoclasts using 30 ng/µl M-CSF and 30 ng/µl RANKL in alpha-MEM for 14 days. Lysates were collected and equal amounts of protein were loaded for cathepsin zymography.

3.2.4 Cathepsin zymography

This protocol is based on our previously published protocol [124]. All recombinant cathepsins are from human sequences. Procathepsins K and V from NSO cells (Enzo) were activated using 100 mM sodium acetate buffer, pH 3.9, 10 mM DTT, and 5 mM EDTA for 40 minutes at room temperature. All others were purchased in mature forms.

Cells and tissue were extracted in lysis buffer (20 nM Tris-HCl at pH 7.5, 5 mM EGTA, 150 mM NaCl, 20 mM β-glycerol-phosphate, 10 mM NaF, 1 mM sodium orthovanadate, 1% Triton X-100, 0.1% Tween-20) with 0.1 mM leupeptin freshly added to stabilize enzymes during electrophoresis and lysates were collected and cleared by centrifugation. Protein concentration was determined by micro BCA assay (Pierce). 5X non-reducing loading buffer (0.05% bromophenol blue, 10% SDS, 1.5M Tris, 50% glycerol) was added to all samples prior to loading. Equal amounts of cell or tissue protein were resolved by 12.5% SDS-polyacrylamide gels containing 0.2% gelatin at 4°C. Gels were removed and enzymes renatured in 65 mM Tris buffer, pH 7.4 with 20% glycerol for 3 washes, 10 minutes each. Gels were then incubated in activity buffer (0.1 M sodium phosphate buffer, pH 6.0, 1 mM EDTA, and 2 mM DTT freshly added) for 30 minutes at room temperature. For different pH conditions, 0.1 M sodium acetate buffers of pH 4, and sodium phosphate buffers of pH 6, 7, and 8 were used. Then this activity buffer was exchanged for fresh activity buffer of the same pH and incubated for 18-24 hours (overnight) incubation at 37˚C. The gels were rinsed once with deionized water and incubated for one hour in Coomassie stain (10% acetic acid, 25% isopropanol, 4.5% Coomassie Blue) followed by destaining (10% isopropanol and 10% acetic acid). Gels were imaged using an ImageQuant LAS 4000. For elastin zymography, 0.2% soluble elastin (Elastin products) was polymerized in the polyacrylamide gels in place of gelatin substrate.

3.2.5 Western blots

SDS-PAGE was performed as described above without a gelatin or elastin substrate polymerized. Protein was transferred to a nitrocellulose membrane (Bio-Rad) and probed with monoclonal anti-human cathepsin K clone 182-12G5 (Millipore), anti-human cathepsin S and V antibodies (R&D Biosystems), or anti-mouse cathepsin L antibody (R&D Biosystems). Secondary donkey anti-mouse or anti-goat antibodies tagged with an infrared fluorophore (Rockland) were used to image protein with a Li-Cor Odyssey scanner.

3.3 Results

3.3.1 Mature cathepsins K, L, S, and V activities can be detected by gelatin zymography

Recombinant cathepsins K and S from *E. coli,* cathepsin V with mutated glycosylation sites purified from *P. pastoris*, and cathepsin L isolated from human liver were loaded for zymography. Cathepsins K, S, and V are the nonglycosylated forms of the enzymes and cathepsin L contains both forms. All were active in the cathepsin zymography with bands at ~29 kDa for cathepsin K, ~21 kDa for cathepsin L, ~25 kDa for cathepsin S, and ~23 kDa for cathepsin V (Figure 1A). To confirm the identity of the cathepsin bands, aliquots were loaded for Western blot, probed with their respective anti-cathepsin antibodies (Fig 3.1C). Cathepsins L and V had multiple immunodetectable bands, but only one band was zymographically active under these conditions (open arrows).

To determine if glycosylation affects electrophoretic migration, recombinant cathepsins K, S, L, and V from eukaryotic expression systems were loaded for cathepsin

zymography and a representative zymogram is shown in figure 3.1B. Cathepsin S maintained similar electrophoretic migration distances as that seen in Fig 1A, but cathepsin K migration distance shifted from ~27 kDa to ~50 kDa, and cathepsin V shifted from ~23 kDa to ~37 kDa (Fig 3.1B). All four glycosylated enzymes were loaded into the same well and similar migration distances were seen indicating that interaction between cathepsins in solution, as would occur in cellular extracts, does not alter their individual migration. Again, Western blotting confirmed the identity of the zymographically active bands and the shifts in electrophoretic migration distances (Fig 3.1C). The open arrow indicates the zymographically active band of cathepsin V and cathepsin L on each respective blot. For all subsequent experiments, cathepsins from eukaryotic expression systems were used.

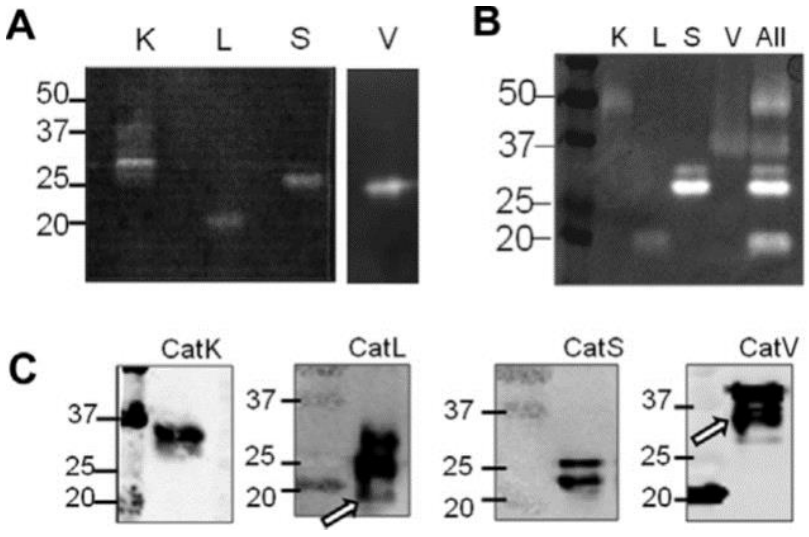

Figure 3.1. Mature cathepsins K, L, S, and V activities can be detected by gelatin zymography. A) Recombinant cathepsins K, S, and V (1, 20, and 50 ng) from E. coli and cathepsin L (50 ng) isolated from human liver were loaded for cathepsin gelatin zymography and incubated overnight in acetate buffer, pH 6. The zymogram reveals zymographically active bands at different electrophoretic migration distances. **B)** Mature,

recombinant cathepsins K, S, and V (10 ng) from eukaryotic expression systems and cathepsin L (50 ng) isolated from human liver were loaded separately and all in one lane (where indicated) for gelatin zymography assayed at pH 6. **C)** Western blot analysis of 50 ng of recombinant glycosylated cathepsin K, L, S, and V from eukaryotic expression systems also were loaded for non-reduced Western blotting.

To test this assay on cellular extracts, we isolated monocytes from peripheral blood mononuclear cells (PBMCs) and differentiated them into macrophages and osteoclasts, two cell types that produce cathepsins, and osteoclasts specifically produce large amounts of cathepsin K under normal conditions [97, 116, 125]. Monocyte derived macrophages and osteoclasts were lysed and duplicates of 5 µg of protein from each were loaded for gelatin zymography. 37 kDa, 25 kDa, and 20 kDa bands were visible in both macrophages and osteoclasts, with the 25 and 20 kDa bands being consistent with cathepsins S and L, from the isolated enzyme studies, respectively (Fig 3.2A). The 35 kDa band was assumed to be cathepsin V to be consistent with Fig 1B, but this band was brighter in osteoclasts and another band appeared just above it, around 37 kDa in the osteoclast lysates.

It is known that osteoclasts express cathepsin K specifically for bone resorption which supported the hypothesis that the upper band was osteoclast expression of cathepsin K. This was a different electrophoretic migration distance than that of the recombinant enzymes. To confirm this band was indeed cathepsin K, lysates from the monocyte derived macrophages and monocyte derived osteoclasts were loaded for reduced, denatured Western blotting, by adding β-mercaptoethanol to break disulfide bonds and boiling to fully denature and linearize the proteins. This differs from the zymography preparation, which maintains the disulfide bonds for proper refolding and renaturation, but does not fully linearize the peptide strand possibly resulting with a

larger hydrodynamic radius which can affect their migration through the polyacrylamide gel during electrophoresis. Reducing Western blots probed with antibodies against human cathepsin K or V verified the identity of the increased cathepsin K in the osteoclasts by the visible detection of the pro- and mature forms of cathepsin K only in the osteoclast lysates where the upper 37 kDa band appeared. Both macrophages and osteoclasts had detectable levels of pro- and mature cathepsin V by Western blot, but a greater amount was present in osteoclasts, consistent with the brighter 37 kDa band in the zymography (Fig 3.2B).

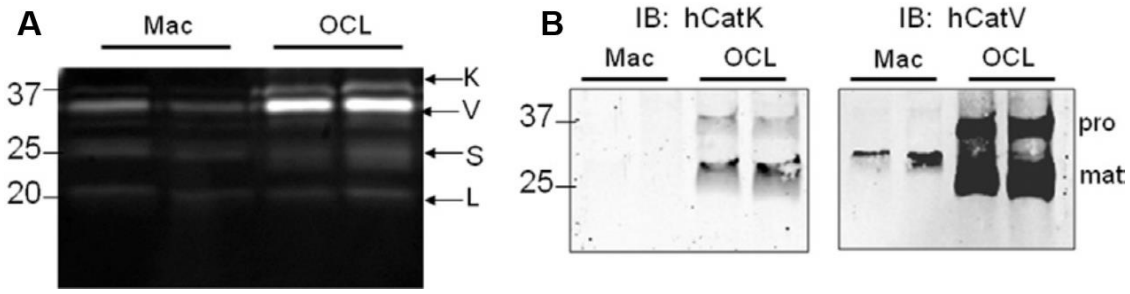

Figure 3.2. Mature cathepsins K, L, S, and V are zymographically active and migrate at distinct electrophoretic distances A) Monocyte-derived macrophages and monocyte-derived osteoclasts were lysed and equal amounts of protein were loaded for cathepsin zymography and **B)** reduced, fully denaturing Western blotting for cathepsins K and V. Procathepsin (pro) bands are at ~37 kDa and mature (mat) cathepsin bands are at ~27 kDa. Increased cathepsins K and V were detected in the osteoclasts compared to the macrophages.

3.3.2 Cathepsin selectivity through pH and substrate modifications.

Given the unexpected location of the cathepsin K band in monocyte derived osteoclasts and its close proximity to a brighter cathepsin V band, we wanted to modify the technique to uniquely distinguish each cathepsin. This would be useful for investigating new cell types or new disease conditions that might alter cathepsin activation or glycosylation. A new approach had to be employed to take advantage of unique cathepsin properties to enable selective distinction among cathepsins migrating at similar distances during the electrophoresis. A number of studies have indicated different substrate and pH-specific changes in proteolytic activity for different cathepsin family members [126, 127] leading us to test the hypothesis that selectivity for cathepsin K, L, S, or V could be obtained by varying pH and substrate. Ten ng of cathepsins K, S, and V and 50 ng of cathepsin L were loaded for gelatin zymography, and 50 ng of each cathepsin were loaded for elastin zymography. These numbers were based on preliminary experiments to obtain visible bands. Gels were incubated in assay buffer at pH 6, 7, or 8 overnight prior to staining with Coomassie blue and visualization of cleared bands of proteolytic activity. Results are shown in figure 3.3.

Cathepsin K maintained activity on gelatin at pH 7 and 8, which contrasted significantly with cathepsins L and V activity (Fig 3.1B and 3.3A) which were not seen at pH 7 or 8 on gelatin. Distinct bands for cathepsin K and S were at different electrophoretic distances and therefore, distinguishable from each other. Thus, a gelatin zymography at pH 7 would select for cathepsin K over V. Cathepsin S activity was stable under all pH conditions tested on both gelatin and elastin. With elastin zymography, cathepsins K and V activities were much weaker than that of cathepsin S (Figure 3.3B) with a drastic reduction in their cleared band signals as pH increased such that at pH 7,

cathepsins K and V retained little to no activity, and the assay conditions selected for cathepsin S (Fig 3.3B).

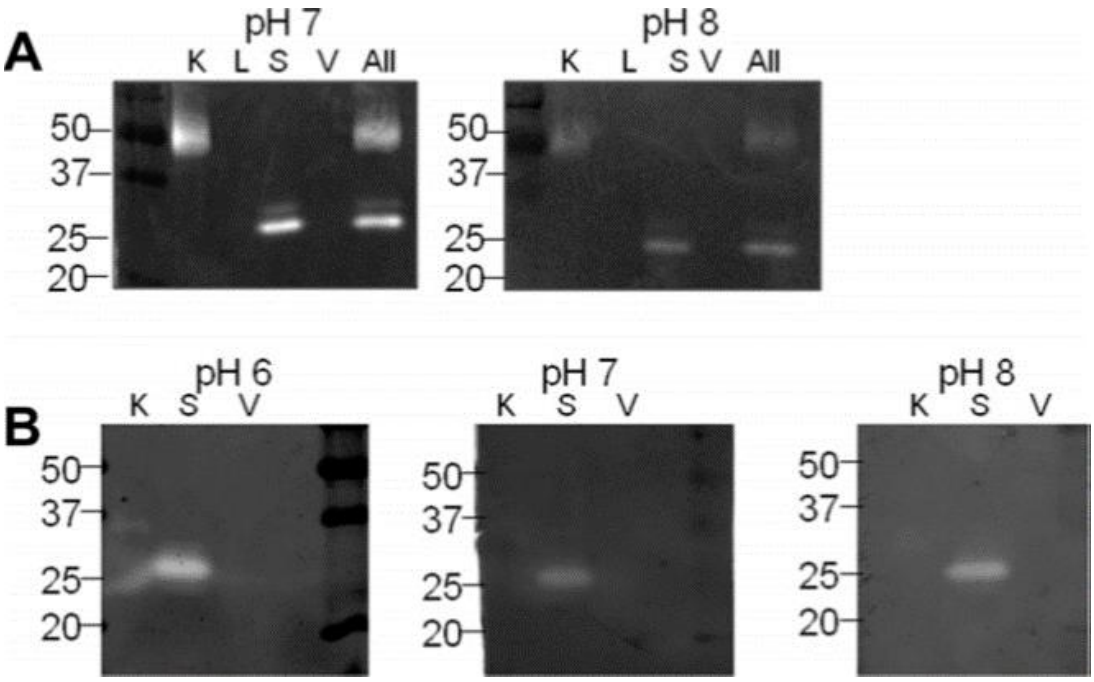

Figure 3.3. Cathepsin zymography selectivity can be obtained through pH and substrate modifications. A) Recombinant, glycosylated human cathepsins K, S, and V (10 ng) and cathepsin L (50 ng) were loaded separately and all in one lane for cathepsin zymography. The samples were incubated overnight in assay buffer, pH 7 or 8 prior to Coomassie staining. **B)** 50 ng of human recombinant cathepsins K, S, and V were loaded for elastin zymography and incubated in pH 6, 7, or 8 assay buffers overnight. There was less cathepsin L and V signal at pH 7 and 8 and only cathepsin S maintained its activity in elastin zymography.

3.3.3 Selectivity for cathepsin V occurs at pH 4 after loss of cathepsin K band of activity.

Unique conditions for cathepsin S had been determined, and cathepsin K had detectable proteolytic activity on gelatin at pH 7 where cathepsins L and V activity was attenuated

(Figure 3.3A), but conditions selective for cathepsin V had not yet been determined. An initial screen of RAW macrophage lysate displayed a strong band of activity at pH 4 that was neither cathepsin K nor S (data not shown), that we hypothesized was due to cathepsin V-like enzyme activity in macrophages. To test this, we loaded a gelatin zymogram with 10 ng of mature cathepsin K, S, and V, and 50 ng of cathepsin L, then incubated it in assay buffer, pH 4 (Figure 3.4A). Cathepsin V band was detectable at ~37 kDa but the cathepsin K band was no longer active. Interestingly, multiple active bands of cathepsin L became visible at ~35 kDa, ~25 kDa, and ~20 kDa after incubation at pH 4, different from just the 20 kDa band detected at pH 6 (Fig 3.1). Next, 5 µg of macrophage lysate and 50 ng recombinant cathepsin V were loaded for zymography and incubated in assay buffer, pH 6 and pH 4, prior to staining to confirm this band in RAW macrophages. Cathepsin V activity appeared at same distance as the cleared band of question in macrophage lysate (Figure 3.4B).

Raw 264.7 cells are a mouse macrophage cell line, and murine cathepsin L is the homolog to human cathepsin V [128]. To confirm the identity of this band as murine cathepsin L, Western blotting was performed with 50 µg of macrophage lysate and probed with either an anti- human cathepsin V antibody or an anti-mouse cathepsin L antibody; mature, recombinant human cathepsin V was loaded as a positive control. Human cathepsin V and the immunodetected band in the macrophage lysate migrated similarly to ~37 kDa (Figure 3.4C) corroborating the active band in macrophages was homologous to cathepsin V. The blot probed with anti-mouse cathepsin L detected the proform and the mature forms of mouse cathepsin L in the RAW264.7 macrophages.

Specificity of mouse cathepsin L antibody is shown by its inability to detect recombinant cathepsin V (Fig 3.4C).

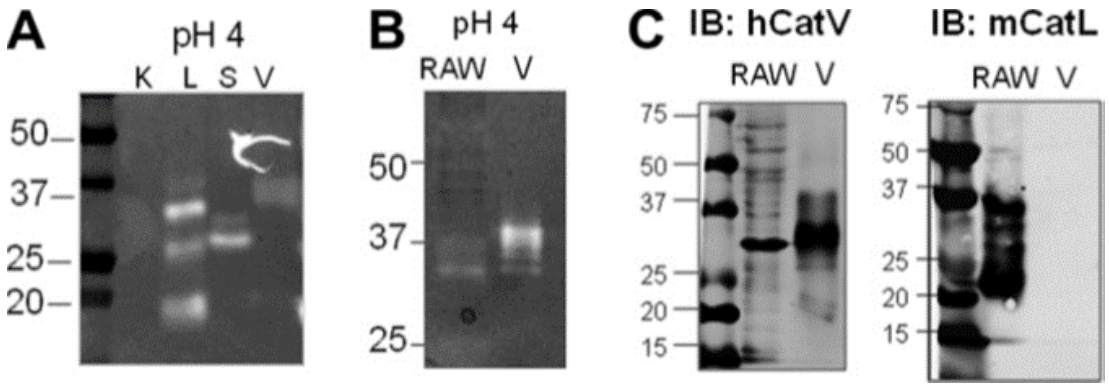

Figure 3.4. Zymography selectivity for cathepsin V occurs at pH 4. A) 10 ng of recombinant human cathepsins K, S, and V and 50 ng cathepsin L isolated from human liver were loaded for gelatin zymography and incubated overnight in assay buffer, pH 4. **B)** Gelatin zymography performed with 5 µg of macrophage extract and 50 ng of recombinant cathepsin V were assayed at pH 4. The active bands at pH 4 in the RAW macrophage extract have similar electrophoretic distance as that of mature, human cathepsin V. **C)** Western blot using anti-human cathepsin V antibodies and anti-mouse cathepsin L antibodies were used on 50 µg RAW 264.7 lysate and 50 ng of recombinant cathepsin V to confirm presence of each in the cell lysates.

3.3.4 Selective zymography at pH 4 distinguishes the activity of cathepsin K from V in human cells and tissue from healthy and diseased conditions.

Our next goal was to apply this technology to natural changes in cells under healthy and diseased states and proper distinction of cathepsin K from V. Endothelial cells express cathepsin K at extremely low basal levels, but increase its expression under disturbed flow, inflammatory conditions, and atherosclerosis [84, 85]. Human aortic endothelial cells (ECs) were grown to confluence and treated with or without 10 ng/mL tumor

necrosis factor alpha (TNFα) for 20 hours, after which lysates were collected for gelatin zymography. Stimulation of ECs with TNFα induced the 37 kDa cathepsin K band with detectable bands of cathepsins V and L for gelatin zymography at pH 6 (Fig 3.5A). To select for cathepsin V, zymograms were incubated at pH 4, which diminished the 37 kDa band, but maintained detectable cathepsin V and cathepsin L bands of activity (Fig 3.5B). Other ECs were transfected with CMVSport6 plasmid containing cathepsin K under the CMV promoter to drive constitutive overexpression and specifically corroborate the identity of the cathepsin K band. Lysates were collected 24 and 48 hours after transfection, and equal protein amounts were loaded for zymography. In these cells, the 37 kDa band appeared, but did not in the control cells, corroborating its identity as cathepsin K.

To test the selective cathepsin V zymography on tissue, human lung tissue from normal and tumor specimens of different cancer stages (indicated by Roman numerals) were obtained and loaded for cathepsin gelatin zymography. Tumor specimens (II – IV) had greater cathepsin activity than the normal specimens and bands appeared at 37, 35, 25, and 21 kDa. To confirm the top band was cathepsin K and the 35 kDa band was cathepsin V, aliquots of the specimens were loaded for selective zymography, incubated at pH 4. No detectable active cathepsin bands in the presence of E-64 indicated that bands are products of active cysteine proteases (data not shown). The 35 kDa band of interest remained in the lung specimens above the intensity of the other cathepsin signals confirming it as cathepsin V (Figure 3.5D), cathepsin K (37 kDa) and S (25 kDa) bands were diminished, but lower molecular weight bands remained at the cathepsin L electrophoretic migration distance (~21 kDa).

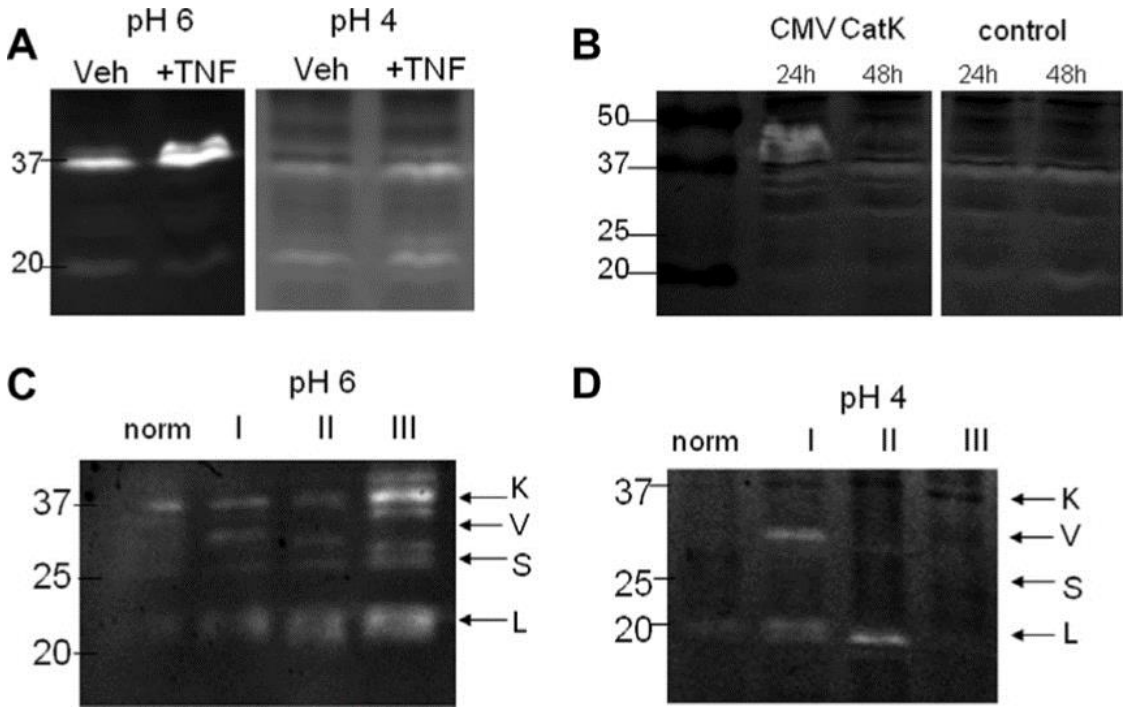

Figure 3.5. Selective zymography at pH 4 distinguishes the activity of cathepsin K from V in human cells and tissue from healthy and diseased conditions. **A)** ECs were cultured in the presence or absence of 10ng/mL TNFα for 24 hours prior to lysis and loading for cathepsin zymography. Gels were incubated at pH 6 or pH 4 to select for cathepsin V over cathepsin K. Representative zymogram is shown. **B)** ECs were transfected with cathepsin K gene on pCMVSport6 and cultured for 24h or 48h to overexpress cathepsin K. Zymogram at pH 6 is shown **C)** Lung tissue specimens from normal and from different stages of cancer progression were homogenized, and 10 µg of soluble total protein were loaded for gelatin zymography and incubated overnight in assay buffer, pH 6 and **D)** pH 4 assay buffers. The bands of cathepsins K and S disappear from the gels leaving only cathepsins V (~33 kDa / 21 kDa) and L (21 kDa) bands.

3.4 Discussion

This study shows that cathepsins K, L, S, and V can all be detected by zymography in one cell lysate or tissue preparation under healthy and diseased states. Cathepsin K, L, S, and V activities were detected and distinguished in human endothelial cells, human monocyte derived macrophages and osteoclasts, murine macrophages, and normal and

cancerous human lung tissue. Employing this assay with monocyte derived macrophages and monocyte derived osteoclasts, we were able to identify increased cathepsin V in osteoclasts compared to macrophages, and this is the first report to do so. Also, this assay was able to detect cathepsin V activity in human lung cancer in the absence of the pro-forms and other immunolabeled bands. It is not surprising that cathepsins V and L both have activity at pH 4, as they share 80% sequence homology, which may account for their renaturing ability and stability at the lower pH.

The ability to detect specific cathepsin activity in a complex cell or tissue lysate is critical in identifying the regulation of these proteases in healthy and diseased states; overdosing of cathepsin inhibitors due to improper quantification can block homeostatic functions of these enzymes and induce serious side effects [129]. We have also shown how different migration distances must be taken into account when interpreting results obtained from diseased states; although differential glycosylation exist for these enzymes, they seem to be active in zymography as shown with the recombinant cathepsins from prokaryotic and eukaryotic sources. It must also be considered that since the recombinant enzymes are from different sources, there is a possibility of different post-translational modifications. The apparent molecular weight and electrophoretic migration distances of cathepsins are different, partially due to glycosylation and secretion mechanisms. As an example, cathepsin V has been shown to have two putative N-glycosylation sites on the mature enzyme and when these sugars are cleaved the migration of the enzyme is altered by 4-7 kDa [90]. Improper glycosylation mistargets these cathepsins to other cellular compartments or for secretion [107, 111, 112], which occurs during pathological overexpression of cathepsins.

Cathepsin zymography has multiple advantages over other methods. Individual cathepsin activity can be visually confirmed by band location and quantified with densitometry analysis. This is an advantage over fluorescent reporter substrate assays that, when cleaved, release aminomethylcoumarin or other quenched fluorescent motifs. Enzyme concentrations, reporter substrate concentrations, and cross-reactivity with reporter substrates, all add confusion to accurate interpretation of the total fluorescent signal. Serine proteases, matrix metalloproteinases, and other enzyme families also contribute to hydrolysis of these reporter substrates confounding proteolytic readout and attribution of that activity to a particular enzyme.

The zymography method described here overcomes these challenges by a) incubating gels in acidic conditions to drastically reduce activity of MMPs and serine proteases, b) allowing the addition of inhibitors that block enzymatic activity of other proteases, c) selecting for enzymes capable of thermodynamically favorable renaturation after non-reducing, partial denaturation by SDS and d) exploitation of unique enzyme structural properties (size, glycosylation, disulfide bridge number and locations) that impart distinct electrophoretic migration distances that may not be seen in reduced, fully linearized SDS-PAGE and immunoblotting. As an added benefit, this assay does not require antibodies which expands its use to different species as cathepsin structures are fairly well conserved; here we have used mouse and human specimens. This also reduces costs compared to immunobased methods such as ELISA, Western blotting, and immunohistochemistry, and remove concerns of nonspecific antibody binding and pro-cathepsin detection interference.

Limits of detection for each enzyme at each pH and substrate will need to be determined. We have already determined that cathepsin K can be detected as low as 0.1 ng at pH 6 [124] and 0.8 ng at pH 7 (data not shown), but cathepsins L, S, and V limits are higher and required a greater amount of enzyme to elicit a detectable signal after Coomassie staining (Fig 1). Fair comparisons of cathepsin activity of different samples loaded in the same gel can be made, but absolute standards can also be loaded to fit the quantified densitometry signal and calculate an actual value to compare across different gels [124, 130].

3.5 Conclusions

Many types of cancers and tissue destructive diseases are caused by altered cathepsin activity and regulation. Understanding and detecting this cathepsin mediated tissue remodeling is important not only for basic science research, but also for clinical purposes. Broad application of this cathepsin K, L, S, and V multiplex zymography will provide a medium throughput and inexpensive protocol with widespread utility. Tools that add greater selectivity such as the zymography protocols and modifications presented here, that enable proper cathepsin identification, and quantification of those signals will assist appropriate pharmaceutical inhibitor dosing and the determination of pathological functions due to upregulated cathepsins for future investigations and, hopefully, answer previously unsolved questions of proteolytic activity.

CHAPTER 4

Broad spectrum cathepsin inhibitors E-64 and cystatin C differentially regulate cathepsin S and L due to differences in localization

4.1 Introduction

Cathepsin protease inhibitor therapies targeting active cathepsins have been developed, and although these therapies have been efficacious in inhibiting cathepsins and stopping the progression of the disease, only odanacatib, the selective cathepsin K inhibitor, has been found to be efficacious in a phase III trial [13, 15, 17]. Even though some of the cathepsin inhibitors are highly selective for specific isolated recombinant cathepsins, off target effects to other cathepsin species are increased when the inhibitors enter into the intracellular environment [24, 131, 132]. In addition, data recently published demonstrated that treatment with the cathepsin S inhibitor LY3000328 resulted in elevated cathepsin S activity and protein mass in the plasma of healthy subjects after treatment [133]. Both the off target effects and the upregulation of active cathepsins due to cathepsin inhibitors highlight the need to study cellular feedback mechanisms that occur with cysteine cathepsin inhibition in order to assist with proper therapeutic dosing.

Cathepsins play important roles in matrix turnover, mesenchymal stem cell differentiation, and apoptosis [96, 102, 104, 134-137], but have also been shown to assist cancer invasion due to their secretion and degradation of extracellular matrix (ECM) proteins in the surrounding environment [6, 137, 138], and even play roles intracellularly. Beyond just degradation of internalized ECM proteins and fragments [5, 137, 139], there are other intracellular functions. Intracellular cathepsins activate other procathepsins into

the mature, active form by proteolytic cleavage of the pro-peptide [140]. Cathepsins L and S shed surface bound proteins from cancer cells reducing Ras GTPase intracellular signaling in breast cancer cells, pancreatic cancer cells, glioblastoma cells, and melanoma cells [141]. Cathepsin S transcriptionally regulates CCL2, a pro-inflammatory chemokine which promotes metastasis [142], via cleavage of the intracellular domain of the surface membrane protein CD74 [143]. Cathepsins have also been implicated in apoptotic pathways due to their release into the cytoplasmic space [100-102]. Cathepsin S expression is specific to tissue and cell type such as epithelial cells and has been detected in lysosomes and the extracellular environment [107]. This is in contrast to cathepsin L which is ubiquitously expressed in most cells and tissues, and its cellular locations include lysosomes, the extracellular environment, and the nucleus [107]. When in the nucleus, cathepsin L is suggested to cleave the CCAAT-displacement protein/cut homeobox transcription factor [108].

Cystatins are endogenous proteins that inhibit cysteine cathepsins. Cystatins are ubiquitously expressed and secreted by cells, although the small molecule inhibitor of cysteine cathepsins, E-64, is not. E-64 was originally isolated from an *Aspergillus japonicus* culture [144] but can be synthesized. The inhibitor is specific to cysteine proteases and forms an irreversible bond at the active thiol group in the active site of cysteine cathepsins. It does not have selective inhibition between proteases within the cysteine cathepsin family making it a broad spectrum cathepsin inhibitor [106, 145]. This small molecule inhibitor is not used clinically, but is useful in studying cysteine cathepsins in vitro because of its potency and specificity to cysteine cathepsins. While E-64 interacts with the active thiol group forming an irreversible bond, cystatin C inhibits

cysteine cathepsins by physically blocking the three domains of the active site, forming a tight bond similar to an irreversible interaction [12, 106]. Both inhibit the members of cysteine protease family and cannot passively cross the plasma membrane. It has been shown that cystatin C can be endocytosed and accumulates in lysosomes at high concentrations. When intracellular, it reversibly dimerizes when in low pH environments and while in the endoplasmic reticulum [146-148]. The dimerized form of cystatin C is not secreted, but upon endocytosis dimerization occurs [147]. Since cathepsin inhibition cannot occur without binding of the inhibitor to the target protease, the intracellular location of the inhibitors is important when trying to understand how their treatment is affecting specific cysteine proteases. Cystatin B, also known as stefin B, is an endogenous cathepsin protein inhibitor that is distributed throughout the cytoplasm of cells, unlike cystatin C [149]. Cystatin C has lower dissociation constants for cathepsins L and S compared to cathepsin B, making it a more potent inhibitor for the aforementioned proteases [12, 150].

All of this has motivated this investigation of the regulation of cathepsins during broad spectrum cathepsin inhibition. The goal is to understand cellular compensatory mechanisms occurring in triple negative MDA-MB-231 breast cancer cells, which are known to have an aggressive phenotype [151-153], when incubated with broad spectrum cathepsin inhibitors E-64 or cystatin C.

4.2 Materials and Methods

4.2.1 Materials

RFP-labeled and non-labeled MDA-MB-231 breast cancer cells were obtained from Cell Biolabs, Inc. (San Diego, CA, USA) or American Type Culture Collection (ATCC) (Manassas, VA, USA), respectively. Normal breast tissue was provided by our collaborators at the DeKalb Medical Center (Decatur, GA, USA) and purchased from National Disease Research Interchange (NDRI) (Philadelphia, PA, USA). Anti-human cathepsin S, L, and V antibodies (R&D Biosystems), anti-actin (Santa Cruz Biotechnology), and secondary donkey anti-mouse or anti-goat antibodies tagged with an infrared fluorophore (Li-Cor) were used to detect protein with a Li-Cor Odyssey scanner.

4.2.2 Cell Culture

RFP tagged MDA-MB-231 breast cancer cells (Cell Biolabs, Inc.) were transfected with one of the plasmids containing full-length expression sequences of either cystatin C, cystatin B, or an empty vector control under control by the CMV promoters (Origene) using Lipofectamine 2000 (Invitrogen). The cells were then cultured in DMEM (Lonza) medium with 10% FBS, 1% L-glutamine, and 1% non-essential amino acids and incubated for 24 hours at 37°C. GFP tagged human THP-1 monocytes (ATCC) were cultured in RPMI with 10% FBS, 1% L-glutamine, 1% penicillin-streptomycin, and 0.05 mM 2-mercaptoethanol. Cells were incubated with either the cysteine cathepsin broad-spectrum small molecule inhibitor E-64 (Calbiochem), the intracellular cysteine cathepsin inhibitor E-64d (Calbiochem), the protein inhibitor of cysteine cathepsins recombinant cystatin C (BBI Solutions), the cathepsin L inhibitor Z-FY-CHO (Calbiochem), or the broad spectrum MMP inhibitor GM6001 (Calbiochem).

4.2.3 Multiplex Cathepsin Zymography

Tissue and cell lysates or conditioned media was collected after a specified incubation duration. Total protein amounts in the cell lysates were determined using the Pierce Micro BCA Protein Assay (Thermo Scientific) and prepared as previously described [124]. The conditioned media was concentrated using VivaSpin 500 concentrators (Sartorius Stedim Biotech GmbH) and the same amount of volume per sample was loaded. The cell lysates and conditioned media were assayed as previously described, but briefly, equal amounts of protein or volume were loaded in gelatin embedded polyacrylamide gels to separate the protein using SDS-PAGE techniques [154]. The gel was washed in renaturing buffer and assay buffer followed by staining with a Coomassie blue stain and destain. The gel was then imaged using an ImageQuant LAS 4000 (GE Healthcare Life Sciences). The bands were then quantified using ImageJ.

4.2.4 Western Blots

Tissue and cell lysates or conditioned media was collected after a specified incubation duration. Total protein amounts in the cell lysates were determined using the Pierce Micro BCA Protein Assay (Thermo Scientific). The conditioned media was concentrated using VivaSpin 500 concentrators (Sartorius Stedim Biotech GmbH) and the same amount of volume per sample was loaded. The cell lysates and conditioned media were assayed as previously described, but briefly, equal amounts of protein or volume were loaded in gelatin embedded polyacrylamide gels to separate the protein using SDS-PAGE techniques. Protein was transferred to a nitrocellulose membrane (Bio-Rad) and proteins

were then probed with primary antibodies overnight at 4°C followed by an hour secondary antibody incubation.

4.2.5 Immunocytochemistry

Non-tagged MDA-MB-231 breast cancer cells were incubated with or without 50µM of the cathepsin broad-spectrum small molecule inhibitor E-64 (Calbiochem). For the gelatin degradation assay, cells were also incubated with 0.05 mg/ml DQ-gelatin from bovine skin, fluorescein conjugate (Invitrogen) at 37°C for 24 hours. Cells were fixed with 4% paraformaldehyde and permeabilized with 0.1% Triton-X. After which cells were incubated overnight with a primary antibody against cathepsin S, cathepsin L (R&D Systems), cystatin C (Millipore), cystatin B (Santa Cruz Biotechnology), or LAMP1 at 4°C. The cells were then rinsed with PBS and incubated with a secondary antibody (Invitrogen) for an hour at room temperature.

4.2.6 Statistical Analysis

To calculate the weighted colocalization coefficients, the pixels with intensities from both red and green fluorescent channels were summed and divided by the sum of total red pixels. Each pixel having a value equal to its intensity value in order to take into account the brightness of the pixel and ranges from zero to one.

Two tailed student paired T-test with two-sample equal variance was performed on all statistical analysis.

4.3 Results

4.3.1 E-64 increases intracellular active cathepsin S in a dose dependent manner in breast cancer cells

To determine the effects of inhibitor treatment on active cathepsins in breast cancer cells, a range of E-64 up to 50 µM was incubated with MDA-MB-231 breast cancer cells for 24 hours. This inhibitor range was chosen to include high concentrations to ensure internalization of the inhibitor and inhibition cysteine proteases. The cells were then lysed and processed for multiplex cathepsin zymography to detect the amount of active cathepsins and any changes that occur due to E-64. Although the multiplex cathepsin zymography can detect active cathepsins K, S, L, and V (Fig. 3.1 and 3.2), only cathepsins S and L were detected in the MDA-MB-231 lysates (Fig. 4.1A). Incubation with as low as 10 µM caused a significant increase in the amount of active cathepsin S in the cells ($n=4$, $p<0.05$), while the amount of cathepsin L in the cells was significantly decreased with as low as 5 µM E-64 ($n=5$, $p<0.05$) (Fig. 4.1A), as indicated by the cleared white bands in the multiplex cathepsin zymography. Since cathepsin L can also be detected using the more acidic pH4 assay buffer as previously published and demonstrated in the Chapter 3 results of this work [154], cathepsin zymograms using pH4 assay buffers were also ran. Cell lysates were also prepared for Western blots to quantify the total amount of these cathepsins since the zymograms specifically detect the active forms. Western blots indicated that the small molecule did not significantly change the amounts of pro- and mature- cathepsin S present intracellularly at any of the concentrations ($n=6$, $p<0.05$) (Fig. 4.1A). The amount of pro cathepsin L and short chain cathepsin L was increased with 50 µM E-64 ($n=8$, $*p<0.05$) (Fig. 4.1A). To assess if there was any feedback between E-64 and the endogenous cathepsin inhibitors cystatin C

or cystatin B, Western blots were ran and the amount of cystatin C and cystatin B did not significantly change with any of the small molecule concentrations, indicating that there was no feedback between exogenous cathepsin inhibitors and the endogenous cathepsin inhibitor proteins.

Since the amount of active cathepsin S was elevated and cathepsin L reduced with E-64 after 24 hours, the dynamics of cathepsin S and any changes due to the inhibitor was assessed. Fresh media with either 50 μM E-64 or a vehicle control was added to MDA-MB-231 breast cancer cells and incubated for 0, 2, 4, 8, 12, or 24 hours. At each time point, lysates were collected and equal amounts of protein were loaded for multiplex cathepsin zymography. Without the inhibitor, the amount of cathepsins S and L did not change over time. E-64 incubation stimulated a 94.2% fold increase in the amount of active cathepsin S by as early as 8 hours and a maximum of 160.7% fold by 24 hours compared to 0 hours and 0 μM control (n=5, ** $p < 0.01$)(Fig 1C). Conversely, cathepsin L over the same eight and 24 hour period when treated with 50 μM E-64 led to a 56.5% fold reduction and 77.4% fold reduction, respectively (n=3, ** $p < 0.01$) (Fig 4.1B). The amount of active cathepsin S was quantified using ImageJ (Fig 4.1C).

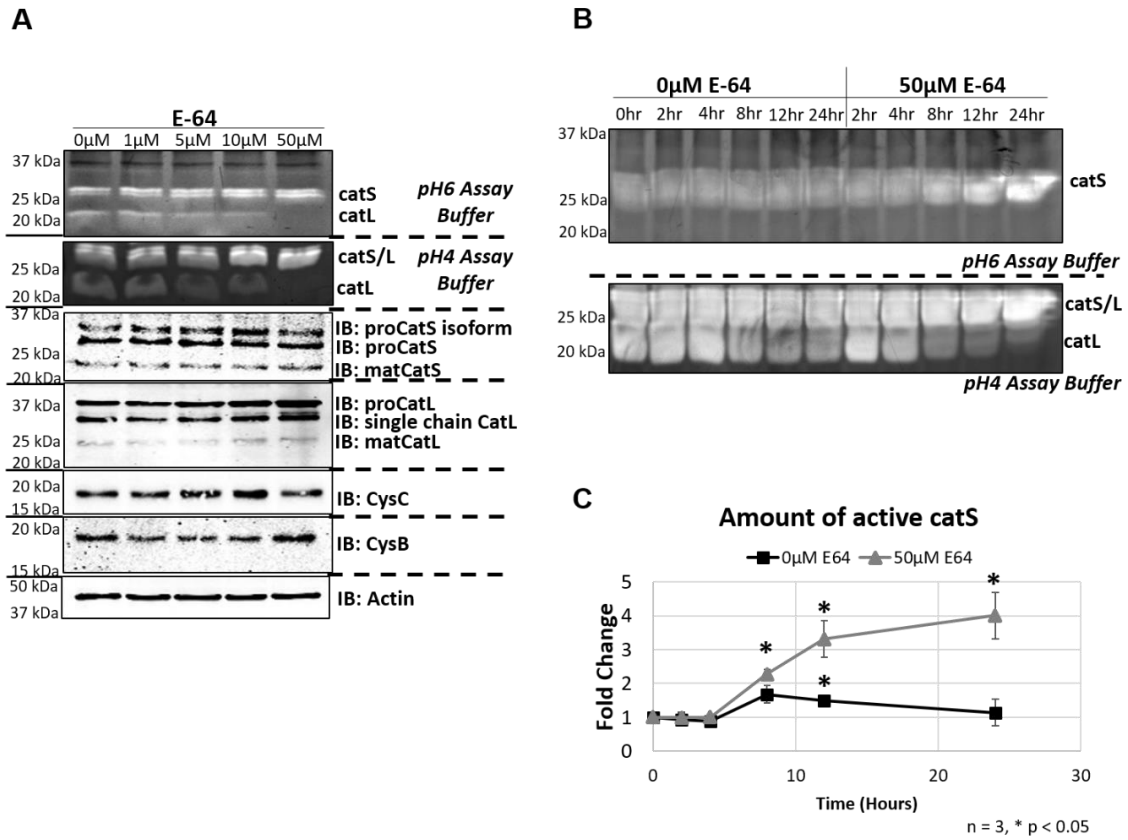

Figure 4.1. Inhibitor-induced increase of active cathepsin S and reduction of cathepsin L occurs intracellularly in MDA-MB-231 breast cancer. (A) MDA-MB-231 cells incubated with increasing amounts of E-64 for 24 hours were lysed and equal amounts of total protein loaded for multiplex cathepsin zymography with either a pH6 or pH4 assay buffer incubation (n=3 for each treatment, * $p < 0.05$, % $p < 0.001$). The amount of active cathepsins were quantified using ImageJ analysis. The same lysates from MDA-MB-231 cells treated with varying inhibitor doses for 24 hours were run with Western blot analysis and probed for intracellular pro- and mature- forms of cathepsin S and cathepsin L. There were no changes in cathepsins S and L protein (n=6). (B) MDA-MB-231 cells were incubated with 50 μM E-64 or a vehicle control for 0, 2, 4, 8, 12, and 24 hours and lysates were collected at each time point. Equal amounts of total protein were loaded for multiplex cathepsin zymography with either a pH6 or pH4 assay buffer incubation. (C) The amount of active cathepsin S was quantified using ImageJ analysis (n=3, * $p< 0.05$).

4.3.2 E-64 treatment causes co-localization of gelatin substrate and cathepsin S, and not cathepsin L

It was important to understand if substrate degradation was co-localized with cathepsin S or L and if E-64 treatment changes the co-localization, thus MDA-MB-231 cells were incubated with fluorogenically quenched DQ-gelatin along with either 50 μM E-64 or a

vehicle control or for 24 hours. The cells were then fixed, immuno-stained for cathepsin S or L, and imaged using confocal microscopy. With the treatment, cathepsin S and the DQ-gelatin was co-localized (Fig. 4.2A), while there was no cathepsin L and DQ-gelatin co-localization (Fig. 4.2B). There was a minimal amount of cathepsin S or L co-localized with DQ-gelatin detected with the vehicle control treatment (Fig. 4.2A-B). This indicates that the inhibitor treatment causes preferential localization of gelatin substrate with cathepsin S, but not cathepsin L.

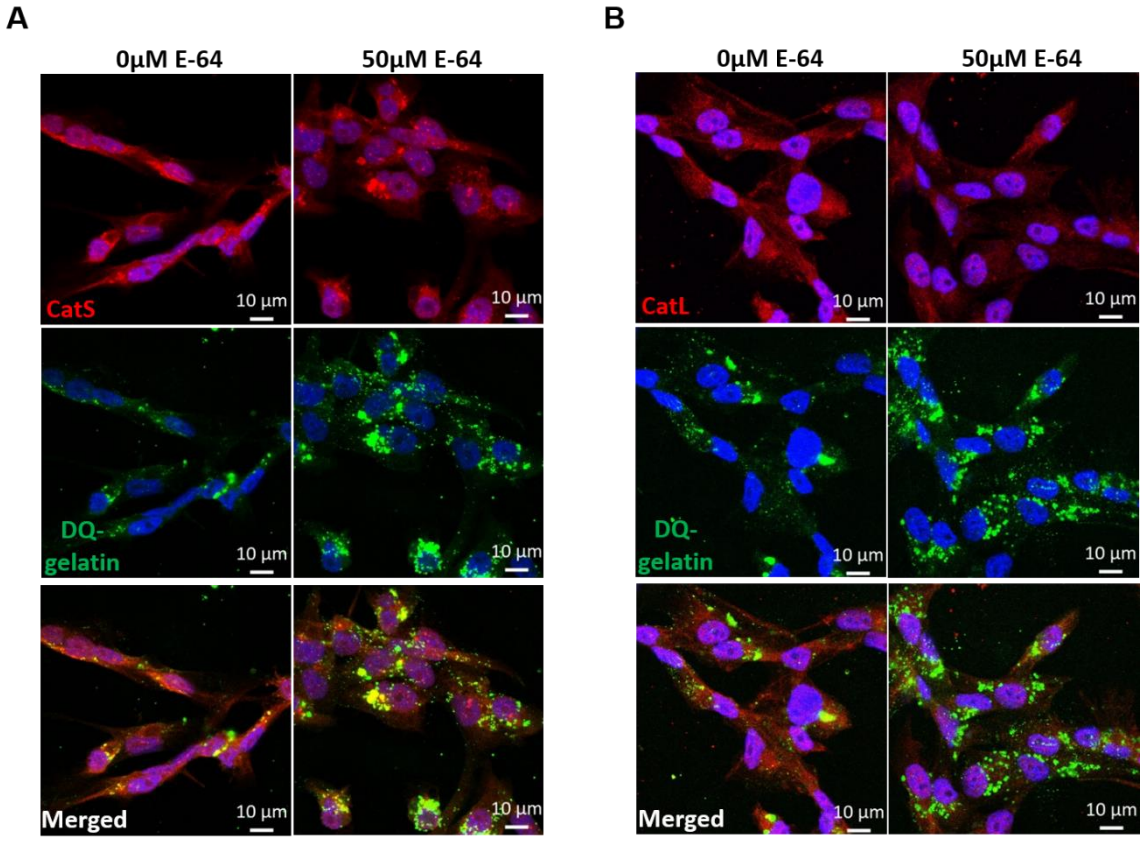

Figure 4.2. E-64 increases cathepsin S, but not cathepsin L, localization with intracellular gelatin substrate degradation. MDA-MB-231 cells were incubated with DQ-gelatin along with either 50 μM E-64 or a vehicle control for 24 hours. The cells were then fixed and stained for (A) cathepsin S (Alexa Fluor® 568, red) or (B) cathepsin L (Alexa Fluor® 594, red). Representative confocal images of degraded DQ-gelatin (green) co-localized with cathepsin S or cathepsin L are depicted. Bars, 10 μm.

4.3.3 Broad spectrum inhibition with cystatin C also upregulates the amount of active cathepsin S

To investigate if this increase in the amount of active cathepsin S was due to the small molecule inhibitor E-64 itself or due to cathepsin inhibition, MDA-MB-231 cells were incubated for 24 hours with increasing concentrations of recombinant cystatin C, the protein inhibitor for the cysteine cathepsin family. The concentrations of cystatin C used in this study were determined based on Abrahamson et al who reported cystatin C concentrations ranging from 0.1 to 3 µM in human body fluids [105]. The cells were then lysed and assayed for active cathepsins by zymography, and cystatin C protein by Western blotting. There was a dose dependent elevation in the amount of active cathepsin S in response to cystatin C treatment with over a 58% increase at 500 nM and 1 µM of cystatin C as detected by zymography ($n=6$, $p < 0.05$ and $p < 0.001$, respectively) (Fig. 4.3A).

There was no significant difference in the amount of active cathepsin L with cystatin C treatment ($n=3$). Intracellular cystatin C levels was also elevated after incubation with increasing cystatin C, suggesting that the exogenous cystatin C protein is being taken up by the cell during treatment ($n=4$-6, $p < 0.05$) (Fig. 4.3A). The upregulation in active cathepsin S due to cystatin C also occurred with E-64. While the amount of cathepsin L remained the same with cystatin C treatment unlike what was seen with small molecule. MDA-MB-231 cancer cells were incubated with cycloheximide (0.75 µg/ml) for 24 hours to inhibit protein synthesis, in the presence or absence of 500 nM recombinant cystatin C to confirm that the increase in intracellular cystatin C protein was due to endocytosis of cystatin C and not upregulated cystatin C production by the cell. Cycloheximide reduced

the amount of intracellular cystatin C by 74% (n=3, $p < 0.001$), except when the cells were also being incubated with exogenous cystatin C (n=3, $p = 0.56$) (Fig. 4.3B).

Since active cathepsin S elevation occurred due to endocytosis of cystatin C, it was hypothesized that not only treatment but overexpression of cystatin C would elevate the amount of active cathepsin S. To test this hypothesis, MDA-MB-231 cells were transfected to overexpress cystatin C or with an empty vector used as a control. Cystatin C overexpression increased the amount of active cathepsin S compared to the empty vector control (n=3, $p < 0.05$) (Fig. 4.3C), while overexpression of cystatin C did not decrease active cathepsin L.

To determine if both treatment in combination with cystatin C overexpression causes a synergistic effect on the amount of active cathepsin S, MDA-MB-231 cells were transfected to overexpress cystatin C or with an empty vector used as a control for 24 hours followed by incubation with 50 µM E-64 or a vehicle control for an additional 24 hours. Cystatin C overexpression and E-64 treatment both individually caused an elevation in the amount of active cathepsin S, while the combination of both inhibitor conditions had the same amount of active cathepsin S as compared to individual conditions. Both the combination of E-64 treatment and cystatin C overexpression along with E-64 treatment alone reduced the amount of cathepsin L (n=3, $p < 0.05$), but overexpression of cystatin C alone did not change the amount of cathepsin L (n=3) (Fig. 4.3C).

In addition, the changes in cathepsins S and L due to cystatin C overexpression are similar to what was seen with the cystatin C treatment. This suggests that overexpression

or exogenous cystatin C can also induce this active cathepsin S elevation, while a reduction in active cathepsin L reduction is specific to the small molecule treatment.

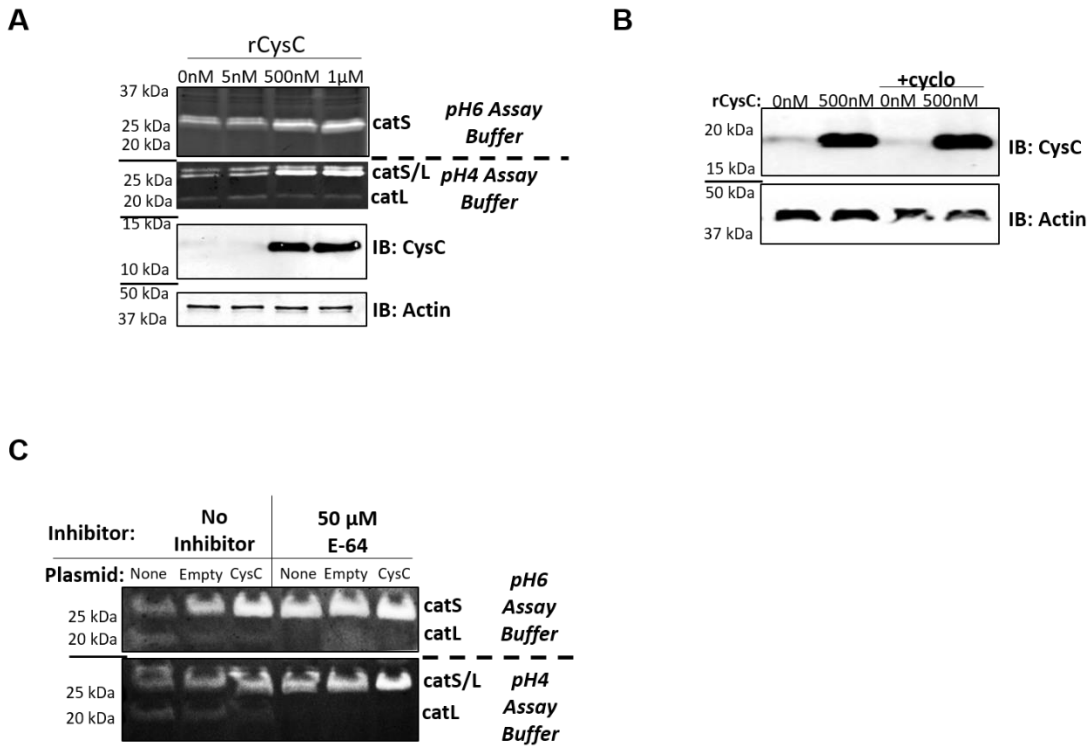

Figure 4.3. Inhibitor induced cathepsin S upregulation also occurs with cystatin C, but it does not reduce active cathepsin L. (A) MDA-MB-231 cells treated with exogenously added recombinant cystatin C inhibitor dose curve for 24 hours were lysed and equal protein amounts of cell lysates loaded for multiplex cathepsin zymography and Western blots probing for cystatin C. The amount of active cathepsin S was upregulated along with cystatin C. (n=3-6, $p < 0.05$). (B) MDA-MB-231 cells were treated with or without exogenous cystatin C and 0.75 μg/ml cycloheximide for 24 hours. After treatment, equal protein amounts were loaded for Western blot assays conducted to determine intracellular cystatin C levels (n=3, $p < 0.001$). (C) MDA-MB-231 cells were transfected with either an empty vector or cystatin C plasmids followed by incubation with E-64 for 24 hours. After 24 hours, the cells were lysed, equal amounts of protein were loaded for multiplex cathepsin zymography with a pH6 or pH4 assay buffer. The amount of active cathepsin S in the cystatin C transfected cells increased compared to the CMV plasmid control (n=3, $p < 0.05$).

4.3.4 Cystatin C and cathepsin S, but not cathepsin L, are co-localized when MDA-MB-231 cells are treated with exogenous cystatin C

Since cathepsin inhibitor treatments have differential effects on the amount of active cathepsins S and L and the co-localization of gelatin with cathepsin S was different compared to the co-localization with cathepsin L, it was hypothesized that cathepsins S and L were not in the same cellular compartments. To test this hypothesis, MDA-MB-231 cells were incubated with either 500 nM cystatin C or a vehicle control, fixed, and immunostained for cathepsins S and L. Cathepsins S and L were in different compartments regardless of the cystatin C treatment (Fig. 4.4A). This suggests that the differential response of cathepsins S and L by broad spectrum inhibitors could be due to differences in cellular locations.

To determine if cystatin C would be co-localized with either cathepsin S or L, MDA-MB-231 cells were incubated with or without 500 nM cystatin C for 24 hours and immunostained for cystatin C, cathepsin S, and cathepsin L. There was an increase in the amount of cathepsin S and cystatin C co-localization after exogenous cystatin C incubation (Fig 4.4B). Cathepsin L did not co-localize with cystatin C with or without cystatin C treatment (Fig 4.4C). To validate the staining in the confocal images, the co-localization of cathepsins S and L, and cystatin C with either cathepsin S or L was quantified using the Zeiss co-localization analysis to calculate the weighted co-localization coefficient ($n = 3\text{-}6$, $p < 0.005$) (Fig 4.4D).

In order to assess if cathepsins S or L were in the same cellular compartments as other cysteine cathepsins, MDA-MB-231 cells were immunostained for cathepsin S, cathepsin L, or cathepsin V, another cysteine cathepsin. Cathepsins S, L, and V were not co-localized, (Fig. 4.5A-C). Additionally, effects of cathepsin inhibition on the co-location

of cathepsins S or L with cathepsin V was investigated. Immunostaining of cathepsins S, L, or V was conducted in MDA-MB-231 cells. Cathepsin V did not co-localize with cathepsins S or L with or without E-64 treatment (Fig 4.6A-B).

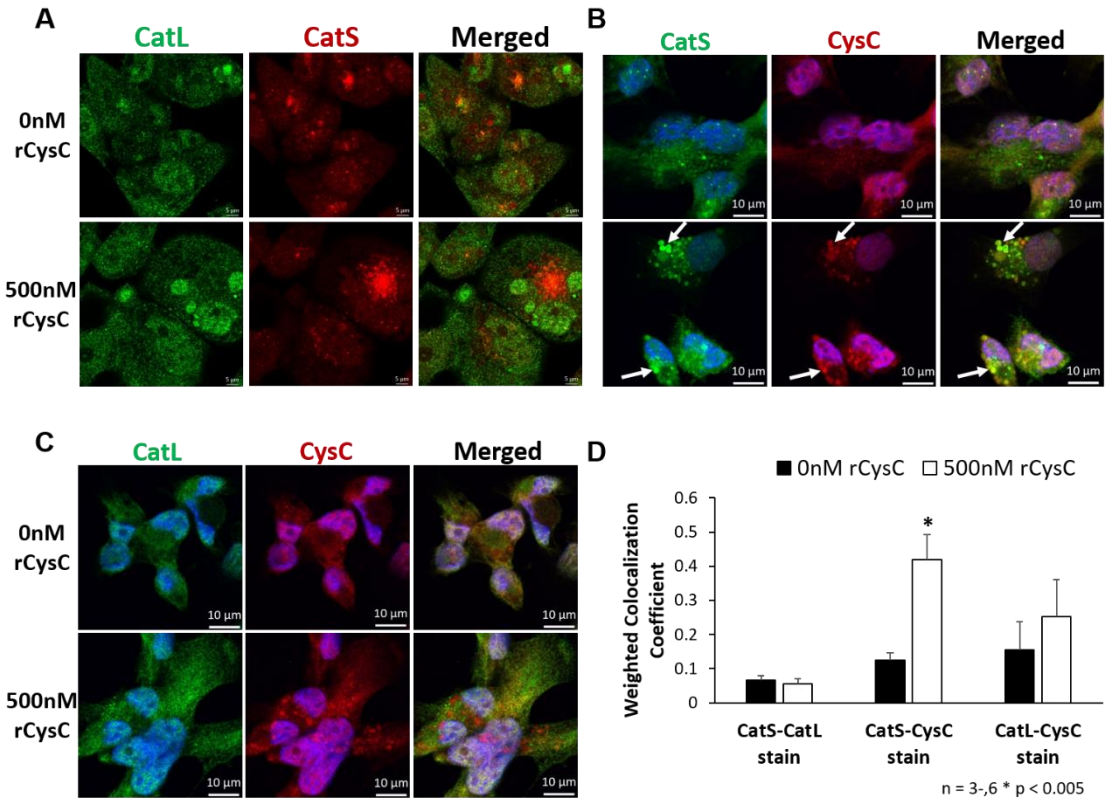

Figure 4.4. Cystatin C does not co-localize with cathepsin L, but cathepsin S-cystatin C containing vesicles occur with inhibitor treatment. (A) MDA-MB-231 cells were treated with 500nM cystatin C or a vehicle control for 24 hours and fixed and stained for cathepsin S (Alexa Fluor® 568, red) or cathepsin L (Alexa Fluor® 488, green). Bars, 5 µm. (B) MDA-MB-231 cells fixed after 24 hours of exogenous cystatin C treatment were stained for cathepsin S (Alexa Fluor® 488, green) and cystatin C (Alexa Fluor® 568, red). Representative confocal images of the stained samples were obtained. Note the cathepsin S and cystatin C colocalization in large vesicles after exogenous cystatin C inhibitor treatment (white arrows). Bars, 10 µm. (C) Cathepsin L (Alexa Fluor® 488, green). Bars, 10 µm. (D) The co-localization between cathepsin S and cystatin C and cathepsin L was quantified using Zeiss co-localization analysis to calculate the weighted co-localization coefficient (n=3-5, * $p < 0.005$).

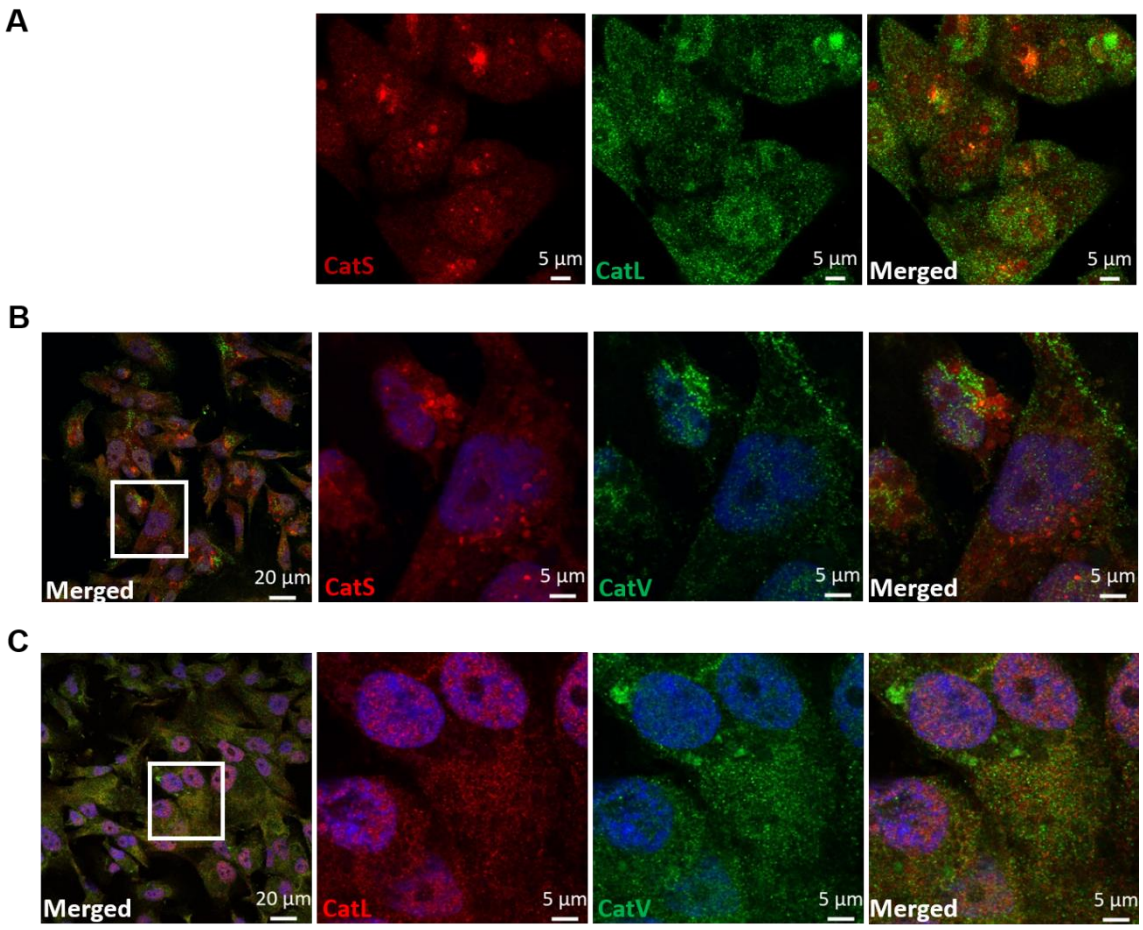

Figure 4.5. Cathepsin S, L, and V are located in different subcellular compartments. MDA-MB-231 cells were fixed and stained for cathepsin S (Alexa Fluor® 568, red), cathepsin L (Alexa Fluor® 488, green; or Alexa Fluor® 594, red), or cathepsin V (Alexa Fluor® 488, green). Bars, 20 µm and 5 µm.

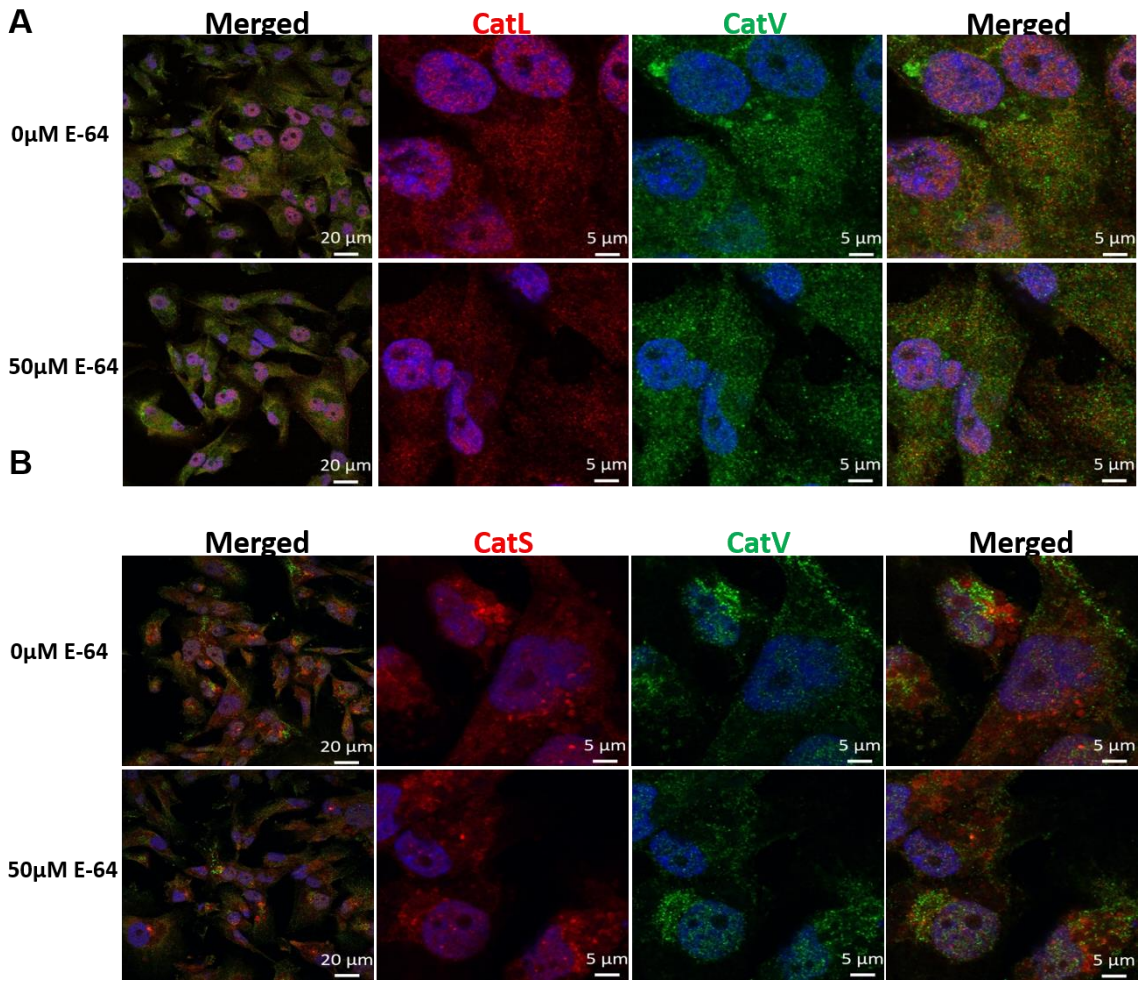

Figure 4.6. E-64 does not change cathepsins S or V co-localization with cathepsin V. (A) MDA-MB-231 cells were treated with a vehicle control or 50μM E-64 for 24 hours and fixed and stained for cathepsin L (Alexa Fluor® 594, red) or cathepsin V (Alexa Fluor® 488, green). Bars, 20 μm and 5 μm. (B) MDA-MB-231 cells were treated with a vehicle control or 50μM E-64 for 24 hours and fixed and stained for cathepsin S (Alexa Fluor® 568, red) or cathepsin V (Alexa Fluor® 488, green). Bars, 20 μm and 5 μm.

4.3.5 Cathepsin L is localized to the cytoplasm of MDA-MB-231 cells while cathepsin S is not

To further investigate the cellular location of cathepsin L since it was not co-localized with cathepsin S or cystatin C and previous studies of cathepsin L have reported cytoplasmic detection [109], cathepsin L localization in the cytoplasm was investigated. To test this, MDA-MB-231 cells were stained for cystatin B, a cysteine protease inhibitor localized in

the cytoplasm; and co-stained for cathepsin L or cathepsin S. There was dominant co-localization between cathepsin L and cystatin B as indicated by the overlapping yellow fluorescence signal. Some cathepsin L was in vesicular compartments not containing cystatin B (Fig. 4.7A). There was no co-localized cathepsin S and cystatin B (Fig. 4.7B).

To confirm this finding, E-64d, which is membrane permeable but converts to the membrane-impermeable E-64c derivative upon cleavage of the ethyl ester intracellularly [106, 155], was incubated with the cells at increasing concentrations for 4 hours and the active cathepsin L band was detected by cathepsin zymography. This early time point was chosen to prevent any inhibitor-induced cathepsin feedback from occurring. Cathepsin L was absent at all E-64d concentrations tested, even as low as 1 µM ($n=4\text{-}5$, $p < 0.05$) (Fig. 4.7C). This indicates that cathepsin L, and not cathepsin S, is susceptible to inhibition by E-64d, which inhibits proteases in the cytoplasm.

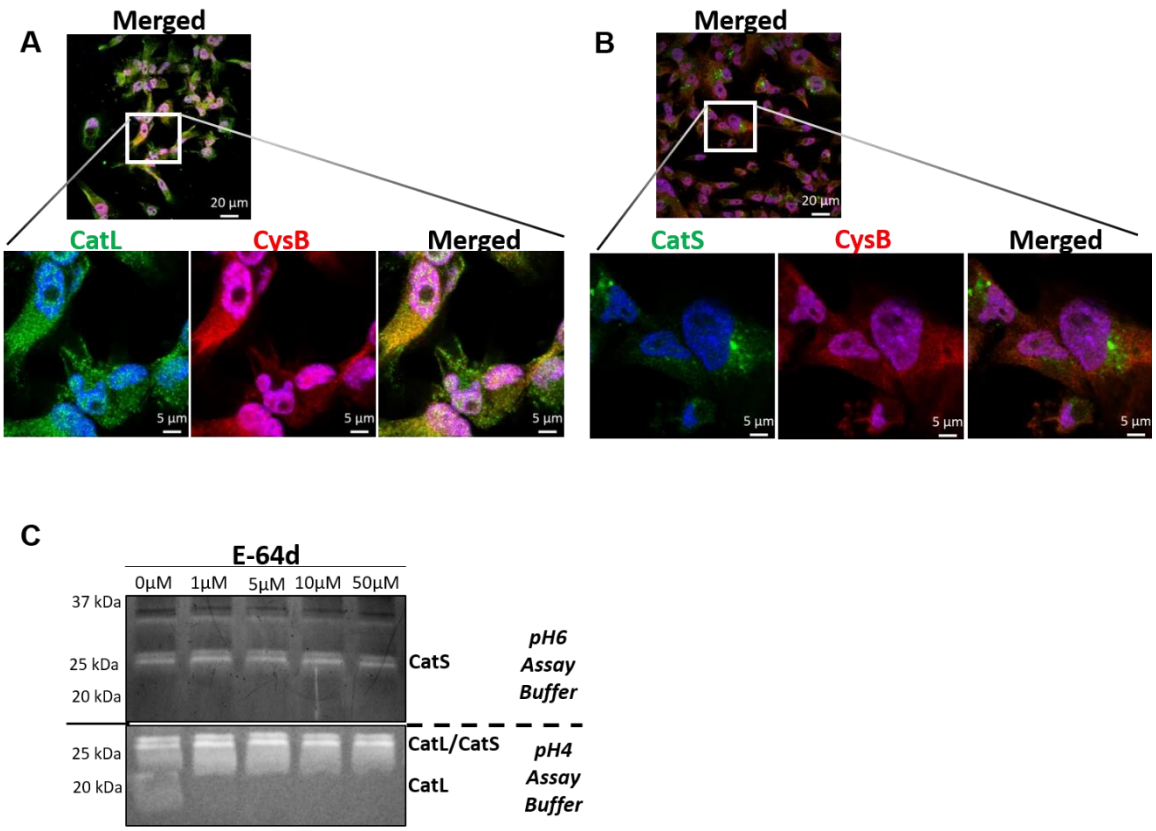

Figure 4.7. Cathepsin L, and not cathepsin S, is colocalized with cystatin B in the cytoplasm. (A) MDA-MB-231 cells were fixed and stained for Cathepsin L (Alexa Fluor ® 488, green), cystatin B (Alexa Fluor® 568, red), and nuclear (DAPI, blue) or (B) cathepsin S (Alexa Fluor ® 488, green), cystatin B (Alexa Fluor® 568, red), and nuclear (DAPI, blue). Representative confocal images of the stained MDA-MB-231 cells shows cathepsin L and cystatin B cytoplasmic colocalization. Bars, 20µm and 5µm. (C) MDA-MB-231 cells treated with E-64d dose curve for 24 hours were lysed and equal amounts of protein lysates were loaded for multiplex cathepsin zymography with pH 6 and pH 4 assay buffers. Intracellular active cathepsin L levels were decreased even with 1 µM E-64d (n=4-5, $p < 0.001$), while the amount of active cathepsin S was not changed (n=5-6).

4.3.6 Cathepsins L is secreted while only minimal amounts of cathepsin S is trafficked for secretion in MDA-MB-231 cells

It was hypothesized that cathepsins S and L are differentially trafficked in the MDA-MB-231 cells since they are not in the same compartments. The amount of secreted cathepsin S and L was investigated to test this hypothesis since the secretion of each cathepsin

depends on the trafficking within transport pathways. The conditioned media from MDA-MB-231 cells incubated with either 50 µM E-64 or a vehicle control was collected after 24 hours incubation, concentrated, and equal volumes of the media were loaded for multiplex cathepsin zymography and Western blot. The membrane was probed for cathepsin S followed by stripping and reprobing for cathepsin L. The active cathepsin L and total cathepsin L protein was detected in both the multiplex cathepsin zymography and Western blot, respectively (n=3) (Fig. 4.8A). Only minimal amounts of active extracellular cathepsin S was detected in the multiplex cathepsin zymography. This corresponds with the low amounts of detectable cathepsin S protein from the conditioned media detected in the Western blot (n=3). Similar results were seen in conditioned media collected from cells incubated with 500nM cystatin C for 24 hours (n=3) (Fig. 4.8B).

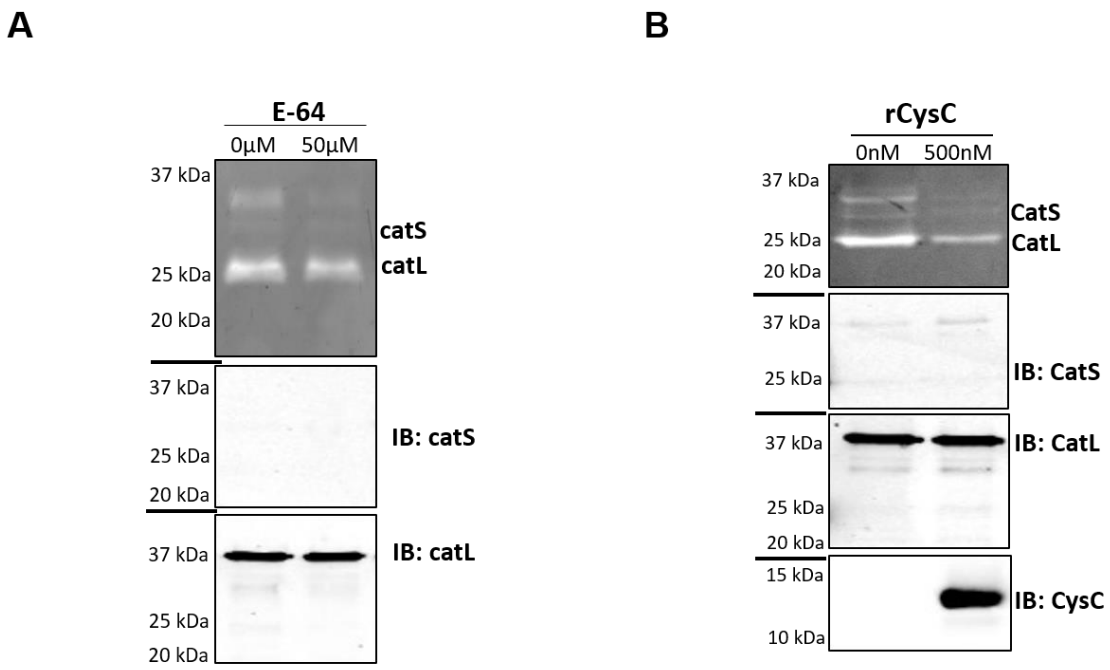

Figure 4.8. Cathepsin L is secreted regardless of inhibitor treatment. (A) Conditioned media from MDA-MB-231 cells incubated with 50 μM E-64 or a vehicle control for 24 hours was collected, concentrated, and equal volumes were loaded for multiplex cathepsin zymography or Western blots (n=3, $p < 0.05$). (B) Similarly, MDA-MB-231 cells were incubated for 24 hours with cystatin C treatment. Conditioned media was then collected, concentrated, and equal volumes were loaded for multiplex cathepsin zymography. Active cathepsins S and L found in the conditioned media demonstrates that minimal amounts of extracellular cathepsin S are detected, while cathepsin L has a higher detectable signal. Active cathepsin S and L is significantly reduced after 24 hours of inhibitor treatment (n=3, % $p < 0.01$). The same samples were analyzed using Western blots and cathepsin S had minimal detection while cathepsin L had abundant amounts.

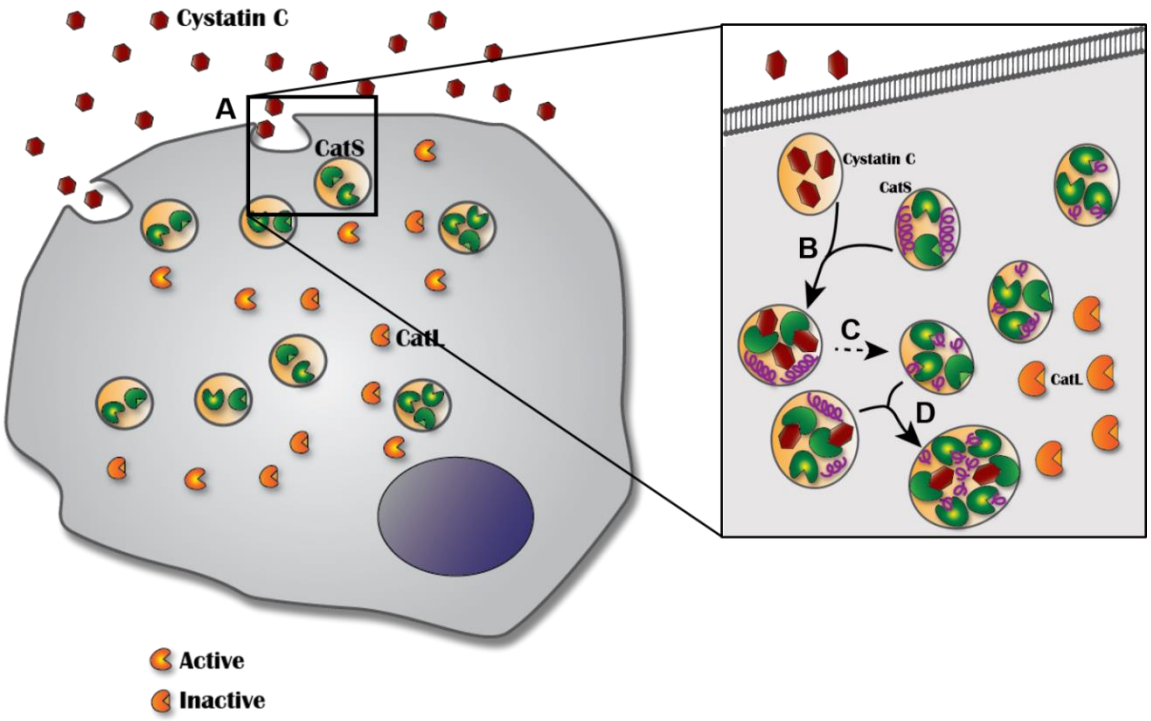

Figure 4.9. Cathepsin inhibitor uptake results in upregulation of active cathepsin S as a compensatory mechanism. The current working model of cathepsin inhibitor treatment of MDA-MB-231 breast cancer cells is during cathepsin inhibitor treatment the inhibitor is taken up by the breast cancer cells (A). After inhibitor uptake, the vesicles containing the inhibitor fuses with vesicles containing cathepsin S and inhibits vesicular cathepsins preventing substrate degradation (B). This results in an upregulation of the amount of active cathepsin S (C) in order to compensate for the decrease in substrate degradation within the system (D).

4.4 Discussion

This study has shown that broad spectrum cathepsin inhibition using either a small molecule inhibitor or protein inhibitor causes compensatory mechanisms in human breast cancer cells to elevate the amount of intracellular active cathepsin S. This suggests that cellular feedback mechanisms within the system upregulated the amount of active cathepsin S in order to compensate for any reduced proteolysis due to the inhibitor. This finding is important for developing and improving cathepsin inhibitors for breast cancer therapies. Thus far, the use of cathepsin inhibitors for cancer therapeutics has been widely discussed, but rarely utilized in part due to the side effects elicited by the

therapies. Previous reports have also investigated the effects of cathepsin inhibitors on cathepsins in vitro and in vivo. The less potent cysteine cathepsin inhibitor leupeptin was shown to increase cathepsin B activity in rat fibroblasts as well as in mouse calvaria while E-64 still maintained inhibitory effects on the cathepsin B activity [156]. In addition, cathepsins B, H, and L protein amounts were elevated in the liver of rats due to the more potent inhibitor E-64-C, also known as EP-475 [145] [157]. While these studies provide important insight into the effects of cathepsin inhibitors, unlike these previous studies we have successfully demonstrated that this unexpected inhibitor-induced feedback occurs in human cells and is capable of occurring in breast cancer. This highlights the need for proper dosing strategies and the development of highly selective inhibitors that maintain their selectivity even in intracellular conditions to prevent off target side effects for breast cancer therapies.

Lysosomal inhibitors have also been shown to elevate cathepsin activity in cells and in vivo [158, 159]. Even though it is thought that the stabilization of the cathepsin proteins due to the inhibitors could be contributing to the elevated protease activities, we have clearly shown that the inhibitor-induced feedback of the cathepsins that occurs in breast cancer cells is dependent on the localization of the cathepsin. Studies have investigated cathepsin L and cathepsin S localization and trafficking [107, 160, 161] and reported detection of cathepsin S and cathepsin L in different cellular compartments in thyroid tissue [161]. This work focuses on the localization of these two proteases in a triple negative breast cancer cell line, and while cathepsin S was co-localized with gelatin substrate and cystatin C, this was in contrast to cathepsin L which was detected in the cytoplasm. Although the inhibitor was co-localized with cathepsin S protein, the

increased cleaved gelatin substrate along with the elevation of active cathepsin S all suggest that cathepsin S could be contributing to the substrate cleavage within the vesicles after inhibitor treatment and feedback within the system increased active cathepsin S. In addition, the inhibitor may be bound to other lysosomal proteases preventing substrate degradation from those proteases and preventing substrate degradation within the vesicles. Both inhibitors used within this study were broad spectrum cathepsin inhibitors capable of inhibiting lysosomal cysteine proteases. While E-64 has similar inhibition rates for both cathepsins S and L, it is also a potent inhibitor for cathepsin B, the most abundant cathepsin [162]. Cystatin C also has sub-nanomolar inhibition constants for cathepsin S and L, making it a potent inhibitor of these proteases, but it still has a 0.25 nM inhibitor constant for cathepsin B [12]. Since the amount of total cathepsin S protein was not increased after inhibitor treatment, the elevated amounts of active cathepsin S could be due to increase activation of the pro-cathepsin S and not due to changes in transcriptional regulation of the cathepsin S gene.

Concurrently, the active cathepsin S elevation due to the inhibitor did not occur with cathepsin L which had reduced active protein with E-64 and unchanged amounts with cystatin C. Although cathepsin L is a lysosomal cysteine protease, it was detected in the cytoplasm of the breast cancer cells. Cytoplasmic cathepsin L has also been detected in podocytes, where it was involved in cleavage of the GTPase dynamin which results in cytoskeleton reorganization [109]. Nuclear cathepsin L has also been reported to cleave the CCAAT-displacement protein/cut homeobox transcription factor [108, 163] and cleave and modify histones [164, 165]. All of this indicates that the cytoplasmic cathepsin L has functional roles and downregulation of cathepsin L during inhibitor

treatment could reduce the transcriptional regulation of other genes and change cellular morphology.

In addition, cathepsin L was also secreted suggesting that it is trafficked in secretory vesicles which could be seen in Figure 4.7A in which some of the punctate cathepsin L protein staining was not co-localized with the cystatin B protein. Cathepsin S was not readily secreted suggesting that, unlike cathepsin L, cathepsin S is not trafficked for secretion. These differences in cathepsins S and L trafficking may explain why active cathepsin L is not upregulated during cathepsin inhibitor treatment like active cathepsin S.

These findings are not only important in understanding how cathepsin inhibitors can induces feedback mechanisms in breast cancer cells, but can also be useful in studying diseases in other tissues since cathepsin L is ubiquitously expressed in different cells and tissues.

4.5 Conclusion

In conclusion, the broad-spectrum cathepsin inhibitor-induced cathepsin S elevation and cathepsin L inhibition is a cellular feedback mechanism that is regulated by preferential localization of the inhibitor to cathepsin S. Understanding this feedback is critical for developing effective therapeutics and dosing strategies targeting cysteine cathepsins for the prevention cancer invasion and metastasis.

CHAPTER 5

Consequences of inhibitor-induced proteolytic network perturbations in breast cancer

5.1 Introduction

According to the American Cancer Society, about one in five diagnosed breast cancer cases are classified as human epidermal growth factor receptor (HER2)-positive. Triple-negative subtypes, which is the most aggressive form of breast cancer [37], accounts for 12% of breast cancer cases [28] while the estrogen receptor (ER)- or progesterone receptor (PR)-positive tumors accounted for 84% of diagnosed breast cancer in 2012 [28].

During cancer progression, transformed tumor cells along with tumor-associated cells within the tumor microenvironment overexpress cysteine cathepsins to assist with the invasion and metastasis of the tumor [5-11]. Proteases, such as cysteine cathepsins and matrix metalloproteinases (MMPs), are secreted by tumor associated macrophages (TAMs), which are differentiated from circulating monocytes from the vasculature, and have been shown to play a significant role in tumor growth and invasion [59, 83, 97, 166-169], due to local degradation of extracellular matrix substrates upon secretion [81, 128, 170, 171]. TAMs, which can account for as much as 50% of tumor volume [13, 59], are often associated with poor prognosis [172-174].

Cathepsins V and K have been shown to be expressed in breast carcinomas [82, 86]. The role of cathepsins and other proteases in cancer cell migration and invasion depends on the mechanisms by which the tumor cells invade. When cancer cells invade

collectively in sheets or clusters, proteolysis at the leading edge occurs, which is in contrast to amoeboid migration that occurs when cells invade individually [175]. Breast cancer cells have been reported to acidify the extracellular milieu [45] providing an optimal environment for cathepsin activity in the pericellular environment. Our own lab has shown that not only the expression, but also the active cathepsins is greater in human breast tumor tissue compared to the patient matched normal breast tissue [9]. While the amount of cathepsins K and L was upregulated in breast cancer tissue and peaked at stage II, active cathepsin S amounts remained comparable to that detected in the normal tissue regardless of cancer stage [9]. Although cathepsins are thought to assist with cancer invasion due to degradation of ECM proteins in the surrounding environment, cathepsins also play an important role intracellularly via the degradation of internalized ECM proteins such as collagen [5, 137, 139], , the shedding of surface bound proteins from cancer cells reducing Ras GTPase intracellular signaling [141], and the cleavage of the surface membrane protein CD74 in endosomes [143] to transcriptionally regulate CCL2, a pro-inflammatory chemokine which promotes metastasis [142]. The multi-functional roles cathepsins play in tumor progression have contributed to targeting them for cancer therapeutics.

Cathepsins are inhibited by the family of protein inhibitors cystatins [12] that are categorized into three families. The family 1 cystatins (also referred to as stefins), such as cystatin B, are cytoplasmic and inhibit cathepsins within the cell, while family 2 cystatins, such as cystatin C, are secreted and inhibit extracellular cathepsins [12, 176]. None of the inhibitors in family 3 act on cathepsins. It is well established that cystatin C is constitutively secreted and found in various human bodily fluids [12]. Cystatin B is

distributed throughout the cytoplasm of cells, but is not found on the cell surface [149]. The ratio of cathepsin to cystatin appears to be a better indicator of cancer prognosis than just cathepsin detection alone [177-179] and can be used to predict cancer invasion [180]. In addition to the cystatins, cathepsins can be inhibited with small molecule cysteine cathepsin inhibitors including E-64 and E-64d. E-64d is a derivative of E-64 which can passively cross cellular membranes and inhibit intracellular cathepsins after ethyl ester cleavage [106, 155].

Traditionally the effect of one protease on substrate cleavage is studied, leaving a gap in exploring interactions between proteases. Within the cathepsin proteolytic network, cannibalistic degradation with cathepsin S preferentially degrading cathepsin K over collagen substrates occurs [181]. Cathepsin S can also activate other cathepsins such as cathepsin C [140].

This study investigated the effects of both protein cathepsin inhibitors cystatin C and cystatin B and the small molecule cathepsin inhibitors E-64 and E-64d on cancer cell invasion, substrate degradation, and active cathepsins L, S, and V amounts. Understanding how broad spectrum inhibitors affect individual cathepsins in different cellular environments and, ultimately, if these effects promote cancer cell invasion is important for therapeutic development. This was accomplished by overexpressing or treating cancer cells, macrophages, and human breast tissue with the above mentioned inhibitors followed by measuring invasion, gelatinase degradation, and the amount of secreted and intracellular active cathepsins. Furthermore, murine and human cells and tissue were studied to determine if the effects of the inhibitor were species specific.

5.2 Materials and Methods

5.2.1 Materials

Normal breast tissue was provided by our collaborator, Dr. John S. Kennedy, at the Dekalb Medical Center (Decatur, GA, USA) and purchased from National Disease Research Interchange (NDRI) (Philadelphia, PA, USA). Anti-human cathepsin S, L, and V antibodies (R&D Biosystems), anti-actin (Santa Cruz Biotechnology), and secondary donkey anti-mouse or anti-goat antibodies tagged with an infrared fluorophore (Li-Cor) were used to detect protein with a Li-Cor Odyssey scanner.

5.2.2 Cell Culture

RFP tagged MDA-MB-231 and GFP tagged MCF-7 epithelial cells were cultured with Dulbecco's Modification of Eagles Medium (DMEM) with 4.5 g/L Glucose (Lonza) supplemented with 10% fetal bovine serum (FBS) – Premium Select (Atlanta Biologicals), 1% L-glutamine (Life Technologies), 1% Eagle′s minimum essential medium (MEM) non-essential amino acids (Sigma Aldrich), and 1% penicillin/streptomycin (Life Technologies). MCF-10A epithelial cells were cultured with the Mammary Epithelium Basal Medium (MEBM) Bullet kit (Lonza). RFP tagged MDA-MB-231 breast cancer cells (Cell Biolabs, Inc.) was transfected with one of the plasmids containing full-length expression sequences of either green fluorescent protein (GFP), red fluorescent protein (RFP), cystatin C (CysC), or cystatin B (CysB) under control by the CMV promoters (Origene) using Lipofectamine 2000 (Invitrogen). Cells were then incubated for 24 hours at 37°C.

GFP tagged human THP-1 monocytes (ATCC) were cultured in RPMI with 10% FBS, 1% L-glutamine, 1% penicillin-streptomycin, and 0.05 mM 2-mercaptoethanol. Cells

were incubated with either the cysteine cathepsin broad-spectrum small molecule inhibitor E-64 (Calbiochem), E-64d (Calbiochem), the cathepsin L inhibitor Z-FY-CHO (Calbiochem), or the broad spectrum MMP inhibitor GM6001 (Calbiochem).

5.2.3 Gelatin degradation assay

Transfected or non-transfected MDA-MB-231 breast cancer cells (Cell Biolabs, Inc.) were incubated with 50 μM or 5 μM of the cathepsin broad-spectrum small molecule inhibitor E-64 or E-64d, or the broad spectrum MMP inhibitor GM6001 (GM) (Calbiochem) along with 0.05 mg/ml DQ-gelatin from bovine skin, fluorescein conjugate (Invitrogen) at 37°C. The amount of degraded DQ-gelatin was measured using spectroscopy (Biotek Synergy H4 Multi-mode Plate Reader) at 1, 2, 4, 8, 12, and 24 hours. After the 24 hour incubation, the conditioned media was collected and concentrated using VivaSpin 500 centrifugal concentrators (GE Healthcare). MDA-MB-231 cells were washed, lysed, sonicated, and centrifuged to collect the soluble fraction. Protein concentration was determined using a micro BCA assay kit (Pierce). Conditioned media and cell lysates were collected and prepared for multiplex cathepsin zymography, Western blots, and qRT-PCR to measure the amount of secreted and intracellular cathepsin K, cathepsin S, cystatin C, and cystatin B. Active- and pro- cathepsin protein were quantified using densitometry (ImageJ).

5.2.4 Cathepsin zymography

This protocol is as previously published by us with minor changes [124]. After non-reducing sodium dodecyl sulfate electrophoresis, proteins were renatured and incubated in activity buffer as previously described [124]. Cathepsins were activated using a sodium

phosphate activity buffer, pH 6. The gels were stained with Coomassie Blue R250 and imaged using an ImageQuant LAS 4000.

5.2.5 Western blots

SDS-PAGE was performed as described above without a gelatin substrate. Proteins were transferred to a nitrocellulose membrane (Bio-Rad) and probed with monoclonal anti-human cathepsin K monoclonal antibody clone 182-12G5 (Millipore), anti-human cathepsin S and V antibodies (R&D Biosystems), or anti-mouse cathepsin L antibody (R&D Biosystems). Secondary donkey anti-mouse or anti-goat antibodies tagged with an infrared fluorophore (Rockland) were used to image protein with a Li-Cor Odyssey scanner.

5.2.6 Invasion assay

RFP tagged MDA-MB-231 breast cancer cells were transfected with either RFP, cystatin C, or cystatin B. Twenty-four hours post-transfection, a 2 mg/ml type I collagen gel (Invitrogen) was polymerized on top of the cells and incubated for 24 hours at 37°C. Invasion into the collagen gel was assessed using a Zeiss LSM confocal microscope.

5.3 Results

5.3.1 Inhibitor-induced cathepsin S elevation occurs in non-cancerous human breast tissue and varies depending on invasiveness of epithelial cell line

The effect of E-64 on active cathepsin S in human cancerous and non-cancerous breast tissue was investigated, since E-64 induced cathepsin upregulation occurred in the MDA-MB-231 breast cancer cells. Non-cancerous breast tissue and patient matched

cancer breast tissue excised during mastectomy or lumpectomy was obtained and cultured ex vivo with increasing amounts of the small molecule for 24 hours. The tissue was homogenized and equal amounts of protein were loaded and assayed for active cathepsins using multiplex cathepsin zymography. Similar to the MDA-MB-231 cells, treatment with 50 µM E-64 significantly increased the amount of active cathepsin S while reducing cathepsin L in the non-cancerous breast tissue ($n=7$, $p < 0.05$) (Fig. 5.1A). In contrast to the non-cancerous tissue, the treatment decreased active cathepsin S along with cathepsin L in the cancerous tissue ($n=4$). Active cathepsin V was elevated in the cancerous tissue compared to the non-cancerous tissue, but the inhibitor had no effect on active cathepsin V ($n=4$) (Fig 5.1A).

Since the cancerous tissue did not have the inhibitor induced response similar to the non-cancerous tissue, human THP-1 monocytes differentiated into macrophages with phorbol 12-myristate 13-acetate (PMA) were incubated with a range of E-64 concentrations for 24 hours to test the hypothesis that upregulation of cathepsin S due to the small molecule inhibitor does not occur in other cell types such as macrophages, which are known to enter the tumor microenvironment and promote tumor growth, invasion, and metastasis [168, 169] in part due to cathepsins [59, 97]. The cells were then lysed and processed for multiplex cathepsin zymography and Western blot. In contrast to the murine RAW 267 macrophages, the amount of intracellular active cathepsin S in the human THP-1 macrophages increased with 50µM E-64 compared to the inhibitor control ($n=3$, $p < 0.05$) (Fig. 5.1B). In addition to the active form, the amount of mature and pro cathepsin S was upregulated with 50µM E-64 ($n=3$, $p < 0.05$) (Fig. 5.1C). While, the amount of intracellular active cathepsin L decreased with 50µM E-64 incubation ($n=3$, p

< 0.05) (Fig. 5.1B), the amount of pro cathepsin L was elevated with 50µM E64 compared to the inhibitor control (n=3, p < 0.05) (Fig.5.1C). The amount of active cathepsin V also increased with 50µM E-64 (n=3, p < 0.001) (Fig. 5.1B). In addition, upon differentiation the PMA-induced THP-1 macrophages had elevated amounts of active cathepsins S and L compared to the non-differentiated THP-1 monocytes (n=3, p < 0.001).

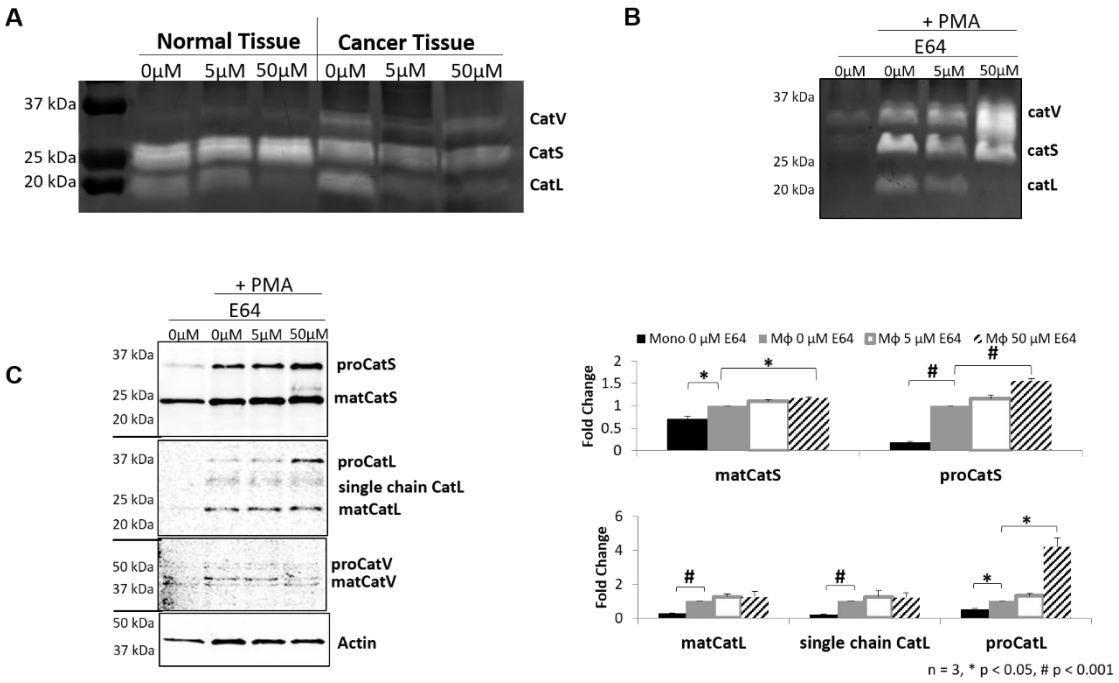

Figure 5.1. E-64 upregulates active cathepsin S in non-cancerous human breast tissue and macrophages. (A) Normal breast tissue was purchased from NDRI and the tissue cultured ex vivo for 24 hours with increasing amounts of E64 inhibitor. The tissue was homogenized and equal amounts of protein were loaded for multiplex cathepsin zymography. The amount of active cathepsin S in the homogenates significantly increased with 50µM E64 treatments (n=7, * p < 0.05), while the active cathepsin L decreased (n=7, * p < 0.05). (B) THP-1 monocytes and PMA-induced macrophages were incubated with E64 for 24 hours. Cells were lysed and equal amounts of total protein were assayed using multiplex cathepsin zymography. Active intracellular cathepsins S, L, and V were detected and quantified (n=3, *p < 0.05, % p < 0.001). (C) The same lysate samples were assayed using Western blot analysis and cathepsin S, L, and V protein amounts in THP-1 monocytes and PMA-induced macrophages was quantified (n=3, *p < 0.05, % p < 0.001).

To determine if the active cathepsin profile varied based on receptor classification, the triple-negative BT-549, HCC-38, HCC-70, HCC-1395, HCC-1806, and MDA-MB-231 breast cancer cell lines; ER-positive MCF-7 breast cancer cell line; and HER2-positive AU-565, HCC-202, HCC-1419, and SkBr-3 breast cancer cell lines were lysed and assayed using multiplex cathepsin zymography. In general, the triple negative breast cancer cells had increased amounts of active cathepsin compared to the HER+ cell lines. In addition, 6 out of 6 triple negative cell lines assayed including the MDA-MB-231 cells had two or more active cathepsins detected, while this was only true for 2 out of 4 HER+ cell lines (Fig. 5.2A).

Since E-64 caused an inhibitor-induced upregulation of cathepsin S in the MDA-MB-231 breast cancer cells, the effect of the small molecule inhibitor on active cathepsins in other epithelial cell lines was investigated. A range of the inhibitor from 0 to 50 μM was incubated with either MCF-10A epithelial cells, estrogen (ER)-positive MCF-7 breast cancer cells, or triple-negative MDA-MB-231 breast cancer cells for 24 hours. The cells were then lysed and processed for multiplex cathepsin zymography to detect the amount of active cathepsins. In the non-transformed MCF-10A epithelial cells, the E-64 treatment did not cause an increase in the amount of active cathepsin S (n=3). The amount of active cathepsin S in the MCF-7 breast cancer cells was not significantly different compared to the vehicle control (n=3). With the more aggressive MDA-MB-231 breast cancer cells, the amount of active cathepsin S was increased with an E-64 incubation as low as 10 μM (n=4, $p<0.05$) (Fig. 5.2B), as indicated by the cleared white bands in the multiplex cathepsin zymography. Cathepsin L was only detected in the

MDA-MB-231 cells and not the less aggressive MCF-7 cells or the MCF-10A epithelial cells.

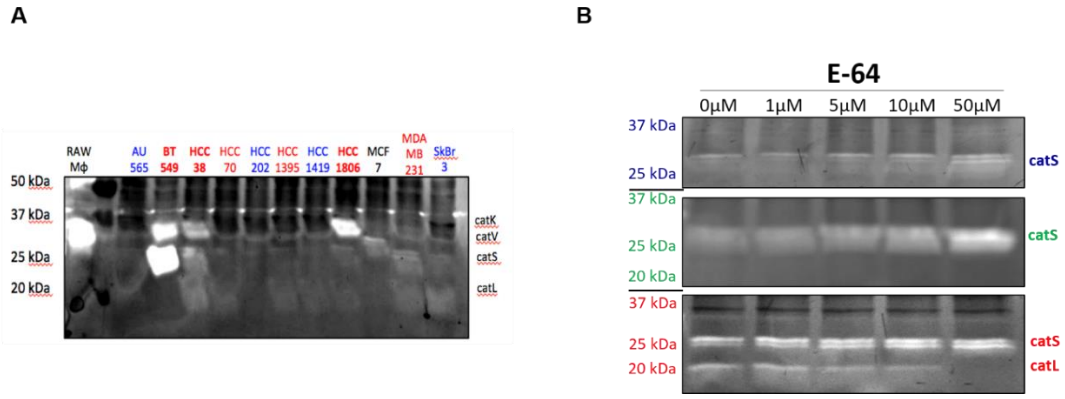

Figure 5.2. E-64 elevation of intracellular active cathepsin S is dependent on the type of epithelial cell line. (A) Equal amounts of lysates from ER-positive and triple-negative breast cancer cell lines were loaded for cathepsin zymography. (B) MCF-10A, MCF-7, and MDA-MB-231 cells incubated with increasing amounts of E-64 for 24 hours were lysed and equal amounts of total protein loaded for multiplex cathepsin zymography (n=3 for each treatment)

5.3.2 Inhibitor-induced elevation of cathepsin S occurs with cathepsin L expression

It was previously reported that activation and degradation among cathepsins occurs [140, 181-183] as well as compensatory elevation of cathepsin expression in cathepsin knockout models [4, 60, 88, 114, 115, 184]. In addition, it was previously demonstrated in Figure 4.1 that E-64 reduces the amount of cathepsin L. Due to all of this, MDA-MB-231 cells were incubated with the cathepsin L inhibitor Z-FY-CHO, E-64, or vehicle control for 24 hours to test the hypothesis that upregulation of cathepsin S with E-64 was due to cathepsin L inhibition. The cells were then lysed and equal amounts of protein loaded for multiplex cathepsin zymography. Z-FY-CHO, the cathepsin L inhibitor, elevated the amount of active cathepsin S similar to that seen with E-64 ($n=6$, $p < 0.05$)

(Fig. 5.3). While the amount of intracellular cathepsin L was reduced with the incubation of E-64, the active cathepsin L was not reduced by Z-FY-CHO. E-64 and Z-FY-CHO both caused an increase in pro cathepsin L, which is an indicator of cathepsin L inhibition.

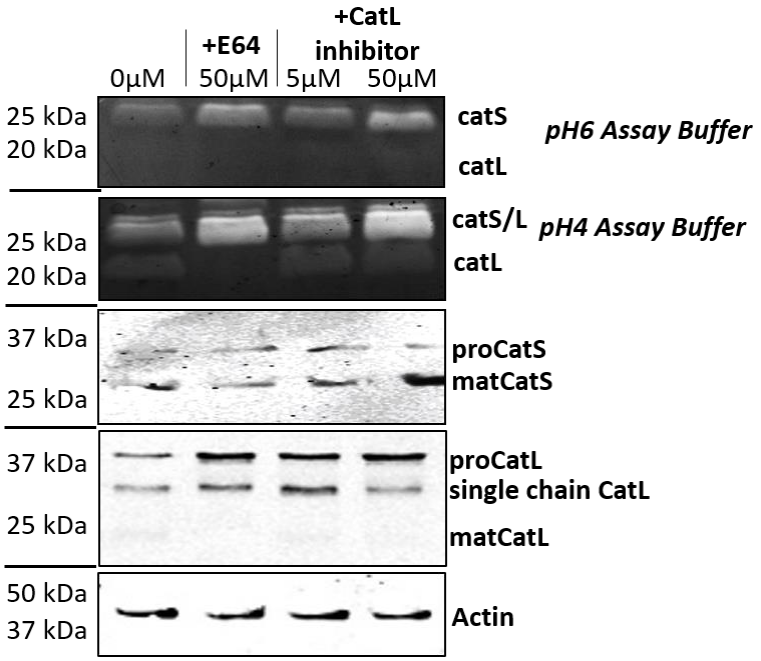

Fig. 5.3. Cathepsin L inhibitor causes cathepsin S upregulation in triple negative MDA-MB-231 breast cancer cells. MDA-MB-231 breast cancer cells were incubated with either the Z-FY-CHO cathepsin L inhibitor or E64 for 24 hours followed by lysing and protein quantification. Equal protein amounts were loaded for multiplex cathepsin zymography. The amount of active cathepsin S was increased with the incubation of 5μM and 50μM of Z-FY-CHO, similar to what was seen with the 50μM E64 treatment (n=6). Cell lysates were also loaded for immunoblotting of cathepsin S, cathepsin L, and actin (n=3).

Thus far, it has been shown that E-64 upregulates intracellular cathepsin S in human cells and tissues (Fig. 4.1 and Fig. 5.1). Mice do not have an orthologue to human cathepsin L, thus a murine system was used to investigate if cathepsin L is involved with the regulation of intracellular active cathepsin S during E-64 treatment. To validate the finding seen with the cathepsin L inhibitor, murine RAW 264.7 macrophages were

incubated with 50 µM E-64 for 24 hours. The amount of active cathepsin S did not increase with the small molecule inhibitor as detected by multiplex cathepsin zymography (n=3) (Fig. 5.4A).

To determine if the small molecule would inhibit the amount of secreted active cathepsins, murine RAW 264.7 macrophages were incubated with 5 µM E-64 or 5 µM E-64d for 24 hours and conditioned media was collected, concentrated, and equal volumes were loaded for multiplex cathepsin zymography or MMP zymography. The amount of secreted cathepsin S was reduced with either E-64, the extracellular inhibitor, or E-64d, the intracellular inhibitor (n=3, $p < 0.05$) (Fig. 5.4B). Both E-64 and E-64d also reduced the amount of secreted murine cathepsin L (n=3, $p < 0.01$) (Fig. 5.4B). This was in contrast to the amount of MMPs which was not affected by either E-64 or E-64d (n=3) (Fig. 5.4B).

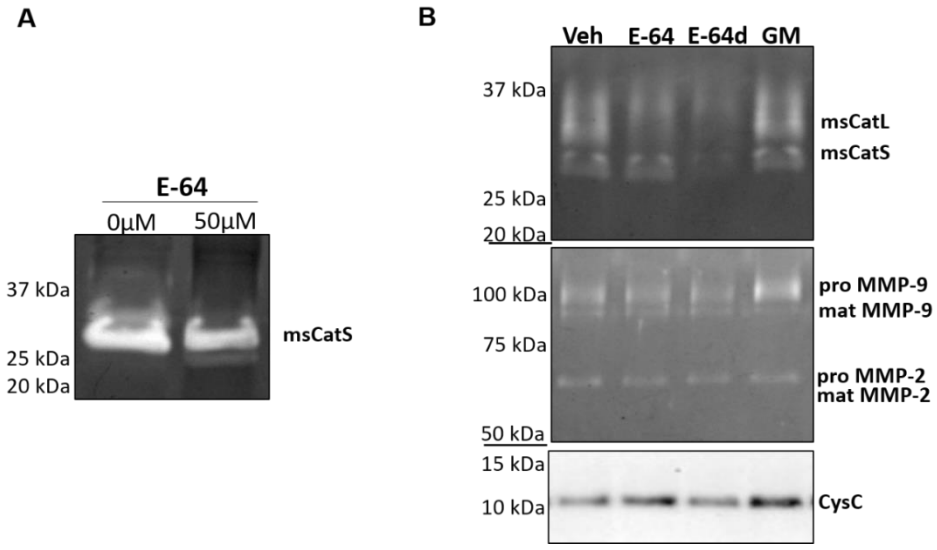

Figure 5.4. E-64 does not cause inhibitor induced cathepsin S upregulation in murine macrophages not expressing human cathepsin L. (A) RAW 264.7 macrophages were treated with 50 µM E-64 for 24 hours. The cells were lysed, equal amounts of protein were loaded for multiplex cathepsin zymography. (B) RAW 264.7 macrophages were treated with 5 µM E-64, 5 µM E-64-d, or a vehicle control for 24 hours. Conditioned media was collected and equal volume amounts were loaded for cathepsin and MMP zymography.

Elevation of cathepsin S due to E-64 did not occur in murine macrophages, which do not have an orthologue for human cathepsin L (Fig.5 4), unlike what was seen in the human mammary tissues and epithelial cells (Fig. 4.1 and Fig. 5.1). Murine mammary fat pads were harvested and incubated with increasing amounts of E-64 for 24 hours to test the hypotheses that human cathepsin L is needed to cause the inhibitor-induced upregulation of cathepsin S in mammary tissue. The tissue was homogenized and equal amounts of protein were loaded for multiplex cathepsin zymography and Western blot analysis. Similar to the RAW 264.7 macrophages, the amount of active cathepsin S did not change due to the incubation of small molecule (n=6) (Fig. 5.5). The amount of pro cathepsin S and murine cathepsin L protein was increased as detected by Western blot (n=3) (Fig. 5.5).

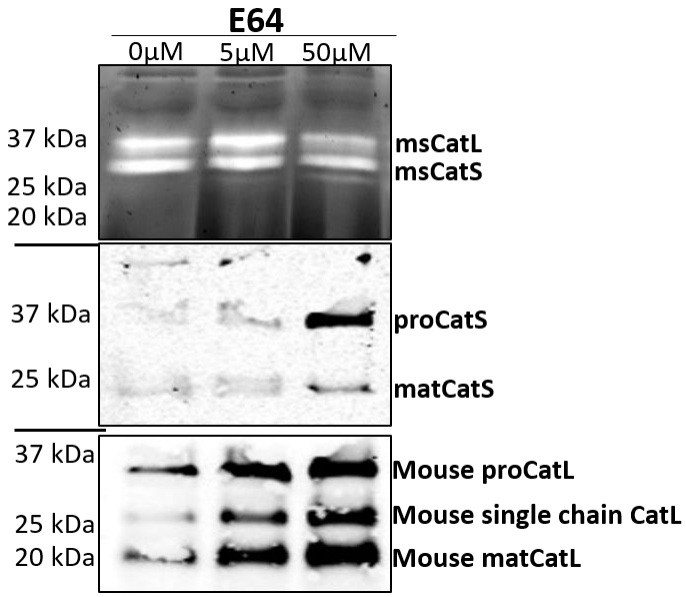

Figure 5.5. Active cathepsin S elevation due to E-64 does not occur in murine mammary fat pads that do not express human cathepsin L. (A) Mammary fat pad tissue samples obtained from apolipoprotein E (apoE) -/- mice were incubated ex vivo with increasing amounts of E-64 for 24 hours prior to being homogenized and equal amounts of protein loaded for cathepsin zymography and Western blot analysis (n=6-8).

To determine if cathepsin inhibition would affect breast cancer cell invasion, a collagen gel was polymerized on top of RFP tagged MDA-MB-231 breast cancer cells transfected to overexpress either cystatin C, cystatin B, or RFP. After 24 hours incubation, the number of invading cells into the collagen gel was visualized using confocal microscopy. There was an increase in the number of invading cells into the collagen gel with the cells overexpressing cystatin C compared to the RFP control cells. The same was seen with MDA-MB-231 cells overexpressing cystatin B (n=4) (Fig. 5.6A).

Since cancer invasion can occur due to ECM degradation [5, 137, 139], MDA-MB-231 cells overexpressing cystatin C, cystatin B, or a control were incubated with DQ-gelatin for 24 hours and the amount of degraded substrate was quantified using spectroscopy to test the hypothesis that the increase in cancer cell invasion was mediated by substrate degradation. Overexpressing cystatin C or B in MDA-MB-231 cells elevated the amount of degraded gelatin compared to the GFP and non-transfected MDA-MB-231 cells (n=3-5, $p<0.05$) (Fig. 5.6B).

To validate that MDA-MB-231 cells overexpressing cystatin C were producing cystatin C, conditioned media from cystatin C overexpressing MDA-MB-231 cells was collected and immunoblotted for cystatin C using Western blot techniques. Cystatin C protein was upregulated compared to all of the control MDA-MB-231 cells (Fig. 5.6C). Cystatin B protein was also increased in the MDA-MB-231 cells overexpressing cystatin B while none was detected in any of the controls confirming cystatin B overexpression (Fig. 5.9C). To determine the contribution of gelatinase degradation due to either cathepsins or MMPs, the cells were incubated with either 5 μM E-64 or 5 μM E-64d, the cathepsin small molecule inhibitors, or 20 μM GM6001, the broad spectrum MMP small

molecule inhibitor, along with DQ-gelatin for 24 hours. This concentration of E-64 and E-64d was less than what was used in Chapter 4 in order to prevent cellular uptake of the small molecule inhibitors and solely inhibit extracellular proteases. Neither the cathepsin or MMP small molecule inhibitors were able to significantly reduce the amount of gelatinase activity after 24 hours from the cystatin overexpressing cells or the controls (n=5-8) (Fig. 5.6D). This suggests that either cathepsin or MMP activity was not contributing to the gelatin degradation since the inhibitors did not affect substrate degradation, or alternatively, during the incubation period an increase in the amount of secreted active cathepsins or MMPs occurred in response to the inhibitor stimulation to compensate for the cathepsin inhibition.

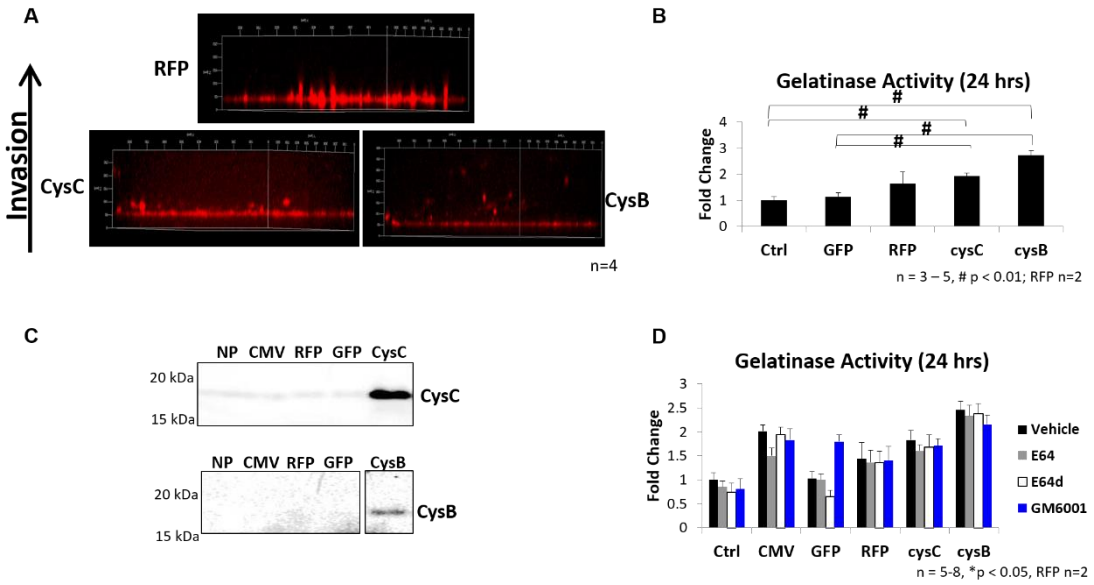

Figure 5.6: Breast cancer cells with cystatins C and B increase cancer cell invasion and gelatin degradation. (A) A 0.5mg/ml collagen gel was polymerized on RFP-labeled MDA-MB-231 breast cancer cells overexpressing cystatin C or cystatin B and incubated for 24 hrs. After the incubation, cell invasion into the collagen gel was determined using confocal imaging. Representative images of the cells were obtained using confocal microscopy. (B) Cystatin C, cystatin B, or control MDA-MB-231 cells were incubated with DQ-gelatin for 24 hours and the amount of gelatin degradation quantified using

spectroscopy. (C) Equal amounts of cell lysates of MDA-MB-231 cells overexpressing cystatin C or B or controls were loaded for immunoblotting analysis. (D) Cystatin C overexpressing, cystatin B overexpressing, or control MDA-MB-231 cells were incubated with DQ-gelatin with or without E-64, E-64d, or GM-6001 for 24 hours and the amount of gelatin degradation quantified using spectroscopy.

Since compensation mechanisms could be occurring with cathepsin and MMP inhibitors to maintain gelatinase degradation, MDA-MB-231 cells were transfected to overexpress either cystatin C, cystatin B, or a control to test the hypothesis that the amount of secreted cathepsins was increased due to cystatin overexpression. After 24 hours, conditioned media was collected, concentrated, and equal volumes were loaded for multiplex cathepsin zymography or MMP zymography. The amount of secreted active cathepsin S did not differ between cells overexpressing cystatin C or B compared to the transfection controls (n=3) (Fig. 5.7A). There was also no difference in the amount of secreted cathepsin V. Even though the total amount of secreted cathepsins did not change after 24 hours, MMP zymography was ran on the conditioned media to determine if the amount of secreted MMPs was altered with cystatin overexpression. Similar to the secreted cathepsins, the cystatin overexpression did not cause any changes in the amount of pro or mature MMP-2 or MMP-9 as detected by MMP zymography (Fig. 5.7A).

Cathepsins S and cathepsin L were incubated with increasing amounts of recombinant cystatin C to test the hypothesis that cystatin C remains bound to cathepsins and decrease the active cathepsin signal as detected by the multiplex cathepsin zymography. The samples were then loaded for multiplex cathepsin zymography and Western blot. The zymography signal from cathepsin S decreased 90% while the cathepsin L signal was reduced by 26% when incubated with cystatin C at a 1:5 ratio (Fig. 5.7B). This indicates that the interactions between the cathepsins S or L and cystatin C proteins remain intact

and the reduction in the active cathepsin signal seen in the zymography of the conditioned media could have been due to the inhibition and sustained binding between the cathepsins and cystatin C.

Although the secreted active cathepsins amounts was not affected by cystatin C or B overexpression, MDA-MB-231 cells overexpressing cystatin C or B were incubated with 5 μM E-64, 5 μM E-64d, or 20 μM GM6001 for 24 hours to ascertain if addition of the small molecule inhibitors would inhibit the secreted cathepsins or MMPs. Neither E-64 nor E64d was able to decrease the amount of active secreted cathepsins L or V. GM6001, the MMP inhibitor, also had no effect on the amount of secreted MMP-2 or MMP-9 (Fig. 5.7C).

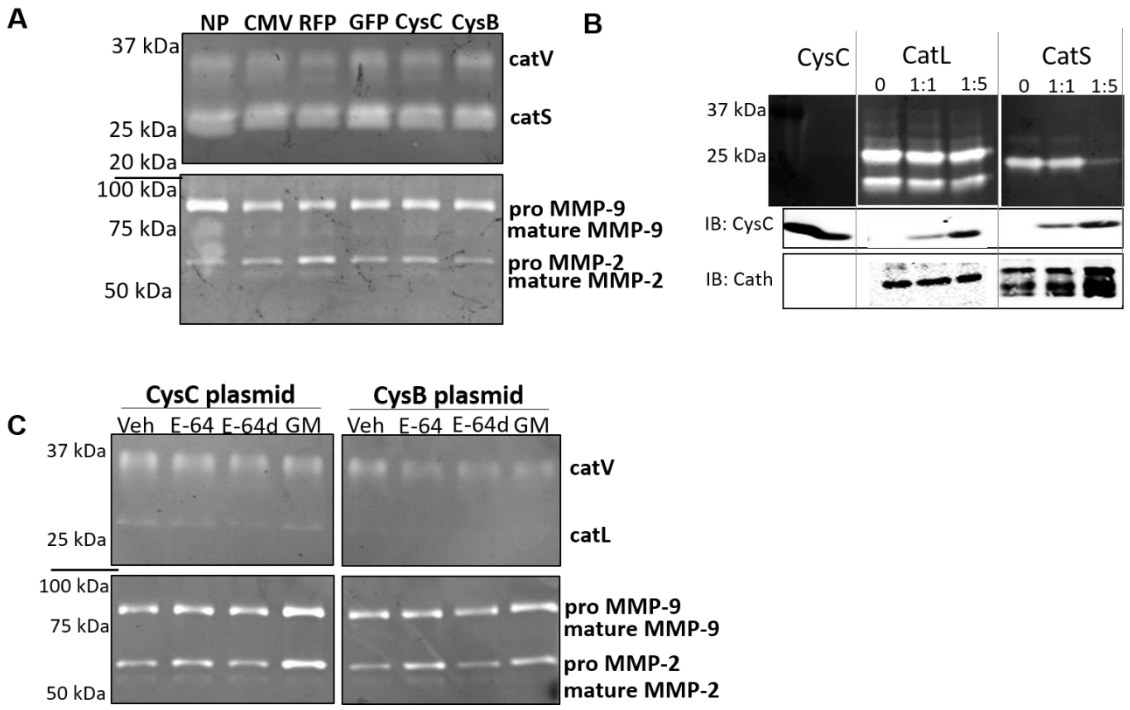

Figure 5.7. Cystatin C overexpression does not change the amount of secreted cathepsins. (A) MDA-MB-231 cells were transfected to overexpress cystatin C, cystatin B, or a control. After 24 hours the conditioned media was collected, concentrated, and assayed using cathepsin and MMP zymography. (B) Recombinant cathepsin S and cathepsin L protein was incubated with increasing amounts of cystatin C protein for 1 hour, followed by multiplex cathepsin zymography and Western blot analysis. (C) Conditioned media of MDA-MB-231 cells transfected with cystatin C or B plasmids and treated with the cathepsin inhibitors E64, E64d, the MMP inhibitor GM6001 (GM), or a control (Veh) was collected and assayed using cathepsin or MMP zymography. NP, no plasmid, CMV, CMV promoter.

Albeit, neither overexpression of cystatin C or B nor the addition of small molecule inhibitors affected the amount of secreted cathepsins after 24 hours, it was hypothesized that this was due to changes in the amount of intracellular cathepsins that could be targeted for secretion. Since cystatin C is a more potent cathepsin inhibitor [12], the following studies focused on the effect of cystatin C overexpression. To test this hypothesis, MDA-MB-231 cells were transfected to overexpress cystatin C or a control followed by incubation with 50 µM E-64 or 50 µM E-64d for 24 hours. A higher

concentration was used compared to the previous experiments to ensure that the small molecule inhibitors were taken up by the cells. Overexpression of cystatin C increased the amount of active cathepsin S compared to the empty vector control (n=3, $p < 0.05$) (Fig. 5.8A). This was in contrast with the secreted cathepsins (Fig. 5.8A) which did not change due to cystatin C overexpression. Not only cystatin C overexpression, but incubation with 50 μM of the small molecule E-64 increased the amount of active cathepsin S to the same amount detected when overexpressing cystatin C. Cathepsin L was only decreased with E-64 incubation and not with cystatin C overexpression (n=3) (Fig. 5.8A). This suggests that cystatin C overexpression elevated the total amount of intracellular active cathepsin S, but not the secreted amounts. In addition, E-64d incubation caused active cathepsin S elevation along with active cathepsin L reduction.

To determine if cathepsin S mRNA expression was upregulated with the elevation in cathepsin S due to cystatin overexpression, MDA-MB-231 cells were transfected to overexpress cystatin C or cystatin B. After 24 hours, the cells were lysed and quantitative real-time RT-PCR was conducted to measure the amount of cathepsin S mRNA. Overexpressing cystatin B significantly elevated cathepsin S mRNA expression compared to the control cells (n=3, $p<0.05$) (Fig. 5.8B). MDA-MB-231 cells overexpressing cystatin C did not significantly upregulate cathepsin S mRNA (n=3, $p=0.22$) (Fig. 5.8B). This suggests that cystatin C overexpression did not increase active cathepsin S levels due to increased cathepsin S transcriptional regulation.

Since cystatin C and cathepsin S co-localized after cystatin C treatment (Fig. 4.4), MDA-MB-231 cells overexpressing cystatin C were incubated for 24 hours, fixed, immunostained for cathepsin S, cathepsin L, or Cystatin C, and imaged using confocal

microscopy to test the hypothesis that overexpressed cystatin C protein would co-localize with cathepsin S and not with cathepsin L. In representative confocal images of MDA-MB-231 cells overexpressing cystatin C, cathepsin S and cystatin C were co-localized, compared to the lack of co-localization found in the control cells. Cathepsin L was not co-localized with cystatin C in the cystatin C overexpressing cells or the controls (Fig. 5.8C).

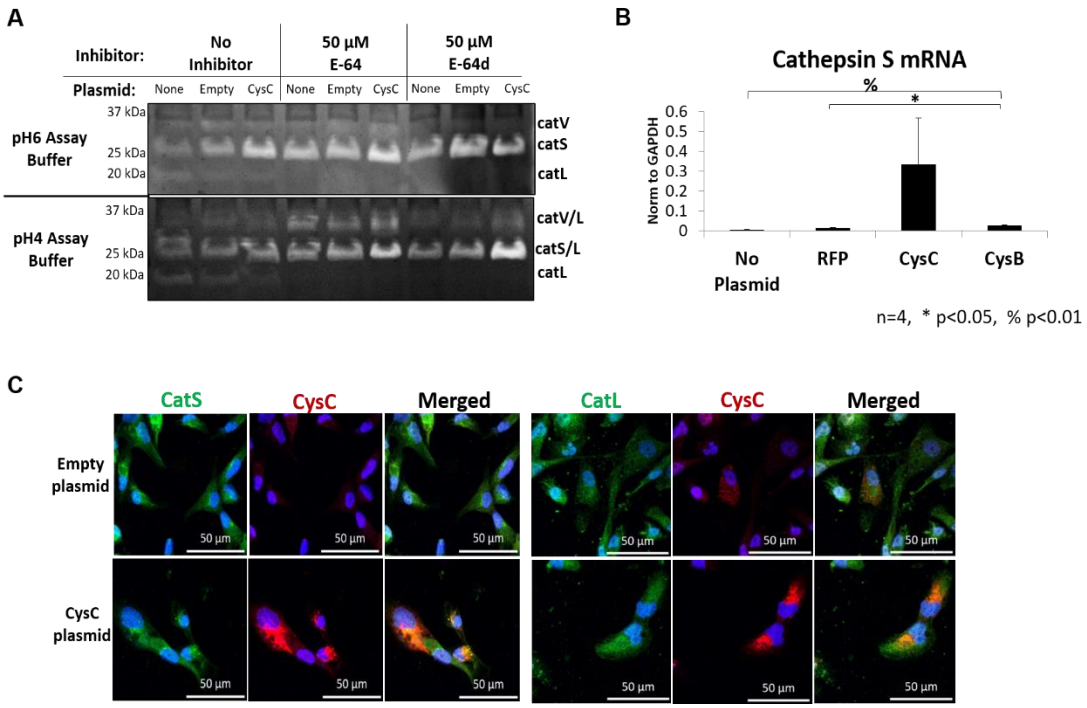

Figure 5.8. Intracellular active cathepsin S elevation occurs with cystatin C overexpression. (A) MDA-MB-231 cells were transfected with either an empty vector or cystatin C plasmids followed by incubation with E-64 or E-64d for 24 hours. After 24 hours, the cells were lysed, equal amounts of protein were loaded for multiplex cathepsin zymography with a pH6 or pH4 assay buffer, and the active cathepsin bands were quantified using ImageJ. The amount of active cathepsin S in the cystatin C transfected cells increased compared to the CMV plasmid control (n=3, $p < 0.05$). (B) MDA-MB-231 cells overexpressing cystatin C, cystatin B, or a control were lysed and cathepsin S mRNA expression quantified with qRT-PCR (n=4). (C) MDA-MB-231 cells were transfected with either an empty vector plasmid or plasmid containing cystatin C for 24 hours. The cells were fixed and stained for cathepsin S (Alexa Fluor® 488, green), cathepsin L (Alexa Fluor® 488, green), or cystatin C (Alexa Fluor® 568, red). Bars, 50 µM.

5.4 Discussion

Cathepsins have been linked to cancer progression and overexpression of cystatins, including cystatin C, reduced primary tumor volume and metastasis in mice. [7, 10, 11]. Our results have demonstrated overexpression of cystatin C not only elevates the amount of intracellular active cathepsin S, but also increases human MDA-MB-231 breast cancer cell invasion and gelatinase activity. This was validated with E-64 which elevated intracellular active cathepsin S in human mammary non-cancerous tissue, MDA-MB-231 human breast cancer cells, and THP-1 human macrophages. This unexpected finding is also seen in data published in the British Journal of Clinical Pharmacology during November 2014 from a clinical trial that detected an increase in cathepsin S activity and protein mass in the plasma of healthy patients a few days after treatment with the cathepsin S inhibitor LY3000328 [133]. This inhibitor-induced upregulation of cathepsin S appears to be specific to human, and not murine, cells and tissues. This study also used murine cells and tissues to investigate the effects of the cathepsin inhibitor E-64 on macrophages and mammary fat pads. Interestingly, the cathepsin inhibitor did not change the amount of active cathepsin S in the murine macrophages and mammary fat pad, which does not contain an orthologue to the human cathepsin L. All of this suggests that human cathepsin L is involved with regulating the inhibitor-induced cathepsin S upregulation and highlights the importance of interpreting *in vivo* mouse model studies and clinical trials using mice since mice do not express the orthologue to human cathepsin L. In addition, this work demonstrates a cathepsin inhibitor response which elevates the amount of the target cathepsin. This will provide insight into understanding how perturbations due to inhibition within a proteolytic network can effect individual

cathepsins which could lead to increased invasion or metastasis. This knowledge can help guide the development and optimization of cathepsin inhibitors for therapeutic usage.

This study demonstrates that even in non-cancerous tissue, the broad spectrum cysteine cathepsin inhibitor is capable of reducing active cathepsin L while elevating the amount of active cathepsin S, although the cancer tissue does not exhibit the inhibitor-induced feedback. The upregulation of active cathepsin S due to E-64 is dependent on the aggressiveness of the epithelial cancer cell. The triple-negative MDA-MB-231 breast cancer cells were the only epithelial cell line with a significant increase in active cathepsin S due to E-64 treatment compared to the ER-positive MCF-7 cells and the non-transformed MCF-10A cells. This could be due in part to the differences in initial baseline amounts of active cathepsins indicating that the upregulation of cathepsin S in response to the inhibitor correlates with the amount of active cathepsins and the aggression of the cell type. Similar to some of the other triple negative cells lines HCC38, HCC 1395, and HCC 1806; the MDA-MB-231 cells had detectable amounts of cathepsins S, L, and V, while cathepsin S was the only detectable cathepsin in the estrogen-positive MCF-7 cells (Fig. 5.2). In addition, there is patient variability with cathepsin proteolytic profiles from human macrophages isolated from peripheral blood mononuclear cells [185]. This is important to note since macrophages invade breast tumors and promote tumor invasion. It has also been reported that the cathepsin proteolytic profile of breast and lung tumors can vary depending on the cancer stage [9]. Thus characterization of baseline cathepsin levels in breast tissue prior to treatment is important in order to understand how a cell or tissue might respond to cathepsin inhibitor treatments. The inhibitor-induced cathepsin S upregulation did not occur in the cancerous

tissue, suggesting that this could be due to the tumor-associated cells within the tumor or due to emergent behaviors that occur with biochemical or biophysical signaling between tumor and tumor-associated cells. We demonstrated here that a feedback mechanism within the proteolytic network upon broad-spectrum inhibition of cysteine cathepsins in breast cancer cells elevates the amount of intracellular active cathepsin S. Since this upregulation is due to cysteine cathepsin inhibitor treatments, it suggests that the elevation of cathepsin S could be due to cellular mechanisms compensating for inhibition of other members in the cysteine cathepsin family. Interestingly, the amount of secreted cathepsins remained the same unlike the intracellular cathepsins. This could be accounted by an upregulation in secretion of intracellular cathepsins to compensate for inhibition of extracellular cathepsins although further investigation would need to be conducted to validate. This could also suggest the mechanism behind the increased invasion and gelatinase activity with cystatin C overexpression.

All of this, along with the reports of compensatory responses in cathepsin knockout mouse models [60, 113-115, 171], suggests the use of cathepsin inhibitors for therapeutic uses. However, the use of cysteine protease inhibitors will need to be further studied since we have clearly shown here that the broad inhibitors E-64- and cystatin C-induced cellular feedback upregulates the active cathepsin S protein. This could have negative physiological consequences since cathepsin S is known to have specific cellular functions [75, 140, 181, 186, 187].

It was also demonstrated here that using the broad spectrum inhibitor E-64 upregulated the pro-form of cathepsin L. Jung et al and colleagues also used the broad-spectrum intracellular cathepsin inhibitor E-64d, and reported an increase in pro-

cathepsins L, B, and D protein and suggested this was due to impaired processing of cathepsins. This, in turn, resulted in lysosomal dysfunction [188]. This is important since signaling between lysosomes and the nucleus, which occurs due to nuclear translocation of Transcription Factor EB (TFEB) from lysosomes, regulates lysosomal biogenesis [189, 190]. Inhibition of active cathepsin L due to E-64 treatment could result in reduced autocatalytic activation of pro-cathepsin L into the mature form or the activation of other cathepsins activated or regulated by the mature cathepsin L. This is especially critical for cathepsin S since this study was able to show the involvement of cathepsin L in cathepsin S regulation. It was also seen that both the pro- and mature forms of cathepsin S were upregulated, this indicates that activation of cathepsin S into the mature form was still occurring, but suggests an increase in production. This was the first report of cathepsin L involvement of cathepsin S regulation between cathepsins S and highlights the importance of maintaining proteolytic homeostasis between the two proteases especially when using therapeutic cathepsin inhibitors to prevent substrate degradation and invasion.

5.5 Conclusion

These results demonstrate an inhibitor-induced feedback that occurs upon cathepsin inhibition and one molecular mechanisms regulating the cellular feedback response. This response between inhibition and cathepsin proteolytic activity appears to be an attempt to maintain a proteolytic homoeostasis. Not only are these findings important for understanding and preventing breast cancer metastasis, but also for other diseases such as HIV, atherosclerosis, and osteoporosis where these proteases are upregulated and highlights a need to understand cathepsin interactions in a proteolytic network.

.

CHAPTER 6

Future Considerations

6.1 Major Findings

The work presented in this thesis focused on addressing the issues accompanied with the use of cysteine cathepsin therapies in breast cancer. While cathepsins are upregulated in cancer and are potential candidates for breast cancer therapies, adverse side effects occurred with cathepsin protease inhibitor therapies. Although cathepsin inhibitor therapies have been efficacious in inhibiting cathepsins and stopping the progression of the disease, both the off target effects and the upregulation in active cathepsins due to compensatory networks complicate the development and use of cathepsin inhibitors. This work elucidated the cellular response of cathepsins due to broad spectrum cysteine cathepsin inhibitors in breast cancer using small molecule or protein cathepsin inhibitors in human cells and tissues. This could assist with the development of more effective cathepsin inhibitors for cancer therapies, as well as provide insight for proper therapeutic dosing options. Pharmaceutical cathepsin inhibitors being developed are designed to be highly selective for a specific protease such as cathepsin S or cathepsin K [13, 24, 215]. Selectively targeting one cathepsin may help reduce some of the feedback that is occurring with the broad spectrum cathepsin inhibitors. All of this points to a compensatory mechanism that is induced in an attempt to maintain proteolytic homoeostasis. This is critical for developing effective therapeutics and dosing strategies for cancer invasion and metastasis since high doses of cathepsin inhibitor would increase cathepsin activity while low doses would be more effective at inhibiting cathepsins. In addition, although some cathepsin inhibitors have been designed to not passively cross

the cellular membrane, uptake of the inhibitor could still occur due to pinocytosis or endocytosis. Since the cellular uptake of cystatin C was correlated with elevated active cathepsin S, it is important that proper dosing strategies are considered to lower the pericellular concentration of the inhibitor and prevent uptake of the inhibitor due to pinocytosis. As this work has demonstrated, high doses of cathepsin inhibitor could potentially increase cancer cell invasion. Use of lower doses that prevent internalization of the inhibitor would be more effective at inhibiting invasion.

The work in this thesis suggest that the upregulation of cathepsin S due to cathepsin inhibitors is due to post-transcriptional regulation such as increased activation. The increased active cathepsin is probably not due to the inhibitor acting as an agonist since cystatin C and E-64 form near irreversible or irreversible bonds, respectively, at the active site of the cysteine cathepsins [106] and the inhibitors have not been shown to interact with any other sites on the cathepsin protein structures.

In order to develop a multiplex cathepsin zymography assay that can selectively distinguish multiple cathepsins, cathepsin specific pH and substrate modifications were made [154]. While previous studies established the detection of cathepsin K activity by cathepsin zymography at femtomole quantities [124], this study developed tools to selectively detect cathepsins K, L, S, and V activity from one cell extract or preparation was established. This technique has many benefits: 1) it does not require antibodies making it relatively inexpensive and species-independent, 2) separation of proteins by molecular mass and electrophoretic migration visually confirm enzyme identity, 3) densitometry can be used for quantitative analysis, and 4) pH change can confirm specific cathepsin activity. In addition, the broad application of these tools allows use in basic

science research and for clinical purposes involving cathepsin-mediated tissue remodeling. It is medium throughput and inexpensive protocol with widespread utility that can be used in a variety of settings.

Elucidating cellular feedback mechanisms between cathepsins and inhibition is important when studying tissue remodeling in physiology and pathophysiology. However, little is known about the cellular feedback mechanisms that initiate cathepsin production and activation and its effect on proteolytic matrix degradation. This work has effectively shown that both small molecule inhibitors and protein cathepsin inhibitors cause cellular responses in human epithelial cancer cells and macrophages which elevate intracellular active cathepsin S. This response was due to preferential localization of the inhibitor to cathepsin S and not to other proteases such as cathepsin L, which was located in the cytoplasm. Trafficking of the inhibitor to endo-lysosomal vesicles could prevent degradation of lysosomal macromolecules and cargo proteins. Mutation or inactivation of lysosomal proteases has been shown to lead to lysosomal storage diseases [216]. These results suggest that cellular preventative measures such as the upregulation of other lysosomal proteases, i.e. cathepsin S, are taken to ensure degradation of lysosomal cargo during inhibitor treatments. While the specific mechanisms causing this feedback are yet to be determined, it is known that signaling between lysosomes and the nucleus regulates lysosomal biogenesis due to nuclear translocation of Transcription Factor EB (TFEB) from lysosome membrane [189, 190].

Since the inhibitor feedback was seen to be due in part to cathepsin L expression, it is important to study cellular feedbacks that are occurring with cathepsin inhibitor treatments in other diseases and not just for breast cancers especially since cathepsin L is

ubiquitously expressed in different cells and tissues. Cathepsin L usually has a higher binding rate to cathepsin inhibitors compared to other cysteine proteases [12, 162] and off target binding of cathepsin L could induce this cellular feedback. This could also explain why a cathepsin S inhibitor caused increased cathepsin S protein in activity in healthy subjects [133]. Although cathepsin L is a lysosomal cysteine protease, it was detected in the cytoplasm of the breast cancer cells where it has functional roles such as cleavage of the GTPase dynamin which results in cytoskeleton reorganization [109], cleavage of the CCAAT-displacement protein/cut homeobox transcription factor [108, 163], and cleavage and modification of histones [164, 165]. Elevation of active cathepsin S due to E-64 occurred in non-cancerous breast tissue, but not cancer tissue. Even though the cathepsin S upregulation did not occur in the cancerous tissue, this indicates that the tumor-associated cells within the tumor may not have this inhibitor-induced feedback response or emergent behaviors could occur between tumor and tumor-associated cells due to biochemical or biophysical signaling. The feedback response was dependent on the type of epithelial cancer cell since it did not occur in the non-transformed MCF-10A, but was prominent in the triple negative MDA-MB-231 cells, the most aggressive form of breast cancer [37]. This suggests that this differential response could be due to differences in the amount of cathepsins or due to the aggressive phenotype with each cell type within the individual tissues and highlights the tissue-dependency of this inhibitor-induced response. This could be due in part to the differences in initial baseline amounts of active cathepsins indicating that the upregulation of cathepsin S in response to the inhibitor correlates with the amount of active cathepsins and the aggression of the cell type. Epithelial cells were not the only cells that had the inhibitor-induced cathepsin S

elevation, but it was also detected in human macrophages. This could be critical when using cathepsin inhibitors for cancer therapies since the inhibitor-induced cathepsin upregulation occurred in cancer cells and macrophages such as TAMs, which can account for 50% of tumor volume [13, 59]. Thus characterization of baseline cathepsin levels in breast tissue prior to treatment is important in order to understand how a cell or tissue might respond to cathepsin inhibitor treatments.

In addition, breast cancer cell invasion and gelatinase activity was increased due to overexpression of the cathepsin inhibitor cystatin C. The inhibitor overexpression also upregulated intracellular active cathepsin S. In this study the cellular invasion that occurred due to inhibition was associated with elevated substrate degradation suggesting protease-mediated cellular invasion.

6.2 Development of multiplex cathepsin zymography

This work has shown the use of multiplex cathepsin zymography with various cells and tissues and a different of types of diseases. This is important since cathepsins are upregulated in many diseases in which tissue remodeling occurs including cancer, bone metastasis [13, 15-17], cardiovascular disease[2, 73-75], and other diseases associated with elastinolytic remodeling [79]. Not only can this tool be used to study multiple diseases but can study multiple cathepsins using one assay. This has limited previous studies investigating cathepsins. With this platform, cathepsins K, L, S, and V can all be studied concurrently which is significant when studying these proteases as a system especially since this group of four cathepsins includes the most potent collagenase, the most potent elastase, and a ubiquitously expressed cathepsin. Using these tools has

potential use clinically as a diagnostic tool to detect diseased tissues due to its sensitivity and specificity [9]. This also can be used in low resource settings due to its affordability.

6.3 Understanding compensatory networks

This report revealed compensatory mechanisms that upregulate cathepsin S during broad spectrum cathepsin inhibition in human breast tissue, breast cancer cells, and macrophages. This is supported by other reports that have shown that double deletion of cathepsins S and B, causes an upregulation of cathepsin Z demonstrating compensatory mechanisms that occur in the tumor microenvironment [113]. Compensatory mechanisms which upregulate cathepsins can also occur in single cathepsin knockout models [60, 114, 115].

The work here that identifies inhibitor-induced upregulation of cathepsins and possible mechanisms could be extended to other protease families such as MMPs, serine, and aspartic proteases, especially since substrate promiscuity, activation, and degradation occurs within each of these families similar to that in the cysteine proteases. The findings of this work could also be extended to study how proteases in one family affects other proteases in other families. Protease activation between protease families has already been shown [217] which suggests that inhibition within one network could affect other protease families.

This work has highlighted the regulation of cathepsin S due to cathepsin L inhibition or expression. While this response was primarily shown in epithelial cancer cells, it was not specific to epithelial cancer cells but also occurred in macrophages. Both the MDA-MB-231 breast cancer cells and THP-1 macrophages used in this report expressed multiple cathepsins including cathepsins S and L. This suggests that the inhibitor-induced

response may occur in high cathepsin producing cells such as invasive cancers or in cells expressing cathepsin L, which is ubiquitously expressed.

The cathepsin proteolytic network contains 11 proteases, but the expression and activity of individual cathepsins depends on the cell and tissue type. Due to such variation, there has been a large focus on investigating the effect of single proteases on substrate cleavage. This has made it difficult to investigate the dynamics and interactions among proteases within the cathepsin proteolytic network and its overall effect on matrix degradation. Previously, our lab has examined and modeled cathepsin S and cathepsin K interactions and its effect on collagen degradation [181]. This model can be expanded to include cystatins, MMPs, and tissue inhibitor of MMPs (TIMPs) and their subsequent interactions. An ordinary differential equations based computational model can be developed to better understand the interactions and dynamics within the cathepsin proteolytic network. Ultimately, the information in this study will play an important role in the potential development of a model that can be used to better understand relationships between the cathepsin proteases and their inhibitors. This model could help discover other compensatory mechanisms that would have consequences on substrate degradation in matrix-remodeling diseases such as atherosclerosis, osteoporosis, and metastatic cancers.

APPENDIX A

Uncovering breast cancer mediated ECM remodeling and paracrine signaling effects on mesenchymal stem cell differentiation and cancer cell survival

A.1 Introduction

With a dismal five year survival rate of 26% for patients with metastatic breast cancer tumors there is a critical need for more research focused on prevention and treatment of metastases [28]. In order to develop therapies for cancer metastasis, a better understanding of biochemical signaling between cancer cells and cells within the surrounding metastatic microenvironment is essential. Bone is the 5th most common metastatic site in breast cancer patients accounting for ~9.5% of the metastatic sites [191]. Bone metastatic breast cancers tend to form osteolytic lesions as a result of osteoclast stimulation [192, 193] and result in a higher risk of fractures due to brittle bone [194].However, when cancer cells arrive in the bone marrow niche they begin to interact with and influence native bone marrow cells [195, 196] including mesenchymal stem cells (MSCs), which differentiate into either osteoblasts, adipocytes, or chondrocytes depending on the biochemical and biophysical signals [197-199]. More studies need to be conducted to understand the effect of breasts cancer cells on MSCs' differentiation into osteoblasts or adipocytes.

Osteoblasts synthesize collagen to promote bone formation in response to osteoclast bone resorption [200, 201]. When there is an imbalance in bone remodeling skeletal disorders such as osteoporosis occurs [200]. Metastatic prostate cancer cells, which form osteoblastic lesions, induce osteogenesis in MSCs [196]. It was previously suggested that bone diseases such as osteoporosis are associated with adiposity [202].

Cysteine cathepsins K and S are involved with adipocyte differentiation [136, 203]. In 2007, Yang et al showed that the protease mouse cathepsin L, which is orthologous to human cathepsin V, controls adipogenesis in mice through fibronectin degradation, demonstrating that proteolysis is linked to adipocyte differentiation[135]. Investigating cathepsin activity is important since their expression and activity is upregulated in breast cancer [5, 6, 82]. Cathepsins degrade extracellular matrix (ECM) proteins including type I collagen[3], an important matrix protein for osteogenic differentiation [204, 205].

There is a need to understand how breast cancer cells subvert and alter the bone microenvironment to promote their own survival. It is important to investigate how breast cancer cells affect MSC differentiation and cathepsin expression in order to understand their role in promoting osteolytic lesions. Due to all of this it was hypothesized that metastatic breast cancer cells would cause preferential differentiation of MSCs toward an adipogenic lineage.

A.2 Materials and Methods

A.2.1 Cell Culture

Human MSCs (hMSCs) (Obtained from Tulane University) were cultured in complete culture medium consisting of Minimum Essential Medium, Alpha 1X (Corning Cellgro) supplemented with 16.5% fetal bovine serum (FBS) – Premium Select (Atlanta

Biologicals), 1% L-glutamine (Life Technologies), and 1% penicillin/streptomycin (Life Technologies). The osteogenic differentiation media contained the complete culture medium with 10 nM dexamethasone, 20 mM β-glycerolphosphate, and 50 μM L-ascorbic acid 2-phosphate. The adipogenic differentiation media contained the complete culture medium with 0.5 μM dexamethasone, 0.5 mM isobutylmethylxanthine, and 50 μM indomethacin. The MSCs were differentiated for 6 to 21 days in either complete culture, osteogenic, or adipogenic induction media with media replaced with fresh media every three days. Human MSCs were co-cultured in either complete culture, osteogenic, or adipogenic induction media directly with or without RFP labeled MDA-MB-231 breast cancer cells, GFP labeled MCF-7 breast cancer cells, or non-tumorigenic MCF-10A epithelial cells. In addition, hMSCs were co-cultured indirectly with either MDA-MB-231, MCF-7, or MCF-10A cells in either complete culture, osteogenic, or adipogenic induction media using a 0.2 μm pore sized membrane or conditioned media from the above mentioned tumorigenic and non-tumorigenic epithelial cells. Only passage four to six hMSCs were used in these studies.

A.2.2 Multiplex Cathepsin Zymography

Tissue and cell lysates or conditioned media was collected after a specified incubation duration. Total protein amounts in the cell lysates were determined using the Pierce Micro BCA Protein Assay (Thermo Scientific) and prepared as previously described [124]. The conditioned media was concentrated using VivaSpin 500 concentrators (Sartorius Stedim Biotech GmbH) and the same amount of volume per sample was loaded. The cell lysates and conditioned media were assayed as previously described, but briefly, equal amounts of protein or volume were loaded in gelatin embedded

polyacrylamide gels to separate the protein using SDS-PAGE techniques [154]. The gel was washed in renaturing buffer and assay buffer followed by staining with a Coomassie blue stain and destain. The gel was then imaged using an ImageQuant LAS 4000 (GE Healthcare Life Sciences). The bands were then quantified using ImageJ.

A.2.3 Western Blots

Cell lysates or conditioned media was collected after a specified incubation duration. Total protein amounts in the cell lysates were determined using the Pierce Micro BCA Protein Assay (Thermo Scientific). The conditioned media was concentrated using VivaSpin 500 concentrators (Sartorius Stedim Biotech GmbH) and the same amount of volume per sample was loaded. The cell lysates and conditioned media were assayed as previously described, but briefly, equal amounts of protein or volume were loaded in gelatin embedded polyacrylamide gels to separate the protein using SDS-PAGE techniques. Protein was transferred to a nitrocellulose membrane (Bio-Rad) and proteins were then probed with primary antibodies overnight at 4°C followed by an hour secondary antibody incubation.

A.2.4 Osteogenic and adipogenic differentiation assays

Osteogenic differentiation was measured using an alkaline phosphatase assay. Briefly, cells were rinsed with phosphate buffer saline (PBS) and cells were lysed with 0.2% NP-40 lysis buffer in 1 mmol/L $MgCl_2$. Lysates were collected and incubated with a 1:1 solution of the substrate p-Nitrophenyl phosphate and 221 Alkaline Buffer Solution for 30 minutes at 37°C. The reaction was stopped using 1N NaOH. Absorbance was measured using spectroscopy. Adipogenic differentiation was measured by rinsing cells with PBS and staining with 0.3% Oil Red-O (made fresh) for 20 minutes at room

temperature to detect the fat lipid droplets. The cells were rinsed with PBS and imaged using microscopy. The dye was then extracted with isopropanol and the absorbance of the Oil Red-O dye was quantified using spectroscopy.

A.2.5 Quantitative real time PCR

Human MSCs were cultured in expansion, osteogenic, or adipogenic induction media and were co-cultured with or without breast cancer cells. Cells were lysed and RNA isolated using the RNeasy Mini Kit (Qiagen). The RNA was reversed transcribed using SuperScript™ III Reverse Transcriptase (Invitrogen) and cDNA was amplified using SYBR® Green PCR Master Mix (Applied Biosystems) and primer sequences for osteogenic factors such as runt-related transcription factor 2 (RUNX2), and alkaline phosphatase (Alk Phos); adipogenic factors such as lipoprotein lipase (LPL) and peroxisome proliferator-activated receptor gamma (PPAR-γ); or the housekeeping control GAPDH.

A.2.6. Flow Cytometry

Human MSCs co-cultured indirectly with either MDA-MB-231, MCF-7, or MCF-10A cells in either complete culture, osteogenic, or adipogenic induction media using a 0.2 µm pore sized membrane. The hMSCs were collected using trypsinization and the cell pellet was resuspended in 0.5 mL PBS with 5 µL of a 50 µg/ml 7-AAD (Biolegend) and 5 µL FITC Annexin V (BD Pharmingen^{TM}) per million cells and incubated for 15 minutes at room temperature in the dark before analysis. The cells were then strained into a round bottom polystyrene tube and analyzed using BD LSR II Flow Cytometer.

A.3 Results

A.3.1 Adhesion of osteogenic hMSCs is disrupted during heterotypic culture with breast cancer cells

To test if triple-negative MDA-MB-231 breast cancer cells or estrogen-positive MCF-7 breast cancer cells affect hMSC differentiation due to cell-cell interactions, hMSCs were differentiated for six days in non-inducing, osteogenic, or adipogenic media. Then either RFP tagged MDA-MB-231 cells or GFP tagged MCF-7 cells were added to the culture for an additional three or six days of co-culture. The cells were fixed and imaged using fluorescent microscopy. After three days of co-culture, both the MDA-MB-231 cells and MCF-7 cells were able to form small colonies within the undifferentiated, osteogenic, and adipogenic hMSCs. Osteogenic hMSCs appear more rounded, suggesting loss of adhesion (Fig. A.1A). This was in contrast to the expansion and adipogenic hMSCs which were more spread and were still attached to the culture plate (Fig. A.1A). By day six of the co-culture, the amount of MDA-MB-231 or MCF-7 cells had increased in the co-cultures containing control and adipogenic hMSCs. In the osteogenic co-cultures, the cells had become detached (Fig. A.1B). This occurred with both the triple-negative MDA-MB-231 and estrogen-positive MCF-7 cells.

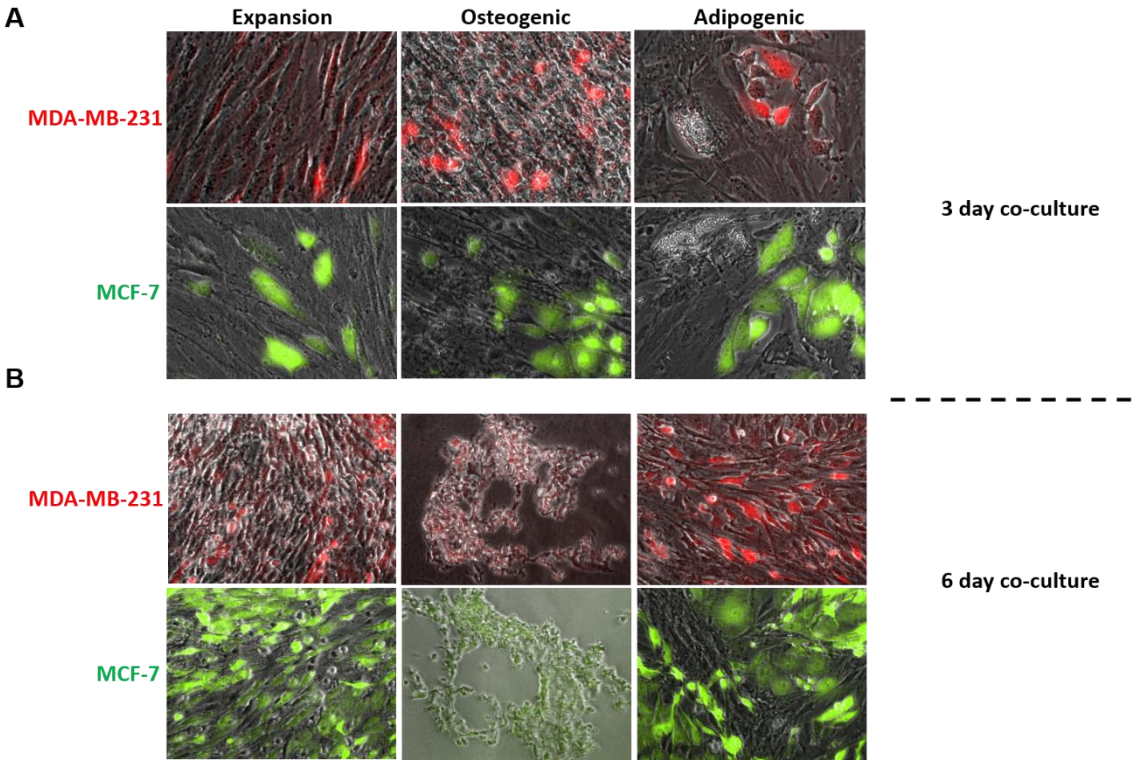

Figure A.1. Cell rounding and detachment increases when breast cancer cells are in direct contact with osteogenic hMSCs. (A) Human MSCs were cultured in non-inducing, osteogenic, or adipogenic media for 6 days. RFP-labeled MDA-MB-231 or GFP-labeled MCF-7 breast cancer cells were seeded directly on the hMSCs and cultured for an additional 3 (B) or 6 days. The location of the cancer cells in relation to the hMSCs was then determined using fluorescent microscopy.

A.3.2 Breast cancer cell paracrine signaling reduces osteogenic differentiation and causes rounded and spindle-like hMSCs

To determine if the cell rounding and detachment that occurred in the osteogenic hMSCs cultured with breast cancer cells was influenced by paracrine signaling, hMSCs were differentiated in osteogenic or control media for six days. To assess the effects of paracrine communication between the cancer cells and hMSCs, MDA-MB-231, MCF-7, or MCF-10A cells were cultured on the apical side of a 0.2 μm pore sized transwell for six days. MDA-MB-231 secreted factors increased the amount of rounded MSCs compared to the cell spread morphology that was detected due to secreted factors of

MCF-10A cells or the hMSCs only control. The same changes in hMSC morphology was observed in the MCF-7 transwell co-culture (Fig. 6.2A). Paracrine signaling from the MDA-MB-231 or MCF-7 cells caused more spindle like projections in the osteogenic hMSCs compared to the controls (Fig. A.2A).

Both the paracrine factors from either MDA-MB-231 or MCF-7 cells were decreasing the spread and affecting the morphology of hMSCs. Cell shape has been reported to influence MSC differentiation down an osteogenic and adipogenic lineage [206]. Due to this osteogenic differentiation was measured in the breast cancer and MSC co-cultures to test the hypothesis that hMSC osteogenic differentiation was decreased with the breast cancer cell co-cultures. hMSCs were cultured in osteogenic or control media for six days followed by co-culture with either MDA-MB-231, MCF-7, MCF-10A transwells or a non-transwell control for and additional six days. After six days of co-culture, hMSCs were lysed and osteogenic differentiation was measured using an alkaline phosphatase assay. Alkaline phosphatase activity was significantly decreased in osteogenic hMSCs that received biochemical communication from MCF-7 cells compared to the osteogenic hMSCs only control ($n=3$, $* p < 0.05$) (Fig A.2B).

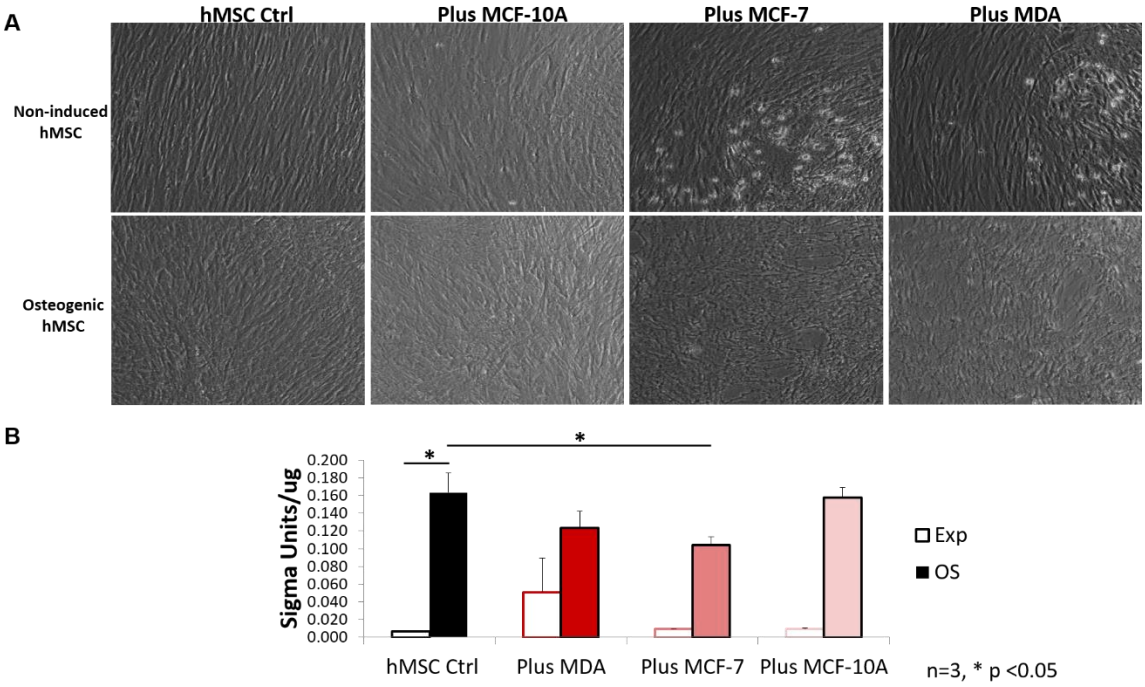

Figure A.2. Human MSCs interacting with breast cancer cells via paracrine signaling form spindle like cell morphology and reduce osteogenic differentiation. (A) Osteogenic differentiation of hMSCs was induced for six days. Induced or non-induced control hMSCs were then incubated with MDA-MB-231 breast cancer cells, MCF-7 breast cancer cells, or non-transformed MCF-10A epithelial cells seeded on a 0.2 μm transwell membrane for 6 days. The hMSCs were fixed and representative images were obtained using microscopy. (B) Cell lysates of the osteogenic and non-induced hMSCs cultured with MDA-MB-231 cells, MCF-7 cells, or non-transformed MCF-10A cells on a 0.2 μm transwell membrane were collected and the amount of alkaline phosphatase activity was quantified by measuring the absorbance of cleaved p-Nitrophenyl phosphate and normalized to total protein (n=3, * $p < 0.05$).

A.3.3 Biochemical signals from breast cancer cells reduces the osteogenic marker RUNX2 mRNA expression in differentiating hMSCs

To validate that the hMSCs were differentiating into osteoblasts, hMSCs were cultured in osteogenic media for three days and then lysed. Equal amounts of cDNA was loaded for quantitative RT-PCR to determine the alkaline phosphatase and RUNX2 mRNA expression. Alkaline phosphatase mRNA expression was upregulated after three days of differentiation unlike the RUNX2 mRNA expression (n=3, *** $p < 0.001$) (Fig A.3A).

Since the biochemical signals from the MCF-7 cells decreased the alkaline phosphatase activity (Fig 6.2B), alkaline phosphatase and RUNX2 mRNA expression, both markers for osteogenic differentiation, was measured in MSCs cultured with MDA-MB-231 and MCF-7 cells in transwells to test the hypothesis that osteogenic mRNA expression would be reduced due to the indirect interactions. Osteogenic or control hMSCs were cultured with MDA-MB-231 or MCF-7 cells on 0.2 μm pore sized transwells, with conditioned media from either breast cancer cell, or a control with hMSCs alone. After six days of co-culture, RUNX2 mRNA expression in the osteogenic hMSCs was decreased due to MCF-7 signaling from the secreted factors from the transwell system or the conditioned media (Fig. A.3B). The same was seen in non-induced control hMSCs cultured with a biochemical cues from the MCF-7 transwell system or conditioned media (n=3, * $p < 0.05$). Alkaline phosphatase mRNA expression in hMSCs was not changed with any of the culture conditions (n=3).

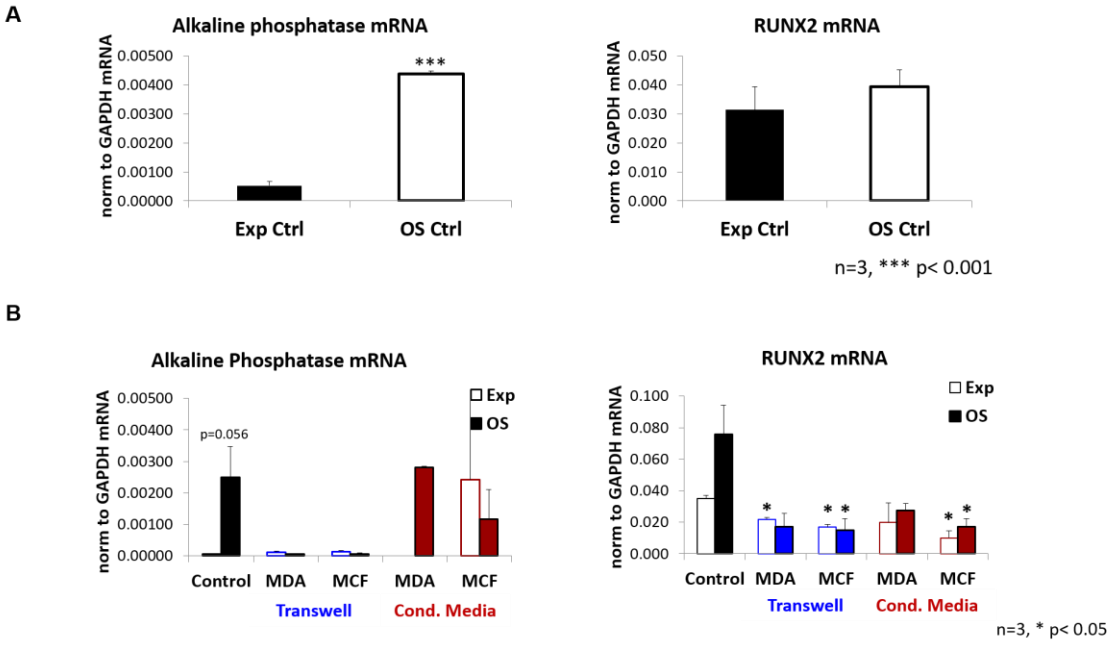

Figure A.3. Breast cancer cells reduce mRNA expression of the late stage osteogenic differentiation marker, RUNX2 in hMSCs. (A) Human MSCs were cultured with osteogenic induction media for 3 days. Cell lysates were collected and alkaline phosphatase and RUNX2 mRNA expression was measured using qRT-PCR (n=3, *** $p < 0.001$). (B) Osteogenic or control hMSCs incubated with MDA-MB-231 breast cancer cells, MCF-7 breast cancer cells, or non-transformed MCF-10A epithelial cells seeded on a 0.2 μm transwell membrane for 6 days were lysed and mRNA expression of alkaline phosphatase and RUNX2 quantified with qRT-PCR (n=3, * $p < 0.05$).

A.3.4 Secreted factors from breast cancer cells reduced the size of osteogenic hMSCs

To test the hypothesis that biochemical communication from breast cancer cells are inducing apoptosis in undifferentiated and osteogenic hMSCs, hMSCs were cultured in osteogenic or control media for six days. For the following six days, the cells were cultured alone or with MDA-MB-231, MCF-7, or MCF-10A cells seeded on 0.2 μm transwell inserts. The hMSCs were then collected and sorted using flow activated cell sorting (FACS). Different subpopulations of the hMSCs were characterized using a scatter plot with side-scattered (SSC), an indicator of cell granularity or internal

complexity, vs forward-scattered (FSC), an indicator of cell surface area or size. There were two subpopulations detected with both the undifferentiated and osteogenic hMSCs. When the hMSCs were cultured alone, 11.9% of hMSCs were found in population 1, which had a smaller cell size as indicated by a lower forward-scattered. A second population detected, that had a larger forward-scatter, contained 64.2% of hMSCs. The number of hMSCs detected in the two populations was similar when the cells were cultured with MCF-10A cells. Biochemical factors from MCF-7 cells increased the amount of undifferentiated hMSCs in population 2 with a 14% fold increase compared to the hMSCs only control. This was in contrast to the hMSCs receiving cues from MDA-MB-231 cells which had a 22% fold decrease in the number of hMSCs found in the 2nd population (Fig. A.4).

Unlike the undifferentiated hMSCs, the number of osteogenic hMSCs in population 2 decreased by 38.6% due to biochemical signaling from MCF-7 cells. Albeit, indirect communication from MCF-7 cells caused a 353% fold increase in the population 1 osteogenic hMSCs. With the paracrine factors from MDA-MB-231 cells, while only a 2.8% fold decrease in the number of osteogenic hMSCs in the 2nd population was detected, there was a 96.4% fold increase in the 1st population (Fig. A.4).

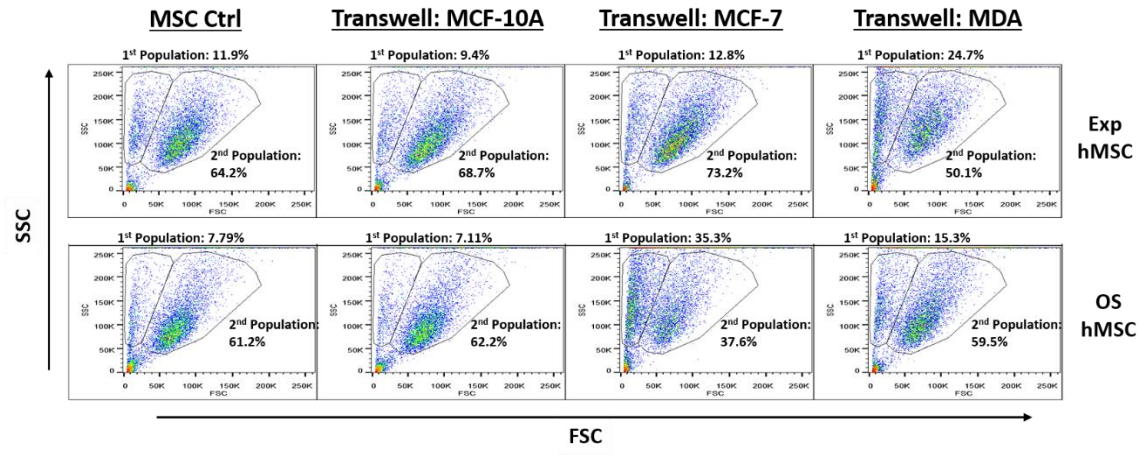

Figure A.4. The size of hMSCs is decreased due to biochemical factors with breast cancer cells. Human MSCs cultured with osteogenic or control media were incubated with transwells seeded with MDA-MB-231 breast cancer cells, MCF-7 breast cancer cells, or non-transformed MCF-10A epithelial cells. Human MSCs were collected and the size and granularity of the cells was determined using FACS.

A.3.5 MDA-MB-231 and MCF-7 cells induce early apoptosis in hMSCs

Since indirect communication from MDA-MB-231 and MCF-7 breast cancer cells increased the number of cells in the 1st population, which has smaller cells as indicated with a lower forward-scattered light; undifferentiated and osteogenic hMSCs receiving indirect cues from the breast cancer cells were collected and stained for Annexin V, an indicator of early apoptosis, and 7AAD, an indicator of late stage apoptosis to test the hypothesis that the smaller hMSCs in population 1 were undergoing apoptosis. All of the hMSCs in population 1, regardless of culture conditions, had over 65 % Annexin V positive staining. MDA-MB-231 biochemical factors caused a 64.9% fold increase in the number of undifferentiated hMSCs that were positive for both Annexin V and 7AAD compared to the hMSC only control. Interestingly, the estrogen-positive MCF-7 cells increased the number of osteogenic hMSCs that were negative for both Annexin V and 7AAD by 182% (Fig. A.5A).

Over 75% of hMSCs in the 2nd population were negative for Annexin V and 7AAD regardless of culture condition. Paracrine signaling from MCF-7 cells elevated the amount of Annexin V staining in both undifferentiated and osteogenic hMSCs by 384% and 315%, respectively. This is in contrast to the MDA-MB-231 paracrine factors which elevated the amount of Annexin V staining only in undifferentiated hMSCs with a 632% fold increase (Fig. A.5B).

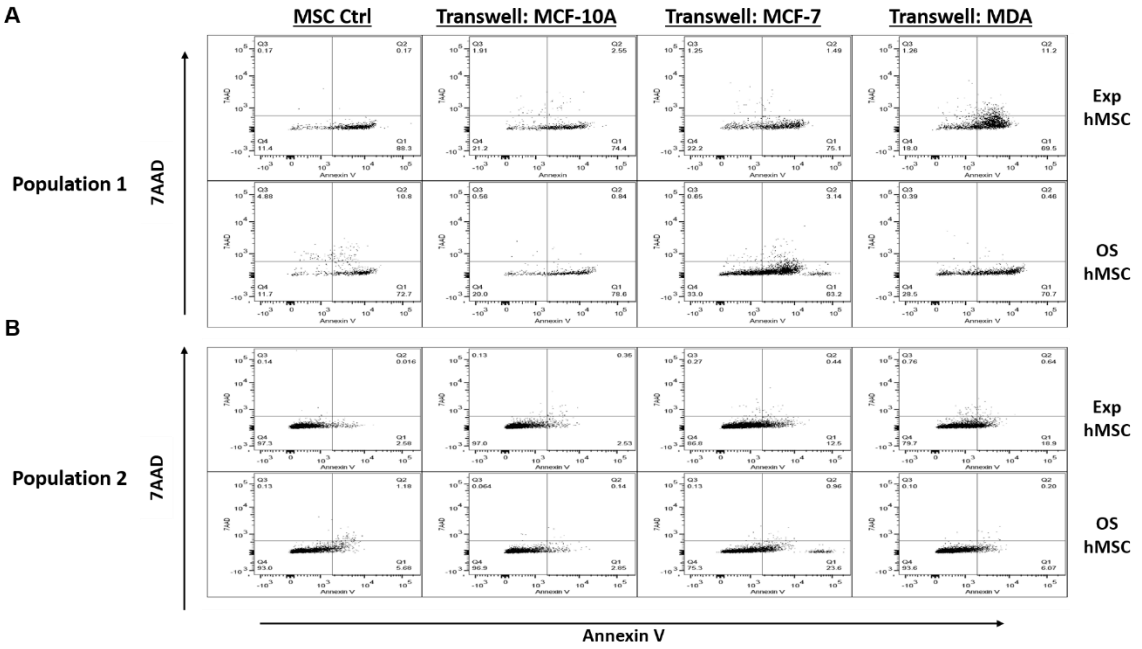

Figure A.5. Secreted factors from breast cancer cells upregulated the early marker for apoptosis, Annexin V, on the hMSCs. Human MSCs cultured with osteogenic or control media were incubated with transwells containing MDA-MB-231 breast cancer cells, MCF-7 breast cancer cells, or non-transformed MCF-10A epithelial cells. Two populations of hMSCs were identified based on the forward scatter and side scatter. Both population 1, which had a smaller forward scatter (A), and population 2 which had a larger forward scatter (B), were stained for the apoptotic markers annexin V and 7AAD.

A.3.6 Breast cancer cells regulate proteolytic remodeling of the ECM to control MSC differentiation

Osteogenic differentiation is mediated in part due to type I collagen [207-209] which is cleaved by the most potent collagenase cathepsin K [3], a protease upregulated in a tumor environment [9]. The effects of paracrine factors from cancer cells overexpressing cathepsin K on MSC differentiation was investigated to test the hypothesis that biochemical factors from breast cancer cells overexpressing cathepsin K and cultured on type I collagen could promote osteogenic differentiation of hMSCs. MDA-MB-231 cells transfected to overexpress cathepsin K, followed by culture on 0.5 mg/ml collagen for 48 hours. Conditioned media was then collected, supplemented with 50% fresh media, and cultured on hMSCs for an additional 72 hours. Following the incubation, the hMSCs were lysed and osteogenic differentiation was quantified by measuring the amount of alkaline phosphatase and RUNX2 mRNA expression using qRT-PCR. Conditioned media from non-transfected MDA-MB-231 cells cultured with or without collagen decreased the amount of alkaline phosphatase mRNA expression detected in hMSCs (n=3) (Fig. A.6A). Alkaline phosphatase mRNA expression in hMSCs was upregulated with indirect communication from MDA-MB-231 cells overexpressing cathepsin K that were cultured on collagen (n=3, $p < 0.05$). In addition, the effects of collagen increased RUNX2 mRNA expression only with MDA-MB-231 cells overexpressing cathepsin K (n=3, $p < 0.01$) (Fig. A.6A).

To determine if the elevation of alkaline phosphatase mRNA expression in hMSCs due to biochemical factors from cathepsin K overexpression in MDA-MB-231 cells was mediated by cathepsins, 5 μM E-64 cathepsin inhibitor was incubated with the cathepsin K overexpressing and control MDA-MB-231 cells cultured with or without collagen. The

amount of alkaline phosphatase mRNA expression was reduced in the hMSCs only when E-64 was incubated with cathepsin K overexpressing MDA-MB-231 cells cultured with collagen (n=3, $p < 0.05$) (Fig. A.6B). Incubation of E-64 with MDA-MB-231 cells overexpressing cathepsin K cultured with collagen did not change the amount of RUNX2 mRNA expression in hMSCs (n=3) (Fig. A.6B).

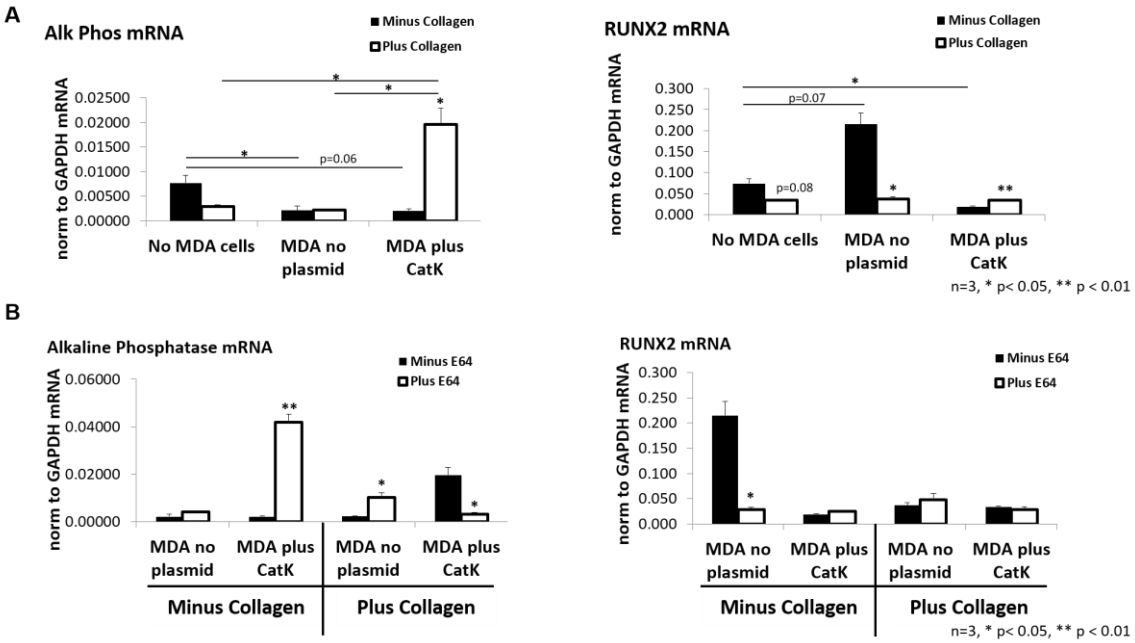

Figure A.6. Biochemical factors from MDA-MB-231 cells overexpressing cathepsin K and incubated on collagen increased osteogenic differentiation. (A) hMSCs were incubated with conditioned media from either cathepsin K overexpressing MDA-MB-231, non-transfected MDA-MB-231 cells, or a control cultured on type I collagen gels for 48 hours. Cell lysates of the hMSCs incubated with or without conditioned media from the MDA-MB-231 cells were collected and qRT-PCR was used to determine alkaline phosphatase and RUNX2 mRNA expression. (B) Human MSCs were incubated with the same conditions with or without E-64 followed by quantification of alkaline phosphatase and RUNX2 mRNA expression

To validate that overexpression of cathepsin K increased the amount of active cathepsin K in MDA-MB-231 cells, the cells overexpressing cathepsin K were lysed and

loaded for multiplex cathepsin zymography. The amount of active cathepsin K was increased in MDA-MB-231 cells overexpressing cathepsin K compared to the control MDA-MB-231 cells (Fig. A.7A). Collagen increased the amount of active cathepsin K in the MDA-MB-231 cells overexpressing cathepsin K (Fig. A.7A). This data was quantified using ImageJ analysis (Fig. A.7B).

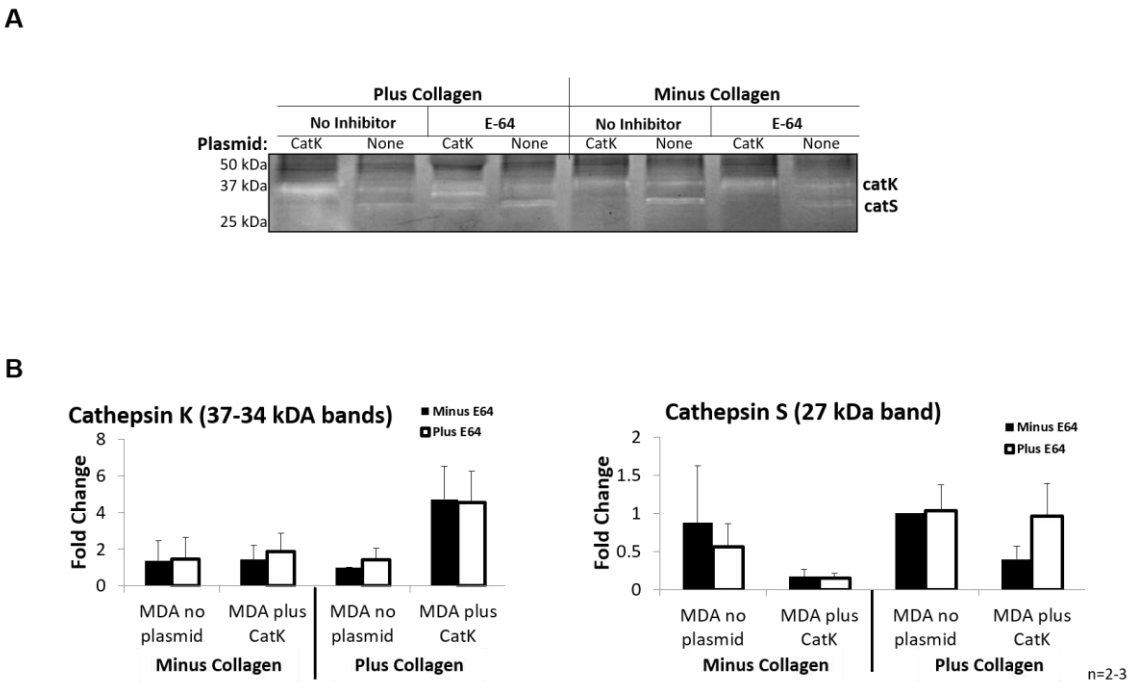

Figure A.7. The amount of active cathepsin K was increased in MDA-MB-231 cells overexpressing cathepsin K. (A) Cell lysates of hMSCs incubated with conditioned media from MDA-MB-231 cells overexpressing cathepsin K cultured with type I collagen gels or E-64 or controls were collected and assayed for active cathepsins using multiplex cathepsin zymography. (B) The amount of active cathepsins was quantified using ImageJ analysis.

A.3.7 Adipogenesis is downregulated with direct or indirect communication from breast cancer cells

To investigate the effects of breast cancer cell paracrine communication on adipogenic differentiation, hMSCs were cultured in adipogenic or control media for six days. This

was followed by six days culture alone or with either MDA-MB-231 or MCF-7 cells seeded on 0.4μm transwell inserts. The amount of adipogenic differentiation was determined using a fat soluble dye Oil Red O which stains lipids. Representative images were obtained and Oil Red O staining was quantified after dye extraction from the cells with isopropanol and absorbance measured using spectroscopy. Lipid accumulation was decreased in adipogenic hMSCs when cultured with either MDA-MB-231 or MCF-7 cells (Fig. A.8A). To determine if this reduction in lipid accumulation was due to biochemical factors from the cancer cells, conditioned media from either MDA-MB-231 or MCF-7 cells was collected and incubated with adipogenic hMSCs. The conditioned media from either the MDA-MB-231 or MCF-7 cells reduced the amount of lipid accumulation as seen in the representative images and quantification (Fig. A.8B).

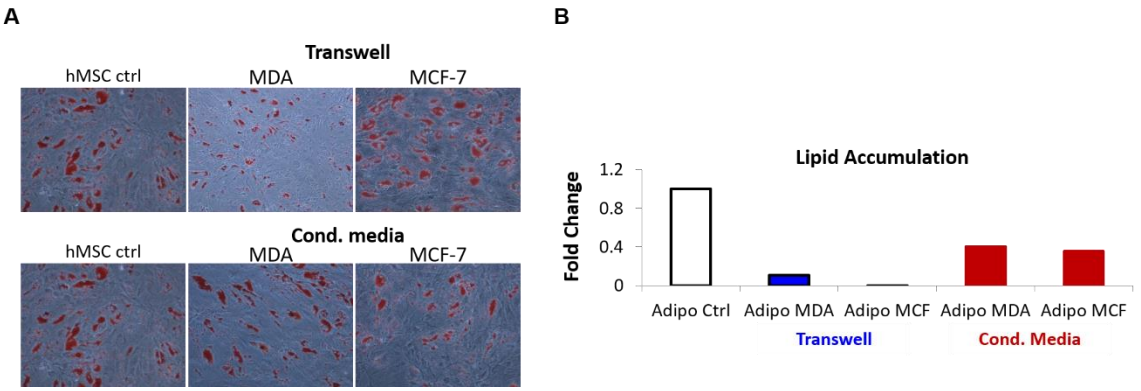

Figure A.8. Lipid accumulation decreased in adipogenic hMSCs due to secreted factors from breast cancer cells. (A) Adipogenic hMSCs were incubated with MDA-MB-231 or MCF-7 breast cancer cells seeded on a 0.2 μm transwell membrane or with conditioned media from the two breast cancer cells. Oil Red O was used to stain lipids and representative images obtained using microscopy. (B) The dye was then extracted with isopropanol and the absorbance was quantified using spectroscopy.

To assess if biochemical signaling from either MDA-MB-231 or MCF-7 cells reduces the adipogenic gene differentiation markers PPAR-γ or lipoprotein lipase (LPL),

adipogenic hMSCs were cultured with either MDA-MB-231 or MCF-7 cells on a 0.4 μm transwell or with conditioned media from the breast cancer cells. Paracrine factors from either of the breast cancer cells reduced both PPAR-γ (Fig. A.9A) and LPL (Fig. A.9B) mRNA expression as seen with both the transwell and conditioned media conditions.

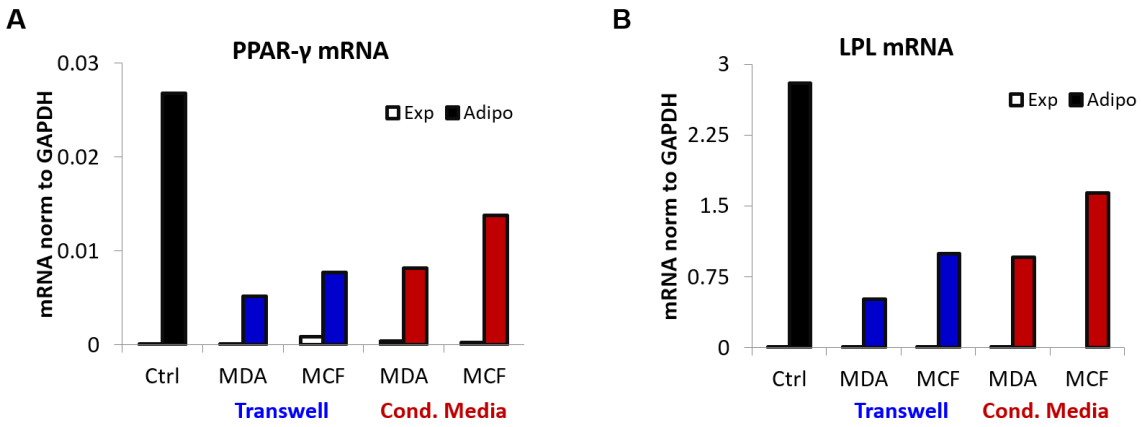

Figure A.9. Biochemical communication from breast cancer cells reduced adipogenic gene expression in MSCs. Adipogenic hMSCs were incubated with MDA-MB-231 or MCF-7 breast cancer cells seeded on a 0.2 μm transwell membrane or with 50% supplemented conditioned media from the two breast cancer cells for 6 days. Cells were lysed and mRNA expression of PPAR-γ (A) and LPL (B) was quantified with qRT-PCR.

Next, the effects of direct cell communication between breast cancer cells and adipogenic hMSCs on adipogenic differentiation was investigated. Either MDA-MB-231 or MCF-7 cells were cultured in direct contact with adipogenic or control hMSCs. The cells were then stained with Oil Red O, and the amount of staining was quantified by extracting the dye with isopropanol and measuring the absorbance. Heterotypic culture of MDA-MB-231 cells and adipogenic hMSCs elevated the lipid accumulation (Fig. A.10A). MCF-7 cells also increased the amount of lipids in adipogenic hMSCs compared

to the adipogenic hMSCs cultured alone. (Fig. A.10B). This was all verified with the quantified absorbance measurements (Fig. A.10C).

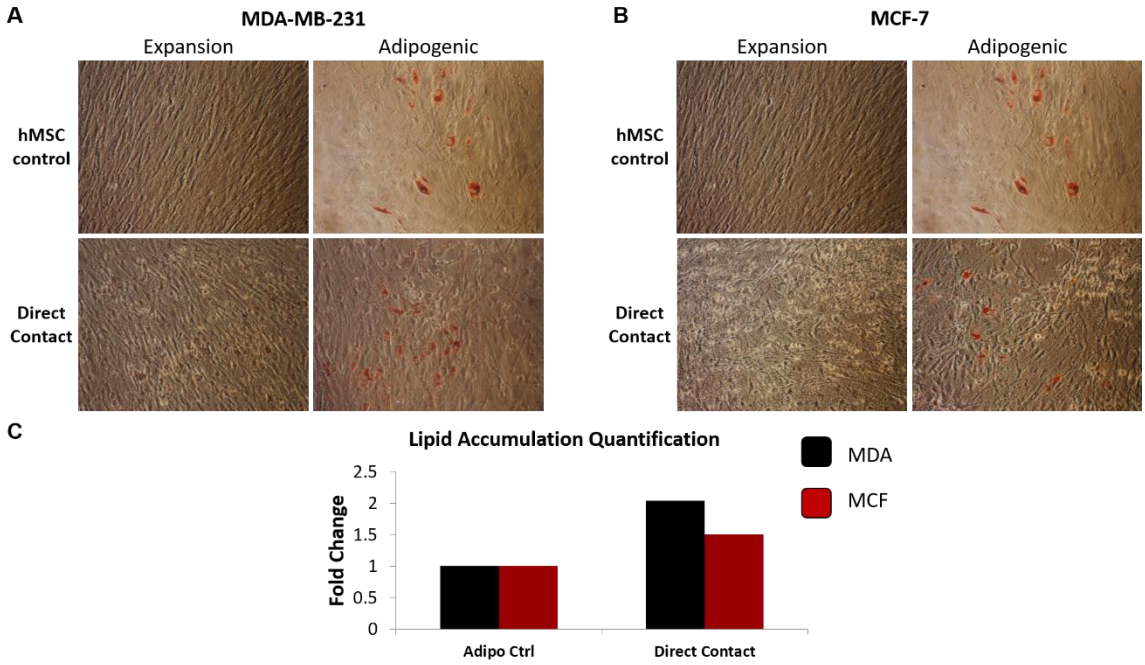

Figure A.10. Lipid accumulation increased with heterotypic culture of breast cancer cells and MSCs. (A) hMSCs were cultured in adipogenic or non-inducing media for 6 days. MDA-MB-231 or MCF-7 breast cancer cells were seeded directly on the hMSCs and cultured for an additional 6 days. (B) The dye was then extracted with isopropanol and the absorbance was quantified using spectroscopy.

A.3.8 Differential regulation of cathepsin proteolytic profiles between osteogenic and adipogenic differentiating hMSCs

Differentiation of hMSCs to adipocytes in mice is controlled by mouse cathepsin L [135]. Human MSCs were cultured in expansion, osteogenic, or adipogenic media for 21 days. Lysates were collected at day 7, 10, 14, 15, 18 and 21 and equal protein amounts were loaded for multiplex cathepsin zymography to assess if hMSCs changed their cathepsin proteolytic profile during osteogenic or adipogenic differentiation. Undifferentiated hMSCs expressed active cathepsins K, S, L, and V on days 7 and 10, but only maintained

active cathepsin K and V by day 14. In contrast, the osteogenic hMSCs had reduced amounts of cathepsins K and V on day 7 compared to the hMSC control cells, but active cathepsins K and V was elevated by day 14 of differentiation and was maintained throughout 21 days of osteogenic differentiation. Adipogenic hMSCs contained active cathepsins V and S at the early stages of differentiation. By the 14th day of differentiation, the amount of active cathepsin L was increased. At the later stages of adipogenesis, cathepsins K, L, S, and V were detected (Fig A.11).

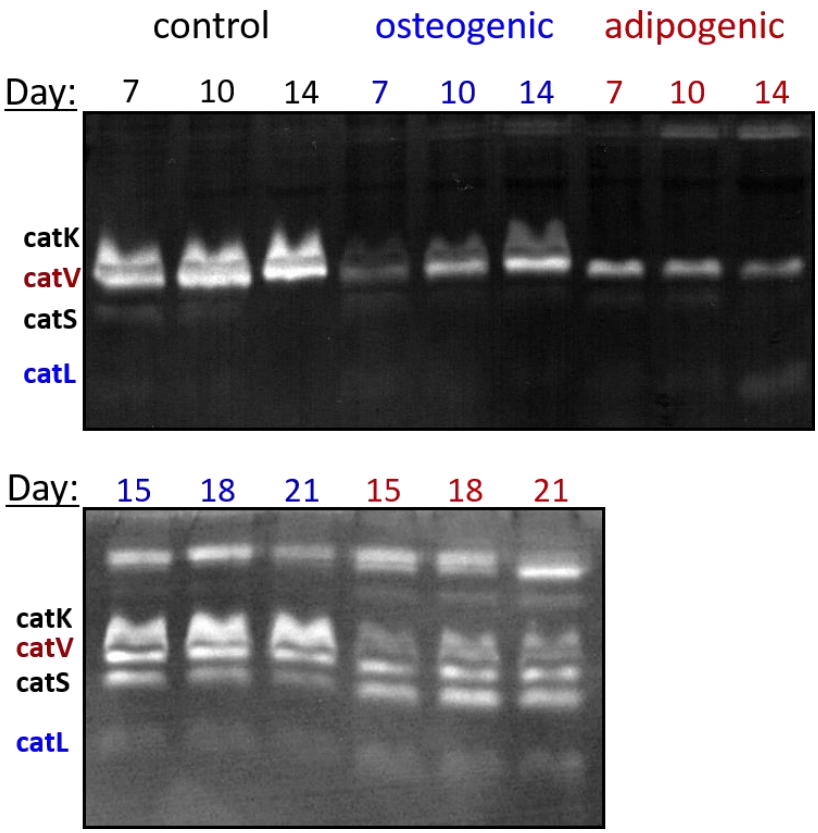

Figure A.11. Human MSCs dynamically regulate cathepsin activity during differentiation. Human MSCs were cultured in osteogenic, adipogenic or non-inducing media for 7, 10, 14, 15, 18, or 21 days. At each time point, cells were lysed and equal amounts of protein were loaded for multiplex cathepsin zymography.

A.3.9 Communication from breast cancer cells reduce the amount of active cathepsins in hMSCs

To determine if the breast cancer cells would influence the proteolytic profiles of hMSCs, hMSCs were cultured for 13 days in adipogenic, or control media; followed by incubation with MDA-MB-231 cells for nine days cultured with adipogenic or un-induced hMSCs. Cells were lysed and equal protein was loaded for multiplex cathepsin zymography. Active cathepsins S, L, and V was detected in the hMSCs cultured without MDA-MB-231 cells. The amount of active cathepsins was reduced by as little as 55% or more when MDA-MB-231 cells were cultured directly or indirectly with the hMSCs. MDA-MB-231 cells cultured indirectly had less of an influence on the active cathepsins in adipogenic hMSCs with only as much as a 27% fold decrease in active cathepsins. The proteolytic profiles of the adipogenic hMSCs cultured directly with MDA-MB-231 cells was comparable to the proteolytic profile of the MDA-MB-231 cells cultured alone (Fig. A.12).

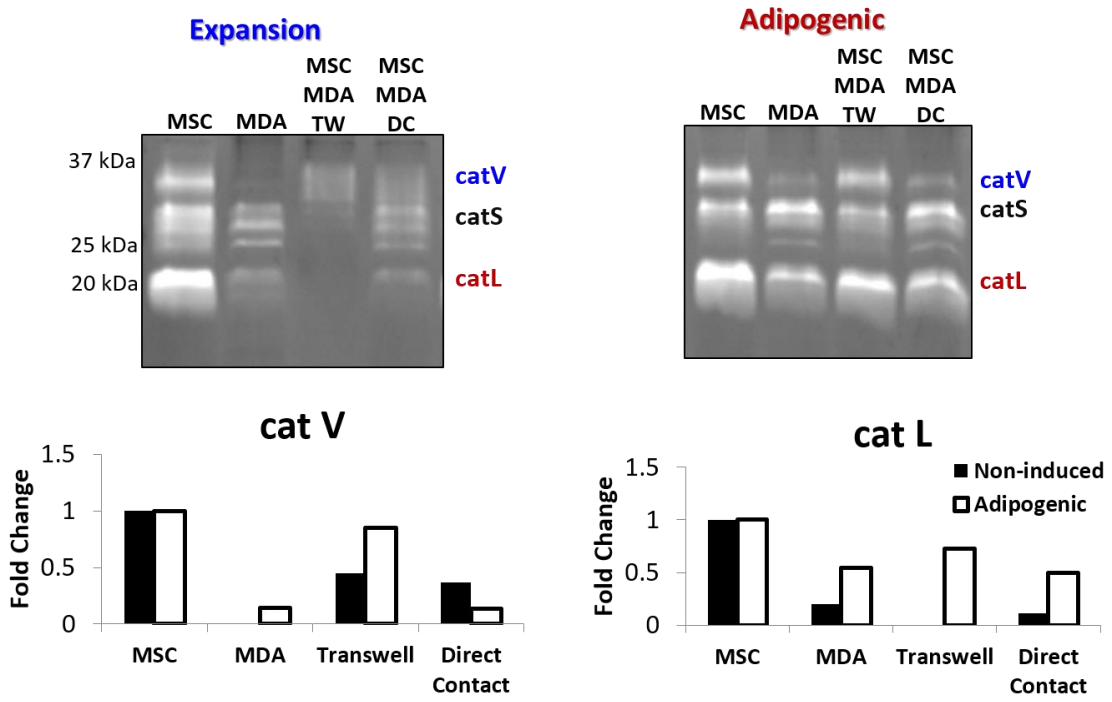

Figure. A.12. Heterotypic cell communication influences proteolytic profiles of adipogenic differentiating MSCs. hMSCs were cultured in adipogenic or non-inducing media for 13 days. MDA-MB-231 breast cancer cells were seeded directly on the hMSCs or indirectly on a 0.2 μm transwell membrane for an additional 9 days. Cells were lysed and equal amounts of protein were loaded for multiplex cathepsin zymography and quantified using ImageJ. TW, transwell; DC, direct contact; MDA, MDA-MB-231 cells.

A.4 Discussion

Breast cancer cells that metastasize to bone promotes formation of osteolytic lesions. The influence of breast cancer cells on MSCs shape and differentiation into osteoblasts or adipocytes was investigated. This study showed that osteogenic MSCs changed their shape and morphology when in direct contact with breast cancer cells. Not only did the direct interaction of the breast cancer cells change the shape, but secreted paracrine factors from the breast cancer cells also caused the non-induced MSCs to take on a more rounded morphology and early stage osteogenic MSCs became more spindle-like. These changes in cellular shape and its potential effect on cellular function is important to

differentiation since cell morphology and shape can determine the MSC cell fate down a osteoblast or adipocyte lineage [206]. Other studies have demonstrated that paracrine factors from breast cancer cells disrupt and decrease f-actin fiber formation and focal adhesion plaques [210], both factors that affect cell morphology and adhesion.

This work not only demonstrates how breast cancer cells alter the cellular morphology of hMSCs and early osteoblasts, but these phenotypic changes were also accompanied with a decrease in osteoblast differentiation as indicated by decreases in alkaline phosphatase activity and osteogenic gene expression of RUNX2 due to indirect communication. While other reports have investigated how chemokine signaling from MSCs promotes breast cancer cell migration recruitment [211], this work examine the effects of direct and indirect communication between breast cancer cells and differentiating MSCs. Breast cancer cells negative influence on early osteogenic MSC could impact the bone marrow niche by preventing osteoblast differentiation and ultimately bone formation and, in turn, promote osteolytic lesion establishment.

In addition, breast cancer cells increased lipid accumulation of adipogenic MSCs but not via paracrine signaling. While direct communication of breast cancer cells increased MSC adipogenesis, lipid accumulation decreased due to secreted factors from breast cancer cells. Paracrine signaling from MDA-MB-231 and MCF-7 breast cancer cells also downregulated the adipogenic gene expression markers LPL and PPAR-γ. This highlights reduce commitment of MSCs to a downstream adipogenic lineage due to paracrine signaling from breast cancer cells. Reduction in adipocytes in a bone niche can also play a vital role in bone formation since paracrine signaling from adipocytes elevates osteogenic differentiation [212].

While previous studies have shown that cathepsins K and S are regulators of adipogenesis [136, 203], this report demonstrates that cathepsins K, L, S, and V are differentially regulated during adipogenic and osteogenic differentiation. This work showed reduced amounts of active cathepsins V, L, and S in MSCs due to breast cancer cells. Down-regulation of cathepsin activity to turn-over ECM proteins could play a role in decreasing adipogenesis and promoting osteolytic lesions.

Osteoblasts and adipocytes secrete and lay down different types of matrix proteins. During early stages of osteogenic differentiation, MSCs produce type I collagen, a matrix protein that has been shown to enhance osteogenic differentiation [213]. This investigation into the effect of breast cancer cells on MSCs differentiation has demonstrated that biochemical factors from breast cancer cells expressing cathepsin K and cultured on collagen can restore osteogenesis that was lost due to paracrine signaling from breast cancer cells alone. This suggests that possible cleavage fragments of collagen due to cathepsin K is sufficient to promote osteoblast differentiation. Although previous reports have used collagen gels to regulate osteogenesis, this report indicates that collagen fragments could also promote osteogenesis. This could have a positive feedback effect on differentiation since collagen fragments were shown to increase cathepsins B, K, and L mRNA expression and activity [214] and cathepsins are regulators of MSC differentiation [136, 203, 214].

The current study uncovered how breast cancer cells affect MSC differentiation into osteoblasts or adipocytes which could promote osteolytic lesion formation in the bone marrow environment. Understanding this regulation can assist with identifying possible therapeutic targets including cathepsins, which are involved in MSC differentiation.

A.5 Conclusion

This study demonstrated the effect of breast cancer cell biochemical interactions on hMSC morphology and differentiation. When breast cancer cell metastasize to bone, osteolytic lesions are established. In this report, not only was differentiation toward an osteogenic lineage reduced, but adipogenesis was also reduced. This is crucial since adipocytes help to promote differentiation of osteoblasts [212]. Cathepsin-mediated regulation of differentiation due to cathepsin overexpression was also suggested. The findings in this report indicate the need to understand how breast cancer cells affect differentiation of bone marrow derived cells, and also how the cathepsin proteolytic profiles is changed within the metastatic site.

REFERENCES

1. Siegel, R.L., K.D. Miller, and A. Jemal, *Cancer statistics, 2016.* CA: A Cancer Journal for Clinicians, 2016. **66**(1): p. 7-30.

2. Samokhin, A.O., et al., *Pharmacological Inhibition of Cathepsin S Decreases Atherosclerotic Lesions in Apoe-/- Mice.* J Cardiovasc Pharmacol.

3. Lecaille, F., D. Bromme, and G. Lalmanach, *Biochemical properties and regulation of cathepsin K activity.* Biochimie, 2008. **90**(2): p. 208-26.

4. Bromme, D., et al., *Human cathepsin V functional expression, tissue distribution, electrostatic surface potential, enzymatic characterization, and chromosomal localization.* Biochemistry, 1999. **38**(8): p. 2377-2385.

5. Mohamed, M.M. and B.F. Sloane, *Cysteine cathepsins: multifunctional enzymes in cancer.* Nat Rev Cancer, 2006. **6**(10): p. 764-775.

6. Chauhan, S.S., L.J. Goldstein, and M.M. Gottesman, *Expression of cathepsin L in human tumors.* Cancer Research, 1991. **51**(5): p. 1478-1481.

7. Kopitz, C., et al., *Reduction of experimental human fibrosarcoma lung metastasis in mice by adenovirus-mediated cystatin C overexpression in the host.* Cancer Res, 2005. **65**(19): p. 8608-12.

8. Podgorski, I., et al., *Bone Marrow-Derived Cathepsin K Cleaves SPARC in Bone Metastasis.* The American Journal of Pathology, 2009. **175**(3): p. 1255-1269.

9. Chen, B. and M.O. Platt, *Multiplex zymography captures stage-specific activity profiles of cathepsins K, L, and S in human breast, lung, and cervical cancer.* J Transl Med, 2011. **9**(109): p. 1479-5876.

10. Zhang, J., et al., *Cystatin m: a novel candidate tumor suppressor gene for breast cancer.* Cancer Res, 2004. **64**(19): p. 6957-64.

11. Li, W., et al., *Overexpression of stefin A in human esophageal squamous cell carcinoma cells inhibits tumor cell growth, angiogenesis, invasion, and metastasis.* Clin Cancer Res, 2005. **11**(24 Pt 1): p. 8753-62.

12. Abrahamson, M., *[49] Cystatins*, in *Methods in Enzymology*, J.B. Alan, Editor. 1994, Academic Press. p. 685-700.

13. Palermo, C. and J.A. Joyce, *Cysteine cathepsin proteases as pharmacological targets in cancer.* Trends in Pharmacological Sciences, 2008. **29**(1): p. 22-28.

14. Jedeszko, C. and B.F. Sloane, *Cysteine cathepsins in human cancer.* Biological Chemistry, 2004. **385**(11): p. 1017-1027.

15. Jensen, A.B., et al., *The Cathepsin K Inhibitor Odanacatib Suppresses Bone Resorption in Women With Breast Cancer and Established Bone Metastases: Results of a 4-Week, Double-Blind, Randomized, Controlled Trial.* Clinical Breast Cancer, 2010. **10**(6): p. 452-458.

16. Chapurlat, R.D., *Odanacatib: a review of its potential in the management of osteoporosis in postmenopausal women.* Therapeutic Advances in Musculoskeletal Disease, 2015. **7**(3): p. 103-109.

17. Bone, H.G., et al., *Odanacatib for the treatment of postmenopausal osteoporosis: development history and design and participant characteristics of LOFT, the Long-Term Odanacatib Fracture Trial.* Osteoporos Int, 2015. **26**(2): p. 699-712.

18. Abbenante, G. and D.P. Fairlie, *Protease inhibitors in the clinic.* Med Chem, 2005. **1**(1): p. 71-104.

19. Turk, B., *Targeting proteases: successes, failures and future prospects.* Nat Rev Drug Discov, 2006. **5**(9): p. 785-99.

20. Tian, M. and W.P. Schiemann, *Preclinical efficacy of cystatin C to target the oncogenic activity of transforming growth factor Beta in breast cancer.* Transl Oncol, 2009. **2**(3): p. 174-83.

21. Coussens, L.M., B. Fingleton, and L.M. Matrisian, *Matrix Metalloproteinase Inhibitors and Cancer—Trials and Tribulations.* Science, 2002. **295**(5564): p. 2387-2392.

22. Lynch, C.C., et al., *MMP-7 promotes prostate cancer-induced osteolysis via the solubilization of RANKL.* Cancer Cell, 2005. **7**(5): p. 485-96.

23. Heppner, K.J., et al., *Expression of most matrix metalloproteinase family members in breast cancer represents a tumor-induced host response.* Am J Pathol, 1996. **149**(1): p. 273-82.

24. Bromme, D. and F. Lecaille, *Cathepsin K inhibitors for osteoporosis and potential off-target effects.* Expert Opin Investig Drugs, 2009. **18**(5): p. 585-600.

25. Torre, L.A., et al., *Global cancer statistics, 2012.* CA: A Cancer Journal for Clinicians, 2015. **65**(2): p. 87-108.

26. *Global Cancer Facts & Figures 3rd Edition*. 2015, American Cancer Society: Atlanta.

27. *Cancer Facts & Figures 2016*. 2016, American Cancer Society: Atlanta.

28. DeSantis, C.E., et al., *Breast cancer statistics, 2015: Convergence of incidence rates between black and white women.* CA: A Cancer Journal for Clinicians, 2016. **66**(1): p. 31-42.

29. *Breast Cancer Facts & Figures 2015-2016*. 2015, American Cancer Society, Inc.: Atlanta.

30. *AJCC Cancer Staging Manual*. 7 ed, ed. S. Edge, et al. 2010, New York, New York: Springer-Verlag New York. XV, 648.

31. Deroo, B.J. and K.S. Korach, *Estrogen receptors and human disease.* J Clin Invest, 2006. **116**(3): p. 561-70.

32. Mauvais-Jarvis, F., D.J. Clegg, and A.L. Hevener, *The role of estrogens in control of energy balance and glucose homeostasis.* Endocr Rev, 2013. **34**(3): p. 309-38.

33. Graham, J.D. and C.L. Clarke, *Physiological Action of Progesterone in Target Tissues.* Endocrine Reviews, 1997. **18**(4): p. 502-519.

34. Yaish, P., et al., *Blocking of EGF-dependent cell proliferation by EGF receptor kinase inhibitors.* Science, 1988. **242**(4880): p. 933-935.

35. Moulder, S.L., et al., *Epidermal Growth Factor Receptor (HER1) Tyrosine Kinase Inhibitor ZD1839 (Iressa) Inhibits HER2/neu (erbB2)-overexpressing Breast Cancer Cells in Vitro and in Vivo.* Cancer Research, 2001. **61**(24): p. 8887-8895.

36. Lodish, H., et al., *Molecular cell biology*. 6 ed. 2008, New York: WH Freeman and Company.

37. Dent, R., et al., *Triple-Negative Breast Cancer: Clinical Features and Patterns of Recurrence.* Clinical Cancer Research, 2007. **13**(15): p. 4429-4434.

38. Bauer, K.R., et al., *Descriptive analysis of estrogen receptor (ER)-negative, progesterone receptor (PR)-negative, and HER2-negative invasive breast cancer, the so-called triple-negative phenotype.* Cancer, 2007. **109**(9): p. 1721-1728.

39. Easton, D.F., D. Ford, and D.T. Bishop, *Breast and ovarian cancer incidence in BRCA1-mutation carriers. Breast Cancer Linkage Consortium.* American Journal of Human Genetics, 1995. **56**(1): p. 265-271.

40. Struewing, J.P., et al., *The Risk of Cancer Associated with Specific Mutations of BRCA1 and BRCA2 among Ashkenazi Jews.* New England Journal of Medicine, 1997. **336**(20): p. 1401-1408.

41. Chen, S. and G. Parmigiani, *Meta-analysis of BRCA1 and BRCA2 penetrance.* J Clin Oncol, 2007. **25**(11): p. 1329-33.

42. Antoniou, A., et al., *Average risks of breast and ovarian cancer associated with BRCA1 or BRCA2 mutations detected in case Series unselected for family history: a combined analysis of 22 studies.* Am J Hum Genet, 2003. **72**(5): p. 1117-30.

43. Moyer, V.A., *Risk Assessment, Genetic Counseling, and Genetic Testing for BRCA-Related Cancer in Women: U.S. Preventive Services Task Force Recommendation Statement.* Annals of Internal Medicine, 2014. **160**(4): p. 271-281.

44. Scheuer, L., et al., *Outcome of Preventive Surgery and Screening for Breast and Ovarian Cancer in BRCA Mutation Carriers.* Journal of Clinical Oncology, 2002. **20**(5): p. 1260-1268.

45. Montcourrier, P., et al., *Breast cancer cells have a high capacity to acidify extracellular milieu by a dual mechanism.* Clinical & Experimental Metastasis, 1997. **15**(4): p. 382-92.

46. Kirschke, H., et al., *Action of rat liver cathepsin L on collagen and other substrates.* Biochemical Journal, 1982. **201**(2): p. 367-372.

47. Bromme, D., et al., *Functional expression of human cathepsin S in Saccharomyces cerevisiae. Purification and characterization of the recombinant enzyme.* J Biol Chem, 1993. **268**(7): p. 4832-8.

48. Turk, B., V. Turk, and D. Turk, *Structural and functional aspects of papain-like cysteine proteinases and their protein inhibitors.* Biol Chem, 1997. **378**(3-4): p. 141-50.

49. Bissell, M.J., et al., *Tissue Structure, Nuclear Organization, and Gene Expression in Normal and Malignant Breast.* Cancer Research, 1999. **59**(7 Supplement): p. 1757s-1764s.

50. Wheelock, M.J. and K.R. Johnson, *CADHERINS AS MODULATORS OF CELLULAR PHENOTYPE.* Annual Review of Cell and Developmental Biology, 2003. **19**(1): p. 207-235.

51. Ingber, D.E., *Cancer as a disease of epithelial–mesenchymal interactions and extracellular matrix regulation.* Differentiation, 2002. **70**(9–10): p. 547-560.

52. Nass, S.J., et al., *Aberrant methylation of the estrogen receptor and E-cadherin 5' CpG islands increases with malignant progression in human breast cancer.* Cancer Res, 2000. **60**(16): p. 4346-8.

53. Owens, D.M. and F.M. Watt, *Influence of β1 Integrins on Epidermal Squamous Cell Carcinoma Formation in a Transgenic Mouse Model: α3β1, but not α2β1, Suppresses Malignant Conversion.* Cancer Research, 2001. **61**(13): p. 5248-5254.

54. Zutter, M.M., et al., *Re-expression of the alpha 2 beta 1 integrin abrogates the malignant phenotype of breast carcinoma cells.* Proceedings of the National Academy of Sciences, 1995. **92**(16): p. 7411-7415.

55. Gocheva, V., et al., *Distinct roles for cysteine cathepsin genes in multistage tumorigenesis.* Genes Dev, 2006. **20**(5): p. 543-56.

56. Bacac, M. and I. Stamenkovic, *Metastatic Cancer Cell.* Annual Review of Pathology: Mechanisms of Disease, 2008. **3**(1): p. 221-247.

57. Bell, C.D. and E. Waizbard, *Variability of cell size in primary and metastatic human breast carcinoma.* Invasion Metastasis, 1986. **6**(1): p. 11-20.

58. Pitts, W.C., et al., *Carcinomas with metaplasia and sarcomas of the breast.* Am J Clin Pathol, 1991. **95**(5): p. 623-32.

59. Gocheva, V., et al., *IL-4 induces cathepsin protease activity in tumor-associated macrophages to promote cancer growth and invasion.* Genes Dev, 2010. **24**(3): p. 241-55.

60. Vasiljeva, O., et al., *Tumor Cell–Derived and Macrophage-Derived Cathepsin B Promotes Progression and Lung Metastasis of Mammary Cancer.* Cancer Research, 2006. **66**(10): p. 5242-5250.

61. Dennemarker, J., et al., *Deficiency for the cysteine protease cathepsin L promotes tumor progression in mouse epidermis.* Oncogene, 2010. **29**(11): p. 1611-21.

62. Lester, J., *Local Treatment of Breast Cancer.* Seminars in Oncology Nursing, 2015. **31**(2): p. 122-133.

63. Veronesi, U., et al., *Twenty-year follow-up of a randomized study comparing breast-conserving surgery with radical mastectomy for early breast cancer.* N Engl J Med, 2002. **347**(16): p. 1227-32.

64. Tuttle, T.M., et al., *Increasing Use of Contralateral Prophylactic Mastectomy for Breast Cancer Patients: A Trend Toward More Aggressive Surgical Treatment.* Journal of Clinical Oncology, 2007. **25**(33): p. 5203-5209.

65. Chung, A., et al., *Comparison of patient characteristics and outcomes of contralateral prophylactic mastectomy and unilateral total mastectomy in breast cancer patients.* Annals of surgical oncology, 2012. **19**(8): p. 2600-2606.

66. Fayanju, O.M., et al., *Contralateral Prophylactic Mastectomy after Unilateral Breast Cancer: A Systematic Review & Meta-Analysis.* Annals of surgery, 2014. **260**(6): p. 1000-1010.

67. Narod, S.A., *Bilateral breast cancers.* Nat Rev Clin Oncol, 2014. **11**(3): p. 157-166.

68. Marta, G.N., et al., *Accelerated partial irradiation for breast cancer: Systematic review and meta-analysis of 8653 women in eight randomized trials.* Radiotherapy and Oncology, 2015. **114**(1): p. 42-49.

69. Sauer, R., et al., *Accelerated partial breast irradiation.* Cancer, 2007. **110**(6): p. 1187-1194.

70. Offersen, B.V., et al., *Accelerated partial breast irradiation as part of breast conserving therapy of early breast carcinoma: a systematic review.* Radiother Oncol, 2009. **90**(1): p. 1-13.

71. King, T.A. and M. Morrow, *Surgical issues in patients with breast cancer receiving neoadjuvant chemotherapy.* Nat Rev Clin Oncol, 2015. **12**(6): p. 335-343.

72. Brömme, D. and K. Okamoto, *Human cathepsin O2, a novel cysteine protease highly expressed in osteoclastomas and ovary molecular cloning, sequencing and tissue distribution.* Biological Chemistry Hoppe-Seyler, 1995. **376**(6): p. 379-384.

73. Lafarge, J.C., et al., *Cathepsins and cystatin C in atherosclerosis and obesity.* Biochimie.

74. Sukhova, G.K., et al., *Deficiency of cathepsin S reduces atherosclerosis in LDL receptor-deficient mice.* J Clin Invest, 2003. **111**(6): p. 897-906.

75. Chapman, H.A., R.J. Riese, and G.P. Shi, *Emerging roles for cysteine proteases in human biology.* Annu Rev Physiol, 1997. **59**: p. 63-88.

76. Sho, E., et al., *Hemodynamic forces regulate mural macrophage infiltration in experimental aortic aneurysms.* Exp Mol Pathol, 2004. **76**(2): p. 108-16.

77. Sukhova, G.K., et al., *Cystatin C deficiency increases elastic lamina degradation and aortic dilatation in apolipoprotein E-null mice.* Circ Res, 2005. **96**(3): p. 368-75.

78. Hou, W.S., et al., *Comparison of cathepsins K and S expression within the rheumatoid and osteoarthritic synovium.* Arthritis Rheum, 2002. **46**(3): p. 663-74.

79. Novinec, M., et al., *Interaction between human cathepsins K, L, and S and elastins: mechanism of elastinolysis and inhibition by macromolecular inhibitors.* J Biol Chem, 2007. **282**(11): p. 7893-902.

80. Vasiljeva, O., et al., *Recombinant human procathepsin S is capable of autocatalytic processing at neutral pH in the presence of glycosaminoglycans.* FEBS Lett, 2005. **579**(5): p. 1285-90.

81. Garnero, P., et al., *The collagenolytic activity of cathepsin K is unique among mammalian proteinases.* J Biol Chem, 1998. **273**(48): p. 32347-52.

82. Littlewood-Evans, A.J., et al., *The osteoclast-associated protease cathepsin K is expressed in human breast carcinoma.* Cancer Research, 1997. **57**(23): p. 5386-5390.

83. Brubaker, K.D., et al., *Cathepsin K mRNA and protein expression in prostate cancer progression.* J Bone Miner Res, 2003. **18**(2): p. 222-30.

84. Lutgens, E., et al., *Disruption of the cathepsin K gene reduces atherosclerosis progression and induces plaque fibrosis but accelerates macrophage foam cell formation.* Circulation, 2006. **113**(1): p. 98-107.

85. Platt, M.O., et al., *Expression of cathepsin K is regulated by shear stress in cultured endothelial cells and is increased in endothelium in human atherosclerosis.* Am J Physiol Heart Circ Physiol, 2007. **292**(3): p. H1479-86.

86. Santamaria, I., et al., *Cathepsin L2, a novel human cysteine proteinase produced by breast and colorectal carcinomas.* Cancer Research, 1998. **58**(8): p. 1624-1630.

87. Tolosa, E., et al., *Cathepsin V is involved in the degradation of invariant chain in human thymus and is overexpressed in myasthenia gravis.* The Journal of Clinical Investigation, 2003. **112**(4): p. 517-526.

88. Reiser, J., B. Adair, and T. Reinheckel, *Specialized roles for cysteine cathepsins in health and disease.* The Journal of Clinical Investigation, 2010. **120**(10): p. 3421-3431.

89. Reiser, J., B. Adair, and T. Reinheckel, *Specialized roles for cysteine cathepsins in health and disease.* J Clin Invest, 2010. **120**(10): p. 3421-31.

90. Bromme, D., et al., *Human cathepsin V functional expression, tissue distribution, electrostatic surface potential, enzymatic characterization, and chromosomal localization.* Biochemistry, 1999. **38**(8): p. 2377-85.

91. Tepel, C., et al., *Cathepsin K in thyroid epithelial cells: sequence, localization and possible function in extracellular proteolysis of thyroglobulin.* J Cell Sci, 2000. **113**(24): p. 4487-4498.

92. Baruch, A., D.A. Jeffery, and M. Bogyo, *Enzyme activity - it's all about image.* Trends in Cell Biology, 2004. **14**(1): p. 29-35.

93. Blum, G., et al., *Noninvasive optical imaging of cysteine protease activity using fluorescently quenched activity-based probes.* Nat Chem Biol, 2007. **3**(10): p. 668-677.

94. Blum, G., et al., *Comparative Assessment of Substrates and Activity Based Probes as Tools for Non-Invasive Optical Imaging of Cysteine Protease Activity.* PLoS ONE, 2009. **4**(7): p. e6374.

95. Brix, K., *Lysosomal Proteases*, in *Lysosomes*. 2005, Springer US. p. 50-59.

96. Wilson, S.R., et al., *Cathepsin K Activity-dependent Regulation of Osteoclast Actin Ring Formation and Bone Resorption.* Journal of Biological Chemistry, 2009. **284**(4): p. 2584-2592.

97. Punturieri, A., et al., *Regulation of elastinolytic cysteine proteinase activity in normal and cathepsin K-deficient human macrophages.* J Exp Med, 2000. **192**(6): p. 789-99.

98. Hashimoto, Y., C. Kondo, and N. Katunuma, *An Active 32-kDa Cathepsin L Is Secreted Directly from HT 1080 Fibrosarcoma Cells and Not via Lysosomal Exocytosis.* PLoS ONE, 2015. **10**(12): p. e0145067.

99. Hashimoto, Y., et al., *Significance of 32-kDa cathepsin L secreted from cancer cells.* Cancer Biother Radiopharm, 2006. **21**(3): p. 217-24.

100. Kirkegaard, T. and M. Jäättelä, *Lysosomal involvement in cell death and cancer.* Biochimica et Biophysica Acta (BBA) - Molecular Cell Research, 2009. **1793**(4): p. 746-754.

101. Stoka, V., et al., *Lysosomal protease pathways to apoptosis. Cleavage of bid, not pro-caspases, is the most likely route.* J Biol Chem, 2001. **276**(5): p. 3149-57.

102. Guicciardi, M.E., et al., *Cathepsin B contributes to TNF-alpha-mediated hepatocyte apoptosis by promoting mitochondrial release of cytochrome c.* J Clin Invest, 2000. **106**(9): p. 1127-37.

103. Ishidoh, K. and E. Kominami, *Multi-step processing of procathepsin L in vitro.* FEBS Lett, 1994. **352**(3): p. 281-4.

104. Bossard, M.J., et al., *Proteolytic Activity of Human Osteoclast Cathepsin K.* Journal of Biological Chemistry, 1996. **271**(21): p. 12517-12524.

105. Abrahamson, M., et al., *Isolation of six cysteine proteinase inhibitors from human urine. Their physicochemical and enzyme kinetic properties and concentrations in biological fluids.* Journal of Biological Chemistry, 1986. **261**(24): p. 11282-11289.

106. Katunuma, N. and E. Kominami, *[37] Structure, properties, mechanisms, and assays ofcysteine protease inhibitors: Cystatins and E-64 derivatives*, in *Methods in Enzymology*. 1995, Academic Press. p. 382-397.

107. Brix, K., et al., *Cysteine cathepsins: Cellular roadmap to different functions.* Biochimie, 2008. **90**(2): p. 194-207.

108. Goulet, B., et al., *Increased expression and activity of nuclear cathepsin L in cancer cells suggests a novel mechanism of cell transformation.* Mol Cancer Res, 2007. **5**(9): p. 899-907.

109. Sever, S., et al., *Proteolytic processing of dynamin by cytoplasmic cathepsin L is a mechanism for proteinuric kidney disease.* The Journal of Clinical Investigation, 2007. **117**(8): p. 2095-2104.

110. Niwa, Y., et al., *Determination of cathepsin V activity and intracellular trafficking by N-glycosylation.* FEBS Letters, 2012. **586**(20): p. 3601-3607.

111. Kane, S.E., *Mouse procathepsin L lacking a functional glycosylation site is properly folded, stable, and secreted by NIH 3T3 cells.* J Biol Chem, 1993. **268**(15): p. 11456-62.

112. Nissler, K., et al., *The half-life of human procathepsin S.* Eur J Biochem, 1999. **263**(3): p. 717-25.

113. Akkari, L., et al., *Combined deletion of cathepsin protease family members reveals compensatory mechanisms in cancer.* Genes & Development, 2016. **30**(2): p. 220-232.

114. Kiviranta, R., et al., *Impaired bone resorption in cathepsin K-deficient mice is partially compensated for by enhanced osteoclastogenesis and increased expression of other proteases via an increased RANKL/OPG ratio.* Bone, 2005. **36**(1): p. 159-172.

115. Tholen, S., et al., *Deletion of Cysteine Cathepsins B or L Yields Differential Impacts on Murine Skin Proteome and Degradome.* Molecular & Cellular Proteomics, 2013. **12**(3): p. 611-625.

116. Shi, G.P., et al., *Molecular cloning of human cathepsin O, a novel endoproteinase and homologue of rabbit OC2.* FEBS Lett, 1995. **357**(2): p. 129-34.

117. Bromme, D., et al., *Human cathepsin O2, a matrix protein-degrading cysteine protease expressed in osteoclasts. Functional expression of human cathepsin O2 in Spodoptera frugiperda and characterization of the enzyme.* J Biol Chem, 1996. **271**(4): p. 2126-32.

118. Bossard, M.J., et al., *Proteolytic activity of human osteoclast cathepsin K. Expression, purification, activation, and substrate identification.* J Biol Chem, 1996. **271**(21): p. 12517-24.

119. Chapman, R.L., S.E. Kane, and A.H. Erickson, *Abnormal glycosylation of procathepsin L due to N-terminal point mutations correlates with failure to sort to lysosomes.* J Biol Chem, 1997. **272**(13): p. 8808-16.

120. Claveau, D. and D. Riendeau, *Mutations of the C-terminal end of cathepsin K affect proenzyme secretion and intracellular maturation.* Biochem Biophys Res Commun, 2001. **281**(2): p. 551-7.

121. McGrath, M.E., *The lysosomal cysteine proteases.* Annu Rev Biophys Biomol Struct, 1999. **28**: p. 181-204.

122. Platt, M.O., R.F. Ankeny, and H. Jo, *Laminar shear stress inhibits cathepsin L activity in endothelial cells.* Arterioscler Thromb Vasc Biol, 2006. **26**(8): p. 1784-90.

123. Desmazes, C., F. Gauthier, and G. Lalmanach, *Cathepsin L, but not cathepsin B, is a potential kininogenase.* Biol Chem, 2001. **382**(5): p. 811-5.

124. Li, W.A., et al., *Detection of femtomole quantities of mature cathepsin K with zymography.* Anal Biochem, 2010. **401**(1): p. 91-8.

125. Rantakokko, J., et al., *Mouse cathepsin K: cDNA cloning and predominant expression of the gene in osteoclasts, and in some hypertrophying chondrocytes during mouse development.* FEBS Lett, 1996. **393**(2-3): p. 307-13.

126. Novinec, M., et al., *Conformational flexibility and allosteric regulation of cathepsin K.* Biochem J, 2010. **429**(2): p. 379-89.

127. Turk, B., et al., *Kinetics of the pH-induced inactivation of human cathepsin L.* Biochemistry, 1993. **32**(1): p. 375-80.

128. Yasuda, Y., et al., *Cathepsin V, a novel and potent elastolytic activity expressed in activated macrophages.* J Biol Chem, 2004. **279**(35): p. 36761-70.

129. Le Gall, C., E. Bonnelye, and P. Clezardin, *Cathepsin K inhibitors as treatment of bone metastasis.* Curr Opin Support Palliat Care, 2008. **2**(3): p. 218-22.

130. Chen, B. and M.O. Platt, *Multiplex Zymography Captures Stage-specific Activity Profiles of Cathepsins K, L, and S in Human Breast, Lung, and Cervical Cancer.* J Transl Med, 2011. **9**: p. 109.

131. Falgueyret, J.-P., et al., *Lysosomotropism of Basic Cathepsin K Inhibitors Contributes to Increased Cellular Potencies against Off-Target Cathepsins and*

Reduced Functional Selectivity. Journal of Medicinal Chemistry, 2005. **48**(24): p. 7535-7543.

132. Desmarais, S., et al., *Effect of cathepsin K inhibitor basicity on in vivo off-target activities.* Molecular Pharmacology, 2007.

133. Payne, C.D., et al., *Pharmacokinetics and pharmacodynamics of the cathepsin S inhibitor, LY3000328, in healthy subjects.* British Journal of Clinical Pharmacology, 2014. **78**(6): p. 1334-1342.

134. Obermajer, N., et al., *Role of Cysteine Cathepsins in Matrix Degradation and Cell Signalling.* Connective Tissue Research, 2008. **49**(3/4): p. 193-196.

135. Yang, M., et al., *Cathepsin L activity controls adipogenesis and glucose tolerance.* Nat Cell Biol, 2007. **9**(8): p. 970-977.

136. Taleb, S., et al., *Cathepsin S Promotes Human Preadipocyte Differentiation: Possible Involvement of Fibronectin Degradation.* Endocrinology, 2006. **147**(10): p. 4950-4959.

137. Szpaderska, A.M. and A. Frankfater, *An intracellular form of cathepsin B contributes to invasiveness in cancer.* Cancer Res, 2001. **61**(8): p. 3493-500.

138. Stonelake, P.S., et al., *Proteinase inhibitors reduce basement membrane degradation by human breast cancer cell lines.* Br J Cancer, 1997. **75**(7): p. 951-9.

139. Premzl, A., et al., *Intracellular and extracellular cathepsin B facilitate invasion of MCF-10A neoT cells through reconstituted extracellular matrix in vitro.* Experimental Cell Research, 2003. **283**(2): p. 206-214.

140. Dahl, S.W., et al., *Human Recombinant Pro-dipeptidyl Peptidase I (Cathepsin C) Can Be Activated by Cathepsins L and S but Not by Autocatalytic Processing.* Biochemistry, 2001. **40**(6): p. 1671-1678.

141. Sobotic, B., et al., *Proteomic Identification of Cysteine Cathepsin Substrates Shed from the Surface of Cancer Cells.* Mol Cell Proteomics, 2015. **14**(8): p. 2213-28.

142. Qian, B.-Z., et al., *CCL2 recruits inflammatory monocytes to facilitate breast-tumour metastasis.* Nature, 2011. **475**(7355): p. 222-225.

143. Wilkinson, R.D., et al., *CCL2 is transcriptionally controlled by the lysosomal protease cathepsin S in a CD74-dependent manner.* Oncotarget, 2015. **6**(30): p. 29725-39.

144. Hanada, K., et al., *Isolation and Characterization of E–64, a New Thiol Protease Inhibitor.* Agricultural and Biological Chemistry, 1978. **42**(3): p. 523-528.

145. Barrett, A.J., et al., *L-trans-Epoxysuccinyl-leucylamido(4-guanidino)butane (E-64) and its analogues as inhibitors of cysteine proteinases including cathepsins B, H and L.* Biochem J, 1982. **201**(1): p. 189-98.

146. Ekström, U., et al., *Internalization of cystatin C in human cell lines.* FEBS Journal, 2008. **275**(18): p. 4571-4582.

147. Merz, G.S., et al., *Human cystatin C forms an inactive dimer during intracellular trafficking in transfected CHO cells.* J Cell Physiol, 1997. **173**(3): p. 423-32.

148. Ekiel, I. and M. Abrahamson, *Folding-related dimerization of human cystatin C.* J Biol Chem, 1996. **271**(3): p. 1314-21.

149. Calkins, C.C., et al., *Differential Localization of Cysteine Protease Inhibitors and a Target Cysteine Protease, Cathepsin B, by Immuno-Confocal Microscopy.* Journal of Histochemistry & Cytochemistry, 1998. **46**(6): p. 745-751.

150. Lenarčič, B., et al., *Differences in specificity for the interactions of stefins A, B and D with cysteine proteinases.* FEBS Letters, 1996. **395**(2–3): p. 113-118.

151. Sudhan, D.R. and D.W. Siemann, *Cathepsin L Inhibition by the Small Molecule KGP94 Suppresses Tumor Microenvironment Enhanced Metastasis Associated Cell Functions of Prostate and Breast Cancer Cells.* Clinical & experimental metastasis, 2013. **30**(7): p. 10.1007/s10585-013-9590-9.

152. Gillet, L., et al., *Voltage-gated Sodium Channel Activity Promotes Cysteine Cathepsin-dependent Invasiveness and Colony Growth of Human Cancer Cells.* Journal of Biological Chemistry, 2009. **284**(13): p. 8680-8691.

153. Sevenich, L., et al., *Analysis of tumour- and stroma-supplied proteolytic networks reveals a brain-metastasis-promoting role for cathepsin S.* Nat Cell Biol, 2014. **16**(9): p. 876-888.

154. Wilder, C.L., et al., *Manipulating substrate and pH in zymography protocols selectively distinguishes cathepsins K, L, S, and V activity in cells and tissues.* Archives of Biochemistry and Biophysics, 2011. **516**(1): p. 52-57.

155. McGowan, E.B., E. Becker, and T.C. Detwiler, *Inhibition of calpain in intact platelets by the thiol protease inhibitor E-64d.* Biochemical and Biophysical Research Communications, 1989. **158**(2): p. 432-435.

156. Montenez, J.P., et al., *Increased activities of cathepsin B and other lysosomal hydrolases in fibroblasts and bone tissue cultured in the presence of cysteine proteinases inhibitors.* Life Sciences, 1994. **55**(15): p. 1199-1208.

157. Kominami, E., et al., *Autodegradation of lysosomal cysteine proteinases.* Biochemical and Biophysical Research Communications, 1987. **144**(2): p. 749-756.

158. Gerard, K.W., A.R. Hipkiss, and D.L. Schneider, *Degradation of intracellular protein in muscle. Lysosomal response to modified proteins and chloroquine.* Journal of Biological Chemistry, 1988. **263**(35): p. 18886-90.

159. Gerbaux, C., et al., *Hyperactivity of cathepsin B and other lysosomal enzymes in fibroblasts exposed to azithromycin, a dicationic macrolide antibiotic with exceptional tissue accumulation.* FEBS Letters, 1996. **394**(3): p. 307-310.

160. Collette, J., et al., *Biosynthesis and alternate targeting of the lysosomal cysteine protease cathepsin L.* Int Rev Cytol, 2004. **241**: p. 1-51.

161. Jordans, S., et al., *Monitoring compartment-specific substrate cleavage by cathepsins B, K, L, and S at physiological pH and redox conditions.* BMC Biochem, 2009. **10**: p. 23.

162. Powers, J.C., et al., *Irreversible Inhibitors of Serine, Cysteine, and Threonine Proteases.* Chemical Reviews, 2002. **102**(12): p. 4639-4750.

163. Goulet, B., M. Truscott, and A. Nepveu, *A novel proteolytically processed CDP/Cux isoform of 90 kDa is generated by cathepsin L.* Biol Chem, 2006. **387**(9): p. 1285-93.

164. Bulynko, Y.A., et al., *Cathepsin L stabilizes the histone modification landscape on the Y chromosome and pericentromeric heterochromatin.* Mol Cell Biol, 2006. **26**(11): p. 4172-84.

165. Adams-Cioaba, M.A., et al., *Structural basis for the recognition and cleavage of histone H3 by cathepsin L.* Nat Commun, 2011. **2**: p. 197.

166. Littlewood-Evans, A.J., et al., *The osteoclast-associated protease cathepsin K is expressed in human breast carcinoma.* Cancer Res, 1997. **57**(23): p. 5386-90.

167. Kleer, C.G., et al., *Epithelial and stromal cathepsin K and CXCL14 expression in breast tumor progression.* Clin Cancer Res, 2008. **14**(17): p. 5357-67.

168. Lewis, C.E. and J.W. Pollard, *Distinct Role of Macrophages in Different Tumor Microenvironments.* Cancer Research, 2006. **66**(2): p. 605-612.

169. Lin, E.Y., et al., *Colony-stimulating factor 1 promotes progression of mammary tumors to malignancy.* J Exp Med, 2001. **193**(6): p. 727-40.

170. Joyce, J.A., et al., *Cathepsin cysteine proteases are effectors of invasive growth and angiogenesis during multistage tumorigenesis.* Cancer Cell, 2004. **5**(5): p. 443-53.

171. Gocheva, V. and J.A. Joyce, *Cysteine cathepsins and the cutting edge of cancer invasion.* Cell Cycle, 2007. **6**(1): p. 60-4.

172. Laoui, D., et al., *Tumor-associated macrophages in breast cancer: distinct subsets, distinct functions.* Int J Dev Biol, 2011. **55**(7-9): p. 861-7.

173. Lee, A.H., et al., *Angiogenesis and inflammation in invasive carcinoma of the breast.* J Clin Pathol, 1997. **50**(8): p. 669-73.

174. Campbell, M.J., et al., *Proliferating macrophages associated with high grade, hormone receptor negative breast cancer and poor clinical outcome.* Breast Cancer Res Treat, 2011. **128**(3): p. 703-11.

175. Friedl, P. and K. Wolf, *Tumour-cell invasion and migration: diversity and escape mechanisms.* Nat Rev Cancer, 2003. **3**(5): p. 362-74.

176. Grubb, A.O., *Cystatin C-Properties and use as diagnostic marker,* in *Advances in Clinical Chemistry*, E.S. Herbert, Editor. 2001, Elsevier. p. 63-99.

177. Kos, J., et al., *Cysteine proteinases and their inhibitors in extracellular fluids: markers for diagnosis and prognosis in cancer.* Int J Biol Markers, 2000. **15**(1): p. 84-9.

178. Sinha, A.A., et al., *Prediction of pelvic lymph node metastasis by the ratio of cathepsin B to stefin A in patients with prostate carcinoma.* Cancer, 2002. **94**(12): p. 3141-9.

179. Sinha, A.A., et al., *Ratio of cathepsin B to stefin A identifies heterogeneity within Gleason histologic scores for human prostate cancer.* Prostate, 2001. **48**(4): p. 274-84.

180. Park, K.-Y., G. Li, and M.O. Platt, *Monocyte-derived macrophage assisted breast cancer cell invasion as a personalized, predictive metric to score metastatic risk.* Scientific Reports, 2015. **5**: p. 13855.

181. Barry, Z.T. and M.O. Platt, *Cathepsin S Cannibalism of Cathepsin K as a Mechanism to Reduce Type I Collagen Degradation.* Journal of Biological Chemistry, 2012. **287**(33): p. 27723-27730.

182. Ménard, R., et al., *Autocatalytic Processing of Recombinant Human Procathepsin L: CONTRIBUTION OF BOTH INTERMOLECULAR AND UNIMOLECULAR EVENTS IN THE PROCESSING OF PROCATHEPSIN L IN VITRO.* Journal of Biological Chemistry, 1998. **273**(8): p. 4478-4484.

183. Vasiljeva, O., et al., *Recombinant human procathepsin S is capable of autocatalytic processing at neutral pH in the presence of glycosaminoglycans.* FEBS Letters, 2005. **579**(5): p. 1285-1290.

184. Hagemann, S., et al., *The human cysteine protease cathepsin V can compensate for murine cathepsin L in mouse epidermis and hair follicles.* Eur J Cell Biol, 2004. **83**(11-12): p. 775-80.

185. Park, K.Y., W.A. Li, and M.O. Platt, *Patient specific proteolytic activity of monocyte-derived macrophages and osteoclasts predicted with temporal kinase activation states during differentiation.* Integr Biol (Camb), 2012. **4**(12): p. 1459-69.

186. Xin, X.Q., B. Gunesekera, and R.W. Mason, *The specificity and elastinolytic activities of bovine cathepsins S and H.* Arch Biochem Biophys, 1992. **299**(2): p. 334-9.

187. Bania, J., et al., *Human cathepsin S, but not cathepsin L, degrades efficiently MHC class II-associated invariant chain in nonprofessional APCs.* Proceedings of the National Academy of Sciences, 2003. **100**(11): p. 6664-6669.

188. Jung, M., et al., *Cathepsin Inhibition-Induced Lysosomal Dysfunction Enhances Pancreatic Beta-Cell Apoptosis in High Glucose.* PLoS ONE, 2015. **10**(1): p. e0116972.

189. Settembre, C., et al., *A lysosome-to-nucleus signalling mechanism senses and regulates the lysosome via mTOR and TFEB.* Embo J, 2012. **31**(5): p. 1095-108.

190. Settembre, C., et al., *Signals from the lysosome: a control centre for cellular clearance and energy metabolism.* Nat Rev Mol Cell Biol, 2013. **14**(5): p. 283-296.

191. diSibio, G. and S.W. French, *Metastatic Patterns of Cancers: Results From a Large Autopsy Study.* Archives of Pathology & Laboratory Medicine, 2008. **132**(6): p. 931-939.

192. Hussein, O. and S.V. Komarova, *Breast cancer at bone metastatic sites: recent discoveries and treatment targets.* Journal of Cell Communication and Signaling, 2011. **5**(2): p. 85-99.

193. Mundy, G.R., *Metastasis: Metastasis to bone: causes, consequences and therapeutic opportunities.* Nat Rev Cancer, 2002. **2**(8): p. 584-593.

194. Guise, T.A. and G.R. Mundy, *Cancer and Bone.* Endocrine Reviews, 1998. **19**(1): p. 18-54.

195. Patel, S.A., et al., *Metastatic breast cancer cells in the bone marrow microenvironment: novel insights into oncoprotection.* Oncol Rev, 2011. **5**(2): p. 93-102.

196. Fritz, V., et al., *Bone-metastatic prostate carcinoma favors mesenchymal stem cell differentiation toward osteoblasts and reduces their osteoclastogenic potential.* J Cell Biochem, 2011. **112**(11): p. 3234-45.

197. Hung, S.-C., et al., *Gene expression profiles of early adipogenesis in human mesenchymal stem cells.* Gene, 2004. **340**(1): p. 141-150.

198. Bianco, P., et al., *Bone Marrow Stromal Stem Cells: Nature, Biology, and Potential Applications.* STEM CELLS, 2001. **19**(3): p. 180-192.

199. Kaveh, K., et al., *Mesenchymal stem cells, osteogenic lineage and bone tissue engineering: a review.* Journal of Animal and Veterinary Advances, 2011. **10**(17): p. 2317-2330.

200. Raisz, L.G., *Physiology and pathophysiology of bone remodeling.* Clin Chem, 1999. **45**(8 Pt 2): p. 1353-8.

201. Theoleyre, S., et al., *The molecular triad OPG/RANK/RANKL: involvement in the orchestration of pathophysiological bone remodeling.* Cytokine & Growth Factor Reviews, 2004. **15**(6): p. 457-475.

202. Rosen, C.J. and M.L. Bouxsein, *Mechanisms of Disease: is osteoporosis the obesity of bone?* Nat Clin Pract Rheum, 2006. **2**(1): p. 35-43.

203. Xiao, Y., et al., *Cathepsin K in Adipocyte Differentiation and Its Potential Role in the Pathogenesis of Obesity.* Journal of Clinical Endocrinology & Metabolism, 2006. **91**(11): p. 4520-4527.

204. Buxton, P.G., et al., *Dense collagen matrix accelerates osteogenic differentiation and rescues the apoptotic response to MMP inhibition.* Bone, 2008. **43**(2): p. 377-385.

205. Chen, X.-D., et al., *Extracellular Matrix Made by Bone Marrow Cells Facilitates Expansion of Marrow-Derived Mesenchymal Progenitor Cells and Prevents Their Differentiation Into Osteoblasts.* Journal of Bone and Mineral Research, 2007. **22**(12): p. 1943-1956.

206. McBeath, R., et al., *Cell Shape, Cytoskeletal Tension, and RhoA Regulate Stem Cell Lineage Commitment.* Developmental Cell, 2004. **6**(4): p. 483-495.

207. Mariman, E. and P. Wang, *Adipocyte extracellular matrix composition, dynamics and role in obesity.* Cellular and Molecular Life Sciences, 2010. **67**(8): p. 1277-1292.

208. Nakajima, I., et al., *Adipose tissue extracellular matrix: newly organized by adipocytes during differentiation.* Differentiation, 1998. **63**(4): p. 193-200.

209. Mizuno, M., R. Fujisawa, and Y. Kuboki, *Type I collagen-induced osteoblastic differentiation of bone-marrow cells mediated by collagen-α2β1 integrin interaction.* Journal of Cellular Physiology, 2000. **184**(2): p. 207-213.

210. Mastro, A.M., et al., *Breast cancer cells induce osteoblast apoptosis: A possible contributor to bone degradation.* Journal of Cellular Biochemistry, 2004. **91**(2): p. 265-276.

211. Molloy, A.P., et al., *Mesenchymal stem cell secretion of chemokines during differentiation into osteoblasts, and their potential role in mediating interactions with breast cancer cells.* International Journal of Cancer, 2009. **124**(2): p. 326-332.

212. Maxson, S. and K.J.L. Burg, *Conditioned media cause increases in select osteogenic and adipogenic differentiation markers in mesenchymal stem cell cultures.* Journal of Tissue Engineering and Regenerative Medicine, 2008. **2**(2-3): p. 147-154.

213. Tsai, K.-S., et al., *Type I collagen promotes proliferation and osteogenesis of human mesenchymal stem cells via activation of ERK and Akt pathways.* Journal of Biomedical Materials Research Part A, 2010. **94A**(3): p. 673-682.

214. Ruettger, A., et al., *Cathepsins B, K, and L are regulated by a defined collagen type II peptide via activation of classical protein kinase C and p38 MAP kinase in articular chondrocytes.* J Biol Chem, 2008. **283**(2): p. 1043-51.

215. Wilkinson Richard, D.A., et al., *Cathepsin S: therapeutic, diagnostic, and prognostic potential*, in *Biological Chemistry*. 2015. p. 867.

216. Neufeld, E.F., *Lysosomal Storage Diseases.* Annual Review of Biochemistry, 1991. **60**(1): p. 257-280.

217. Mason, S.D. and J.A. Joyce, *Proteolytic networks in cancer.* Trends Cell Biol, 2011. **21**(4): p. 228-37.